SLOPE STABILITY ASSESSMENT IN KALIMPONG REGION OF DARJEELING HIMALAYAS

Thesis Submitted
In Partial Fulfillment of the Requirements
For the Degree of

DOCTOR OF PHILOSOPHY

in

Civil Engineering

by

Vaishnavi Bansal
(2K19/PhD/CE/08)

Under the Supervision of

Prof. Raju Sarkar
(Professor, DTU, Delhi)

To the
Department of Civil Engineering
DELHI TECHNOLOGICAL UNIVERSITY
(Formerly Delhi College of Engineering)
Shahbad Daulatpur, Main Bawana Road, Delhi-110042, India

June, 2025

ACKNOWLEDGEMENTS

I express my deep gratitude to my supervisor Prof. Raju Sarkar, for assisting me in identifying and formulating the research problem. His valuable comments and advice gave me the confidence to overcome the challenges in the formulation of this research work. I express my special thanks to Prof. K C Tiwari, Head of Civil Engineering Department, DTU, for his continued inspiration and support during research work.

I sincerely express my profound gratitude to His Holiness Jagadguru Sri Shivaratri Deshikendra Mahaswamiji and the leadership at JSS Mahavidhyapeetha for granting me the opportunity to pursue my Ph.D.

I would like to thank Dr. Ruchi Saraswat (Head of Civil Engineering Department, JSSATEN), Mr. Praful Rao (Founder- Save the Hills, NGO in Kalimpong), Mr. Sanjay Gupta (Spatial Geotech Pvt. Limited), Ms. Samten Tamang (Lecturer, Kalimpong Govt. Polytechnic), Dr. Pankaj Sharma (Post-Doctoral Fellow at the University of São Paulo, Brazil), Mr. Gaurav Bharti (Assistant Professor, JSSATEN) and my fellow colleagues and scholars in JSSATEN and DTU for their valuable feedback during my experimental and thesis work.

I would also like to thank all those who directly and indirectly supported me in carrying out this thesis work successfully. Furthermore, I would like to express my sincere gratitude to my parents, husband, and daughters and also to all members of my family for their endless inspiration, support and guidance throughout my whole life. Last but not least, I express my sincere gratitude to the Almighty for everything.

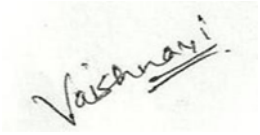

Vaishnavi Bansal
(Roll No. 2K19/PhD/CE/08)

DELHI TECHNOLOGICAL UNIVERSITY
(Formerly Delhi College of Engineering)
Shahbad Daulatpur, Main Bawana Road, Delhi-42

CANDIDATE'S DECLARATION

I **VAISHNAVI BANSAL** hereby certify that the work which is being presented in the thesis entitled "**Slope Stability Assessment in Kalimpong region of Darjeeling Himalayas"** in partial fulfillment of the requirements for the award of the Degree of Doctor of Philosophy, submitted in the Department of **Civil Engineering**, Delhi Technological University is an authentic record of my own work carried out during the period from17-July-**2019** to **14-June-2025** under the supervision of **Prof. Raju Sarkar.**
The matter presented in the thesis has not been submitted by me for the award of any other degree of this or any other Institute.

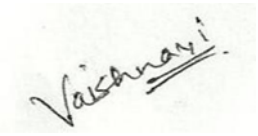

Candidate's Signature

This is to certify that the student has incorporated all the corrections suggested by the examiners in the thesis and the statement made by the candidate is correct to the best of our knowledge.

Signature of Supervisor **Signature of External Examiner**

DELHI TECHNOLOGICAL UNIVERSITY
(Formerly Delhi College of Engineering)
Shahbad Daulatpur, Main Bawana Road, Delhi-42

CERTIFICATE BY THE SUPERVISOR

Certified that **Vaishnavi Bansal** (2K19/PHD/CE/08) has carried out her research work presented in this thesis entitled **"Slope Stability Assessment in Kalimpong region of Darjeeling Himalayas"** for the award of **Doctor of Philosophy** from Department of Civil Engineering, Delhi Technological University, Delhi, under my supervision. The thesis embodies results of original work, and studies are carried out by the student herself and the contents of the thesis do not form the basis for the award of any other degree to the candidate or to anybody else from this or any other University/Institution.

(Signature)
Prof. (Dr.) Raju Sarkar
Department of Civil Engineering
Delhi Technological University, Delhi

Date: …….

ABSTRACT

The Darjeeling Himalayas, particularly the Kalimpong region, experience frequent landslides due to a complex interplay of geological, hydrological, seismic, and anthropogenic factors. This research provides a comprehensive slope stability assessment of Kalimpong using a multidisciplinary approach that integrates geotechnical investigation, numerical modeling, and geospatial analysis. The study begins with a detailed review of the region's geology, geomorphology, and historical landslide activity. Field investigations were conducted to collect soil and rock samples, and extensive laboratory tests were performed to determine key geotechnical parameters such as cohesion, internal friction angle, unit weight, and permeability. Using these inputs, slope stability was evaluated through GeoStudio SLOPE/W software, applying the Morgenstern-Price method under various conditions—static and dynamic, dry and saturated. The results revealed that many natural slopes in Kalimpong are marginally stable under dry conditions but exhibit critical instability when subjected to rainfall infiltration and seismic forces. The Factor of safety (FOS) significantly dropped below 1.0 for several slopes under dynamic-saturated scenarios, indicating a high probability of failure. Furthermore, stabilization strategies such as soil nailing were modelled and validated in SLOPE/W, showing significant improvements in FOS values and thus enhancing slope resilience.

To complement the site-specific analyses, the study incorporated GIS-based landslide susceptibility mapping using the Frequency ratio (FR) model. Geospatial layers representing conditioning factors—including slope angle, aspect, elevation, lithology, proximity to roads and faults, and rainfall intensity—were developed using Shuttle Radar Topography Mission (SRTM) Digital Elevation model (DEM) and remote sensing data. The FR model quantified the correlation between historical landslide events and each parameter, producing a susceptibility zonation map that classified the region into low, moderate, and high-risk zones. Approximately 38% of the study area fell into

moderate-to-high susceptibility classes, aligning with known landslide-prone corridors and anthropogenic ally disturbed slopes. This dual approach—merging deterministic Limit Equilibrium method (LEM) based modelling with probabilistic geospatial assessment—allowed for both micro and macro-scale understanding of slope instability in the region. The study also outlines policy recommendations, emphasizing the integration of slope stability analysis in infrastructure planning, particularly in seismic zones and monsoon-affected terrains. Overall, the thesis delivers a robust framework for landslide hazard mitigation in the Kalimpong region and sets the foundation for future research incorporating machine learning models, real-time monitoring, and climate change projections for improved early warning and slope management strategies.

TABLE OF CONTENTS

Contents

LIST OF TABLES

LIST OF FIGURES

LIST OF SYMBOLS, ABBREVIATIONS AND NOMENCLATURE

Adaboost	Adaptive Boosting
ANFIS	Adaptive network-based fuzzy inference system
ASTM	American Society for Testing and Materials
AHP	Analytical Hierarchy Process
AUC	Area Under the Curve
AI	Artificial Intelligence
ANN	Artificial Neural Networks
CA	Classification Accuracy
CRU	Climatic Research Unit
COD	Coefficient of determination
C	Cohesion
CD	Consolidated Drained
CU	Consolidated Undrained
DT	Decision Tree
DEM	Digital Elevation model
F1	F1 Score
FOS	Factor of safety
F	Failure
FN	False Negative
FP	False Positive
FPR	False Positive Rate
FDM	Finite Difference Methods
FEM	Finite Element Methods
FR	Frequency Ratio
Phi (ϕ)	Friction angle
GLE	Generalized Limit Equilibrium

GIS	Geographic Information Systems
GSI	Geological Strength Index
GB	Gradient Boosting
GSI	Grain Size Distribution
K_h	Horizontal seismic coefficient
IS	Indian standards
CRITIC	Inter Criteria based Correlation
InSAR	Interferometric Synthetic Aperture Radar
IoT	Internet of things
IDW	Inverse Distance Weight
KNN	k Nearest Neighbours
LCF	Landslide conditioning factor
LHZ	Landslide hazard zonation
LSI	Landslide Susceptibility Index
LSI	Landslide susceptibility index
LSM	Landslide Susceptibility Mapping
LHS	Lesser Himalayan Sequence
LiDAR	Light Detection and Ranging
LEM	Limit Equilibrium method
LL	Liquid Limit
LR	Logistic Regression
ML	Machine learning
MBT	Main Boundary Thrust
MCT	Main Central Thrust
MATLAB	Matrix Laboratory
MDD	Maximum dry density
mu	Mean
$\bar{x}$	Mean of the x values
$\bar{y}$	Mean of the y values
MSE	Mechanically stabilized earth
M-P	Morgenstern–Price

NB	Naïve Bayes
NCRB	National Crime Records Bureau
NetCDF	Network Common Data Form
N.P.	Non Plastic
NEHR	North-Eastern Himalayan Region
Wj	Objective weight of any given criterion j
OMC	Optimum moisture content
PSO	Particle swarm optimisation
PSD	Particle-size distribution
r	Pearson's Coefficient of correlation
PL	Plastic Limit
PI	Plasticity Index
P	Precision
PR	Prediction rates
RF	Random Forest
lambda	rate parameter
R	Recall
ROC	Receiver Operating Characteristics
RFV	Relative frequency values
RMR	Rock Mass Rating
SRTM	Shuttle Radar Topography Mission
SA	Slope angle
SH	Slope height
S	Stable
sigma	Standard deviation
I_j	Standard Deviation/Average for each individual parameter j
SVM	Support Vector Machines
SVR	Support vector regression
SoI	Survey of India
SAR	Synthetic Aperture Radar
3D	Three-Dimensional

TN	True Negative
TP	True Positive
TPR	True Positive Rate
2D	Two-Dimensional
USCS	Unified Soil Classification System
UW	Unit Weight
x_i	Value of the x variable
y_i	Value of the y variable
K_v	Vertical seismic coefficient

CHAPTER 1
INTRODUCTION

1.1 General

Earth embankments are frequently needed for levees, roads, railroads, river training projects, and earth dams. Since their failure could result in both enormous financial loss and the loss of human life, the stability of these embankments, also known as slopes, should be carefully examined. In the majority of engineering applications, slope analysis is typically carried out to recommend a safe and cost-effective design for associated structures including earth dams, embankments, and excavations. The identification of crucial geological, material, environmental, and economic aspects is aided by preliminary analyses. Slope stability analysis becomes a crucial component for organizing in-depth studies of the aforementioned structures. Generally speaking, determining the stability of any slope accurately requires prior geotechnical and engineering geology experience in the area. Slope stability assessment is frequently an interdisciplinary endeavor that calls for input from engineering geology, soil mechanics, and rock mechanics. The total mass of soil that contributes to the failure moves outward and downward in each slope failure. Slope failure results from the effect of gravitational forces, Soil seepage forces, and Earthquake loading shown in a generalized Fig 1.1.

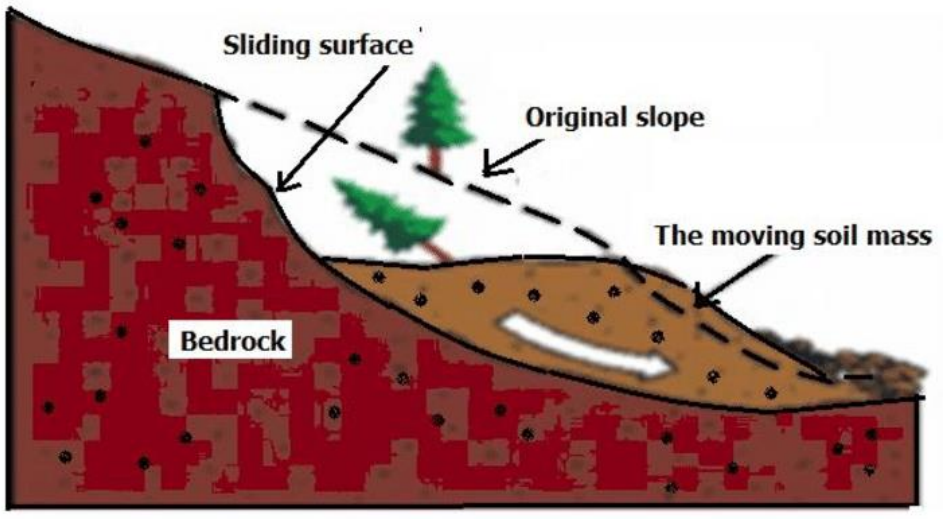

Fig 1.1 Illustration of a landslide in general

Slope failure can also result via excavation and the slow breakdown of the soil's structure. Because gravitational forces try to mobilise a portion of the mass downward to obtain a more level surface, every finite sloping surface is always susceptible to shearing pressures on almost all of its internal surfaces. There are two components to an analysis of slope stability:

a) Identifying the surface that is in a state of limiting equilibrium or about to move.

b) Calculating the shearing strength and stresses along this surface.

Shear stress on any slope surface is dependent on a number of factors, including the slope's shape and material unit weights. The density, drainage, and characteristics of the soil all affect the mobilised shearing strength along any plane.

1.2 Causes of Slope Failures

The gravitational and other forces (such as tectonic stresses and earthquake forces) causethe sliding movement of any slope. The shearing resistance of the soil along the plane of failure tries to prevent the movement. When the shearing resistance is overcome by the mobilizing forces trying to cause movement, the slope becomes unstable. Sudden failure of natural slopes may be caused due to one or several of the following reasons:

a) The current balance of forces is altered when portions of a slope or the ground next to the slope are excavated or filled.
b) Seismic activities (i.e. earth tremors or earthquakes).
c) Sudden rise in water table leads to increase in pore water pressure inside a slope and subsequent reduction in the shear strength of existing soil mass. This may be caused activities such as deforestation, alteration of natural drainage conditions, reservoir construction or excessive rainfall etc.
d) Deformations which are not significant enough to cause instability of the slope but gradually leading to failure. Such deformations help to reduce the shear strength of the soil in a progressive manner. These often occur along major natural discontinuities, ancient slip surfaces and tectonic zones within a slope.
e) Increase in pore water pressure after many years of a cutting or an excavation

(for low permeability soil) leading to considerable reduction of the shear strength of soil.

f) Weathering of soil disturbs the internal structure or the bonds between the soil particles. The shear strength of the soil is greatly reduced by weathering activity. For over-consolidated clays and shales, weathering leads to increase of recoverable strain energy and its tendency to failure (Bjerrum, 1967). Weathering may be accelerated by slope disturbance and exposure to atmosphericand other agencies such as stream action.

1.3 Importance of Slope Stability Analysis

For man-made or natural slopes (e.g. embankments, road cuts, open-pit mining, excavations, landfills etc.), slope stability analysis forms an integral part to assess its safety and economy. Slope stability analysis helps us to find endangered areas, potential causes of failure, sensitivity to different triggering mechanisms etc. The analysis also helps us to arrive at a safe, reliable, economical design of any slope and also find remedial measures against failure of the same.

Slope stability analysis is a crucial component of geotechnical engineering, essential for ensuring the safety and sustainability of infrastructure in regions prone to landslides and soil instability. Unstable slopes pose serious risks to human lives and critical infrastructure such as roads, dams, bridges, and urban settlements. Landslides often triggered by heavy rainfall, seismic events, and anthropogenic activities, result in catastrophic consequences, including fatalities, loss of property, and economic setbacks. For instance, studies highlight that rainfall-induced landslides account for substantial damage to infrastructure annually, particularly in mountainous and tropical regions (Petley, 2012, Pardeshi et al., 2013). Slope stability analysis helps identify potential failures early, enabling mitigation strategies to safeguard lives and assets.

From a sustainability perspective, slope stability is vital for the long-term viability of development projects. Failure to assess and address stability issues can lead to project delays, cost overruns, and environmental degradation. Stabilized slopes are instrumental in preventing soil erosion, preserving topsoil, and

maintaining the ecological integrity of natural landscapes (Lacasse et al., 2009). Furthermore, advancements in computational modeling and remote sensing techniques, such as the use of high-resolution geospatial data, have significantly enhanced the accuracy of slope stability assessments (Fan et al., 2020, MORA C and Vahrson, 1994).

Environmental impacts are another key concern. Landslides often lead to sedimentation of rivers, destruction of vegetation, and disruption of ecosystems. Proactive slope stability measures reduce these impacts, contributing to sustainable land use management (Wang et al., 2021). Additionally, integrating soil reinforcement methods such as soil nailing and geosynthetics can further improve slope stability under static and dynamic conditions (Sharma et al., 2019). Slope stability analysis is indispensable for safeguarding infrastructure, minimizing environmental impacts, and ensuring sustainable development. Comprehensive assessments incorporating modern technologies and mitigation techniques can significantly reduce the risks associated with slope failures. Slopes may be of two types: infinite slope and finite slope. If a slope represents the boundary surface of a semi-infinite soil mass and the soil properties for all identical depthbelow the surface are constant, it is called a finite slope. The present work mainly deals with finite slopes. The examples of finite slopes are the inclined faces of earth dams, embankments and cuts etc. In the present study, the stability analysis is done for finite slopes based on limit equilibrium technique. Evaluation of safety factor (i.e. factor of safety) using limit equilibrium technique utilizes the principle of static equilibrium along discretized failure surface. Limit equilibrium technique based (Morgenstern and Price, 1965) is used to evaluate the FOS of potential failure surface. This method satisfies both moment and force equilibrium for all the slices in the discretized failure mass.

1.4 Research Gap

Following research gaps have been identified despite the known susceptibility of Kalimpong to landslide events, there remains a significant research gap in this area.

1. To date, no comprehensive studies have been undertaken to conduct landslide susceptibility mapping and slope stability analysis in this region. This lack of detailed, site-specific research means that the critical factors contributing to landslide risks in Kalimpong remain poorly understood. Consequently, the development of effective mitigation strategies and risk management plans is hindered, underscoring the urgent need for focused research in this domain.
2. A significant research gap exists in Kalimpong as no comprehensive studies have been conducted on slope stability analysis under both static and dynamic conditions. This lack of research leaves critical uncertainties in predicting and mitigating landslide risks, highlighting the urgent need for detailed studies in this area.
3. A significant research gap exists as no studies have applied machine learning techniques separately to static and dynamic conditions in slope stability analysis taken consideration of Kalimpong. This omission hampers the development of accurate and comprehensive predictive models, highlighting the need for targeted research in this area.

1.5 Research objectives and scope

This research has been carried out to use several metaheuristic optimisation techniques and the limit equilibrium technique to perform slope stability analysis for a number of challenges. Below is a list of the current study's objectives:

a) To locate the critical sites in Kalimpong region as study area.

b) To investigate the soil parameters of the study area based on field and laboratory tests.

c) To prepare models in the software of the slopes and to assign the soil properties.

d) To analyze the models developed in the software under static and dynamic loading in dry condition.

e) To analyze the models developed in the software under static and dynamic loading in saturated condition.

f) To propose the appropriate technique to stabilize the unstable slopes.

g) To analyze the slopes after stabilizing technique adopted.

The overall aim of this PhD research is to comprehensively evaluate the stability of critical slopes in the Kalimpong region through field and laboratory characterization, numerical modeling, and simulation under varying loading and moisture conditions, and to develop effective stabilization measures for enhancing slope safety.

1.6 Presentation of the Thesis

The thesis is composed of six chapters. Brief descriptions of the contents of each chapterare as follows:

Chapter 1 – Introduction: The concept of slope stability and the significance of its assessment in mountainous terrain like Kalimpong are introduced. Causes of slope failures, the impact of rainfall, seismicity, and anthropogenic activities are described. The aim and objectives of the study, focusing on geotechnical analysis, modeling, and mitigation, are outlined.

Chapter 2 – Literature Review: An overview of past research on landslides, slope behavior, and analytical methods is presented. Factors influencing slope failures are explored, and GIS, remote sensing, and machine learning applications are reviewed. Also, the gaps in the present state of the art knowledge in the area of slope stability analysis is provided at the end of this chapter.

Chapter 3 – Materials and Methodology: Field investigation, laboratory testing (Atterberg limits, compaction), and data collection for slope modeling are detailed. The use of SLOPE/W software for analyzing slopes under dry/saturated, static/dynamic scenarios before and after stabilization is explained. The GIS-based Frequency Ratio method used to generate susceptibility maps with thematic layers is described.

Chapter 4 – Results and discussions: The results of slope stability analyses for six slope locations under static as well as dynamic condition emphasizing their combined role in reducing slope safety. It highlights the need for effective stabilization measures to mitigate failure risks. Among the techniques evaluated, soil nailing emerged as an efficient

method for improving slope performance under both static and dynamic conditions.

Chapter 5– Conclusion, future scope and social impact: This chapter presents conclusions based on the current work. Summarizes key outcomes showing that slopes are marginally stable and become critical under extreme conditions.

CHAPTER 2
LITERATURE REVIEW

2.1 General

Natural calamities are inevitable and disastrous. The increasing frequency and magnitude of landslides contribute significantly to natural disasters. However, early warning and detailed study of the landslides and landslide-prone areas have proven to be effective in minimising the risk, which is mainly reinforced by the increasing frequency of socio-economic impacts as well as the rapid population spread out on mountainous environment (Santi et al., 2011, Highland and Bobrowsky, 2008, Aleotti and Chowdhury, 1999). According to the evaluation of Research on the Epidemiology of Disasters (CRED, 2020), India was the third most affected country in the previous two decades by geo hydro-meteorological catastrophes. Aside from all the natural risks in mountainous areas, landslides are perhaps the broadest common and most severe hazards, affecting at least 15% of our country's geographical location.

"Landslide" is characterised as the movements of slope-forming materials made out of rocks or soils down a slope under the direct effect of gravity (Schuster and Wieczorek, 2018, Cruden, 1991, Hutchinson, 1988, Varnes, 1978). This morpho-dynamic phenomenon is widespread in the tectonically active Himalayas, where landslide hazards are most prevalent, especially during intense rainfall. Landslides can happen by sliding, flowing, toppling, or falling movements and numerous avalanches (Hutchinson, 1988, Varnes, 1978, Lugo Hubp, 1999, Crozier, 2010). The occurrence of landslides is triggered by different phenomena, including heavy regional rainfall as a consequence of changing climatic circumstances, rapid snow melting, earthquakes, and a variety of human activities like continued deforestation, unplanned urbanisation, development, etc. in the landslide-prone area (Wieczorek, 1996). India has growing vulnerability towards landslides, particularly in the Himalayan geo-dynamically active region and Arakan-Yoma belt of the Northeastern parts of the country because of their dynamic seismic events, diverse geographical characteristics along with feeble topographical

materials, and stable domains of the Meghalaya Plateau, the Western Ghats in the South West of the nation (van Westen et al., 2012). Hence, the Himalayan region alone contributed around 30% of the world's complete devastations because of landslide and their connected obliterations (Dahal et al., 2009). The rugged topography, steep slopes, and deep and narrow valleys encourage mass movement like earth flow, rockfall cum debris slide, avalanches, rockfall, and rock block slides that can be controlled by gravity which may vary in size from very large scale to small scale (Shroder Jr and Bishop, 1998, van Westen et al., 2012, Gerrard, 1994). On top of that, the climate variables such as rainfall, temperature variation, and freezing and thawing action play a vital role in slope failures (Kumar et al., 2019, Kumar et al., 2018, Lee et al., 2013, Chang et al., 2011, Gupta et al., 2016, Sah and Mazari, 1998). The slopes may be undercut or scoured by the action of the high rate of erosion as a consequence of complicated tectonic activities, rivers, and extreme climate conditions (Wulf et al., 2012, Thiede et al., 2009). In addition, socio-economic development activities in the Himalayan region play havoc with the slope failures considering rapid urbanisation that demands proper infrastructure developments in remote areas and the construction of highways for the communication link between the remote terrains of the Himalayas and the low land areas of peninsular India.

2.2 Site Study

Slope failures are the easiest natural hazard to prevent, reduce, or resolve (Collins and Znidarcic, 2004) Landslides occur on a large portion of land surfaces except snow covered in India (Chawla et al., 2018). As per the Geological Survey of India (2014), approximately 0.42 million square kilometers of land are prone to landslides, with nearly 43% of this area located in the NEHR. Data from the NCRB covering the years 2010 to 2019 reveal that landslides cause an average of 304 accidental deaths annually across India. Alarmingly, the evolving global climate has led to more frequent and intense weather disturbances, which, in turn, have heightened the risk of landslides. This risk is further compounded by rapid, unplanned urban growth and unsystematic land-use modifications in hilly and

mountainous regions (Khanna et al., 2021, Phong et al., 2021, Pourghasemi et al., 2012). Situated within the NEHR, Kalimpong district is highly vulnerable to both minor and major landslides, especially during the monsoon months from July to September. The region features steep mountainous terrain that experiences intense rainfall, contributing significantly to slope instability. The main urban settlement is positioned on a ridge near the Teesta River, while several other rivers—such as the Relli, Neora, Geesh, Leesh, Jaldhaka, and Murti—along with numerous small streams, drain the area. These watercourses actively erode the valley slopes, intensifying their steepness and promoting slope failure. The narrowing of interfluvial zones further escalates the landslide susceptibility. Between June and September, Kalimpong records average monthly rainfall ranging from 119 cm to 417 cm (source: https://worldclim.org). Human-induced developments like road construction, settlements, and hydropower installations disturb the natural slope conditions by stripping vegetation, making the soil more prone to displacement. Even a slight presence of water can trigger the movement of this loose material downhill. These combined factors make Kalimpong an ideal region for studying landslides. Identifying high-risk zones is essential so that appropriate mitigation strategies can be implemented to protect both lives and property (Roy et al., 2022).

Kalimpong, located in the Darjeeling Himalayas of West Bengal, India, forms part of the tectonically active and geologically diverse LHS. This region, shaped by the ongoing Himalayan orogeny, features complex stratigraphy, structural deformation, and active geomorphic processes. The interaction of tectonic activity, lithology, and climatic factors contributes to the region's susceptibility to landslides and slope instability (Steck, 2003). The Himalayan orogeny, initiated during the collision of the Indian and Eurasian tectonic plates in the Cenozoic era, has produced major thrust zones, such as the MCT and MBT, which significantly influence Kalimpong's geology. These tectonic features have resulted in steep slopes, deep valleys, and active river systems that dominate the landscape (Das et al., 2022). The regional geology of the Kalimpong area reflects the broader tectonic and lithological characteristics of the Darjeeling Himalayas. Located south of the MCT, which divides the high-grade metamorphic rocks of the Higher Himalayas from the low- to

medium-grade rocks of the Lesser Himalayas, the region's lithology is significantly influenced by the Lepcha Thrust, a subsidiary fault of the MCT responsible for extensive folding and faulting (Das et al., 2024). Dominated by the Daling Group of Rocks, which include phyllites, quartzites, schists, and gneisses of Precambrian to Paleozoic age, the lithology is highly weathered and fractured, making it mechanically weak and prone to instability under static and dynamic loads(Das et al., 2022). The geomorphology of the region is marked by steep slopes, deeply incised river valleys, and landslide-prone terrain shaped by the Teesta and Rangit rivers through erosion and sediment deposition (Nath et al., 2021). Stratigraphically, the Daling Group forms the foundation, with Lower Dalings comprising weak phyllites and slates and Upper Dalings characterized by schists interbedded with quartzites (Steck, 2003). Overlying these are the Darjeeling Gneiss Complex, consisting of high-grade metamorphic rocks such as banded and augen gneisses, reflecting deep crustal processes of Himalayan orogeny. Recent alluvial and colluvial deposits dominate lower valleys, contributing to slope instability and geomorphological evolution (Das et al., 2022). Structurally, the region exhibits intense deformation with thrust faults like the Lepcha Thrust creating shear zones, tight isoclinal folds aligned northwest-southeast indicating compressive Himalayan forces, and lineaments that act as conduits for groundwater, exacerbating instability during monsoons (Mandal & Maiti, 2015; Sarkar et al., 1995; Das & Basu, 2012). Geomorphological features such as steep slopes shaped by river incision and landslide-prone zones underlain by phyllites and weathered schists, particularly on slopes exceeding 30°, are common (Nath et al., 2021, Das et al., 2024). Seismically, the region lies in Zone IV, experiencing moderate earthquakes that have historically triggered landslides, as seen after the 1934 Bihar-Nepal earthquake (Das et al., 2022). The ongoing tectonic activity along the MCT and related faults underscores the seismic and slope stability hazards in the area (Nath et al., 2021). Before analysing further objectives of this research, let us get into the basics of landslides, categories, types and **m**ethods of slope stability analysis.

2.3 Categories of Landslides

Landslides are classified based on different criteria such as type of sliding surface, material involved, type of movement, age and state of activity. The most common nomenclature scheme is the one proposed by Varnes, 1978, Cruden, 1996 in landslide related literature which is based on two important parameters namely the type of movement and type of material involved. Further modification of Varnes' classification of landslide given by (Hungr et al., 2014), in particular, to improve compatibility with geotechnical and geological terminology of rocks and soils. As a result, four main types of landslides can be described as follows on the basis of movement mechanism and material composition:

2.3.1 Falls

Occurs in steep or overhanging slopes or cliffs by the abrupt movement of rocks along existing natural fractures or joint/ bedding planes. This typically occurs as free falling, bouncing and rolling. Undercut river banks and road cut slopes are prone to such failures. Weathering, gravity and water are controlling forces for such events. Detachment of rock or soil masses, often triggered by undercutting or seismic activity (Aleotti and Chowdhury, 1999).

2.3.2 Slides

It occurs in moderate to steep slopes and is characterized by failure of material at depth and then movement by sliding along a rupture or slip surface. Rotational slides (also referred to as slumps) involve movement of the material on a curved slip surface whereas if sliding is on a planer surface, it is called a transitional or rock slide. Translational (movement along planar surfaces) or rotational (curved slip surfaces) are commonly observed in areas with weak lithological strata.

2.3.3 Flows

Occurs in moderate slopes during or after heavy rain events and involves deformation of an entire soil mass that then flows downslope as a thick viscous fluid. Liquefaction or high-water content thus generates such condition of earth flow. If

downward movement of flow is very rapid it is a debris flow or as it is sometimes known, a mudflow. Fluid-like movement of debris or soil, typically resulting from heavy rainfall (Guo et al., 2022).

2.3.4 Complex Movements

A combination of mechanisms, such as rotational slides transitioning into flows, is often seen in tectonically active zones.

2.4 Slope stability analysis

2.4.1 Slope stability analysis under static conditions integrated with AI/ML

Shear strength as a function of normal stress on the slip surface, cohesion, and internal friction generally determines slope stability. The stability of the slope is reflected in the FOS, which is calculated by dividing the "shear strength" by the "shear stress" produced. When the generated shear stress is greater than the soil's available shear strength, a slope typically collapses (Kabir et al., 2023). Because of their ease of use, low version complexity, and quick processing times, Limit Equilibrium method (LEM) is a fundamental and traditional analytical tool for slope stability investigations, are frequently employed in slope stability studies and can be used to calculate FOS (Mafi et al., 2021). For multi-dimensional (2D and 3D) environments, LEM can be used to both static and dynamic scenarios (Agam et al., 2016, Azarafza et al., 2014). There is multiple equilibrium methods used to estimate the FOS. Fellenius, Bishop, Janbu, Modified Swedish, Morgenstern-Price, and others are some of the most well-known methods (Alejano et al., 2011). When computing FOS, maximum techniques yield comparable results, with the variance in projected values frequently being less than 6% (Huang et al., 2012). For the evaluation of slope stabilisation, LEM has been proposed and studied in great detail in recent decades (Yue and Kang, 2021, Liu et al., 2015, Wang et al., 2011, Cheng et al., 2007, Zhu et al., 2003, Zhu et al., 2005). The LEM technique has remained the preferred approach for the best use of many approaches, regardless of their utilitarian value, depending on the type of problem to be solved (e.g., circular, non-circular), as well as the level of precision that is desired in the results (Matthews et al., 2014). Along with taking

probabilistic soil factors into account, the method of slices is also taken into consideration to determine the most significant slip surface. Because of the difficulties involved in determining FOS values, traditional stability analysis techniques—which are influenced by the stabilisation process—find it difficult to produce trustworthy results. In order to solve this problem, scientists used computational intelligence techniques that provide an extremely accurate prediction of the slope condition, failure mechanism, and slide risk (Zhu et al., 2003, Ahangari Nanehkaran et al., 2022, Li and Yang, 2019, Mathe and Ferentinou, 2021, Azarafza et al., 2022).

In the meantime, there has been a lot of interest in machine learning techniques for reducing uncertainty in FOS calculations.In terms of calculating F.S. using prognostic models, AI, and in particular ML, has been very helpful in predicting the stability of slopes. These models make predictions about FOS based on the rate of machine learning and the models' stated accuracy. These algorithms attempt to develop methods for understanding the current state of "target data," learning, and using "training data" to learn. To generate likelihoods or forecasts, it uses a range of algorithms that fall within the categories of "deep" or "shallow" learning approaches (Raschka et al., 2020). The algorithms' learning mechanism, which can be compared to learning models like controlled, unstructured, or reinforcement learning, has a direct impact on how accurate the predictions are (Schmidhuber, 2015). AI and machine learning techniques have been successfully applied in engineering and science over the past 25 years (Zhang et al., 2021, Zhao et al., 2021, Armaghani et al., 2021, Yang et al., 2020, Kardani et al., 2021, Asteris et al., 2022). Through predictive modelling, risk assessment, and uncertainty analysis, ML models are also used to compute results for slope stability analysis that can provide insights into potential slope collapse processes and rates (Bui et al., 2020, Erzin and Cetin, 2012, Abdalla et al., 2015, Verma et al., 2016, Samui, 2013, Sakellariou and Ferentinou, 2005a, Ferentinou and Sakellariou, 2007). The FOS of slopes was also predicted using MATLAB-based coded programs, ANFIS, and other techniques, and the outcomes of the LEM methodology were compared with the predictions (Mohamed and Kasa, 2014). Another study compares the FOS of slopes with 3D-Finite Element method (FEM) using the PSO technique (Kalatehjari et al., 2014). They showed that

PSO may be used well in 3D situations, but not so well in 2D slope stability scenarios. To predict slope stability many researchers (Ferentinou and Sakellariou, 2007, Lu and Rosenbaum, 2003, Sakellariou and Ferentinou, 2005b) used ANN, a basic and popular AI model, in contrast to the LEM slope stability study.

The results of the LEM and ANN models were found to be consistent, allowing sample data to be categorised according to the expected failure mechanism. In another study, the SVM model was found to be somewhat more accurate than the ANN results when compared side by side (Samui, 2008). SVR and the radius basis function(Wei et al., 2021a) were compared with gradient boosting to ascertain the FOS and its relationship to the triggering factors on slope instabilities (Zhou et al., 2019). Various artificial intelligence-based techniques were used to accurately predict the FOS values for slopes, which were subsequently used for slope stabilisation (Qi and Tang, 2018). Numerous encouraging outcomes have been obtained by the "extreme learning machine" (Liu et al., 2014), "attribute recognition method and ANN" (Tao et al., 2021, Wei et al., 2021b), "fuzzy comprehensive evaluation method" (Wang and Lin, 2021), "particle swarm optimisation" (Gupta et al., 2016), and "cloud model" (Cui et al., 2021). In order to anticipate slope stability using numerical simulation techniques and the limit equilibrium approach, it is essential to consider the stress on the slope's body, demonstrate its deformation and stability, and identify the related back failure mechanism.

2.4.2 Slope stability analysis under dynamic conditions integrated with AI/ML

Slope stability under dynamic loading is a critical research area in geotechnical and seismic engineering, as seismic forces significantly influence slope deformation and failure mechanisms (Zhu, 2008). Dynamic loads include both natural and artificial sources, with earthquakes representing the primary natural load affecting slope stability (Krishnamoorthy, 2007). The interaction between soil dynamic properties and ground motion parameters makes evaluating seismic slope stability more complex than static analysis. Several approaches have been developed for dynamic stability evaluation, including experimental testing, numerical modeling (Jing-shan et al., 2001; Chuhan et al., 1997; Liu et al., 2004), the Newmark sliding block method (Newmark, 1965), and the pseudo-static method (Seed, 1979). Among

these, the pseudo-static approach remains the most widely used because of its simplicity and efficiency in practical engineering applications (Siyahi and Bilge, 1998; Biondi et al., 2002; Ai-Jun and Yong-Hua, 2003; Siad, 2003). It represents the seismic effect through equivalent static forces acting horizontally and vertically on the potential sliding mass (Erzin and Cetin, 2012).

In pseudo-static analysis, seismic loading is simulated as a static force derived from the product of the slope mass and the corresponding acceleration, simplifying earthquake-induced inertial effects shown in Fig 2.1 (Karray et al., 2018). The Factor of Safety (FOS) is determined as the ratio of resisting to driving forces along a potential slip surface, with values above unity indicating stability (Johari et al., 2015). This approach, incorporated within the Limit Equilibrium Method (LEM), assumes equilibrium between forces and moments and is highly effective for both static and dynamic evaluations (Mafi et al., 2021; Agam et al., 2016; Azarafza et al., 2014). In this study, the pseudo-static analysis was performed following IS 1893 (Part 1): 2016, as Kalimpong lies in seismic Zone IV, where horizontal and vertical seismic coefficients of 0.3 and 0.2, respectively, were used (Melo and Sharma, 2004). The simplicity and adaptability of the pseudo-static method make it well suited for regional studies, enabling rapid stability estimation under earthquake loading conditions.

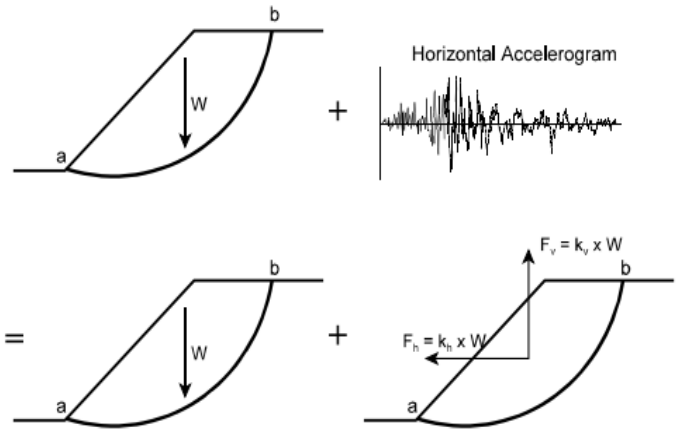

Fig. 2.1 Pseudo-static analysis approach (Melo and Sharma, 2004)

Over the years, LEM-based methods have been extensively applied for assessing seismic slope stability in both natural and engineered slopes (Howland, 1980; Nouri et al., 2008; Leshchinsky and San, 1994; Loukidis et al., 2003; Hynes-Griffin and Franklin, 1984; Baker et al., 2006). They have proven useful in analyzing earth dams, embankments, and natural slopes (Yue and Kang, 2021; Wang et al., 2011; Liu et al., 2015; Cheng et al., 2007; Zhu et al., 2005). Recent advances have introduced computational intelligence and machine learning (ML) to address the limitations of deterministic approaches by improving prediction accuracy and reducing uncertainty in FOS estimation (Asteris et al., 2022; Azarafza et al., 2022; Zhu et al., 2003; Ahangari Nanehkaran et al., 2022; Li and Yang, 2019; Mathe and Ferentinou, 2021). ML techniques, including artificial neural networks (ANNs), support vector machines (SVMs), decision trees (DT), random forests (RF), and hybrid models, have shown remarkable success in learning from complex geotechnical datasets (Cevik, 2011; Das, 2013; Kayabasi et al., 2015; Nanehkaran et al., 2023). Studies demonstrate that ANN and hybrid models such as PSO-ANN outperform traditional LEM approaches in FOS prediction under seismic conditions (Erzin et al., 2016; Erzin and Cetin, 2013; Gordan et al., 2016). Other models like SVM (Samui, 2008), ELM (Hoang and Bui, 2017), ANFIS (Fattahi, 2017), genetic algorithms (Manouchehrian et al., 2014), and ensemble techniques like AdaBoost and gradient boosting (Lin et al., 2021) provide strong predictive capabilities, even for nonlinear and uncertain data (Sousa et al., 2017; Qi and Tang, 2018). Collectively, these methods have advanced geotechnical modeling by enhancing slope stability predictions, particularly under dynamic and seismic stresses, thus contributing to safer and more resilient slope design practices.

2.5 Properties Influencing Slope Stability

The stability of a slope is inherently dependent on its geotechnical properties, which dictate the strength and deformation characteristics of the materials involved. Key factors include soil and rock mechanics, geological parameters, and hydrological factors, seismic and anthropogenic factors all of which play critical

roles in determining the resistance to failure under varying environmental and loading conditions.

2.5.1 Soil and Rock Mechanics

(a)Soil Mechanics: The mechanical behaviour of soils is governed by their composition, structure, and moisture content. Soil classification systems, such as the USCS, provide a basis for categorizing soils into granular (sand and gravel) and cohesive (clay and silt) types. These classifications are crucial for analyzing their response to stress and strain under loading conditions (Mizal-Azzmi et al., 2011, Santoso et al., 2011). Granular Soils exhibit high shear strength due to frictional resistance between particles. Their stability is significantly influenced by compaction and drainage characteristics whereas Cohesive Soils depend on cohesion and capillary forces for shear strength. These soils are prone to plastic deformation and exhibit time-dependent behaviour under loading, often leading to progressive failure.

(b) Rock Mechanics**:** Rock masses are inherently heterogeneous, comprising intact rock material and discontinuities such as joints, faults, and bedding planes. The stability of rock slopes is influenced by the orientation, spacing, and persistence of these discontinuities (Kumsar et al., 2000, Puniya et al., 2023). RMR and GSI are commonly employed to assess the quality of rock masses and their susceptibility to failure. Shear strength along discontinuities is described by parameters such as c and ϕ, which are often reduced due to the presence of water and weathering (Aleotti and Chowdhury, 1999)

2.5.2 Geological Factors

Cohesion, and friction angle govern the resistance to sliding. Weak or weathered materials are more prone to failure (Aleotti and Chowdhury, 1999, Kechik et al., 2023). Rock discontinuities, such as faults, joints, and bedding planes, serve as potential failure surfaces, especially when aligned parallel to the slope (Thakur et al., 2010). The orientation of geological structures relative to the slope plays a crucial role. Adverse dip angles increase the likelihood of translational failures (Puniya et al., 2023). Tectonic activity can create zones of weakness through faulting and

fracturing, reducing overall stability (Kumar et al., 2020). The shear strength of slope materials, defined by the Mohr-Coulomb failure criterion, is a critical factor in determining slope stability.

(a)Cohesion: Cohesion arises from interparticle forces and cementation in soils and rocks. In cohesive soils like clays, cohesion is a dominant factor, but it decreases with weathering and saturation (Kechik et al., 2023)

(b)Friction angle: The friction angle depends on the grain size, shape, and roughness of particles. Granular soils exhibit higher friction angles, whereas clays and silts have lower values. Laboratory tests such as direct shear and triaxial compression tests are commonly used to determine these parameters (Santoso et al., 2011, Zhao et al., 2020b).

(c)Effective Stress Principle: This principle highlights the detrimental impact of elevated pore water pressure on shear strength, especially during rainfall or rapid drawdown scenarios (Liu and Wang, 2023, Kumar et al., 2020).

2.5.3 Hydrological factors

Prolonged or intense rainfall increases pore water pressure, reducing effective stress and shear strength(Liu and Wang, 2023). Perched water tables can form within the slope, creating localized zones of instability (Santoso et al., 2011). Seepage induced by groundwater flow can destabilize slopes by exerting additional forces on soil particles. The effect is particularly pronounced in slopes with fine-grained materials (Kechik et al., 2023). Sudden lowering of water levels, such as in reservoirs, creates a transient imbalance between hydrostatic forces and slope resistance, often triggering failures (Ali et al., 2014). Rainfall-induced landslides in tropical regions, such as the Bhagirathi Valley during the June 2013 flood, highlight the impact of hydrological factors on slope stability(Bhambri et al., 2017). Pore water pressure plays a pivotal role in slope stability, particularly in rainfall-induced and seepage-driven failures. It influences the effective stress and thus the shear strength of soils.

(a) Positive Pore Water Pressure: When water infiltrates the soil, it increases the pore pressure, reducing the effective stress and shear strength. This is especially critical in saturated cohesive soils where prolonged rainfall or rapid drawdown conditions can lead to shallow slope failures (Ali et al., 2014, Liu and Wang, 2023).

(b) Negative Pore Water Pressure (Suction): In unsaturated soils, negative pore pressure (matric suction) contributes to apparent cohesion, enhancing stability. However, this effect diminishes as the soil becomes saturated. The relationship between suction and shear strength is captured by the extended Mohr-Coulomb criterion for unsaturated soils (Kechik et al., 2023, Santoso et al., 2011).

(c) Rainfall Infiltration: Rainfall alters pore pressure distribution, creating perched water tables and zones of increased instability. Analytical models are also developed to predict annual probabilities of slope failure under varying rainfall intensities and durations (Liu and Wang, 2023).

(d) Seepage and Permeability: Seepage forces exacerbate instability by reducing effective stress and inducing erosion. High-permeability materials like sand allow rapid drainage, mitigating pore pressure buildup, whereas low-permeability clays retain water, making them susceptible to failure.

2.5.4 Seismic Factors

Seismic activity induces inertial forces within the slope, which can reduce shear strength and trigger failures. The magnitude of the destabilizing forces depends on ground acceleration and slope geometry (Zhao et al., 2020a, Yin et al., 2009). Earthquakes can generate excess pore water pressure, particularly in saturated soils, reducing effective stress and exacerbating instability (Eberhardt et al., 2004). Loose, saturated sandy soils may lose strength completely during seismic shaking, leading to catastrophic failures. This phenomenon is particularly relevant in seismic zones with high water tables (Kumsar et al., 2000). The 2008 Wenchuan earthquake in China triggered numerous seismic-induced landslides, with significant damage to infrastructure and loss of life (Yin et al., 2009). Seismicity-induced landslides in the Kashmir Himalaya during the 2005 earthquake serve as a stark reminder of the

destructive potential of seismic forces (Ray et al., 2009).

2.5.5 Anthropogenic Factors

Slope cutting for roads, buildings, and mining activities disturbs the natural equilibrium, often leading to failures if proper stabilization measures are not implemented (Malviya et al., 2024, Mizal-Azzmi et al., 2011). Vegetation provides natural reinforcement to slopes through root cohesion and water interception. Deforestation removes this stabilizing effect, increasing susceptibility to erosion and failure (Puniya et al., 2023). The addition of structures or embankments increases the driving forces acting on slopes, particularly when combined with inadequate drainage systems (Kumar et al., 2017). Anthropogenic activities such as road widening in the Lesser Himalayas have led to frequent slope failures, highlighting the need for careful planning and engineering (Ansari et al., 2020).

2.6 Types of failures

Failure mechanisms in slopes are characterized by the type of movement, geometry of the failure surface, and material properties. Understanding these mechanisms is critical to predicting slope behavior under various environmental and loading conditions. The three primary failure types—translational, rotational, and compound—each have unique triggers and characteristics.

2.6.1 Translational Failures

Translational failures occur along a planar or nearly planar failure surface, often dictated by weak geological layers or discontinuities. The movement is typically parallel to the slope surface, and these failures are common in stratified rock masses or slopes with distinct bedding planes (Aleotti and Chowdhury, 1999, Puniya et al., 2023). Failure initiates when the driving forces exceed the resisting forces along a pre-existing plane of weakness. Factors such as excessive loading, rainfall infiltration, and seismic activity reduce the shear strength of the failure surface, triggering sliding (Liu and Wang, 2023, Kumar et al., 2017) Rainfall-induced translational failures in layered Himalayan slopes have been extensively documented, where water infiltration leads to saturation and reduced

effective stress along weak bedding planes (Yin et al., 2009).

2.6.2 Rotational Failures

Rotational failures involve movement along a concave, circular or non-circular failure surface. These failures are most common in homogenous, cohesive soils or rock masses and are associated with deep-seated instabilities (Mizal-Azzmi et al., 2011, Zhao et al., 2020b). A rotational slip occurs when the moment of driving forces about the failure center exceeds the resisting moment. Factors such as increased pore water pressure, overloading, or undercutting at the slope toe promote failure. Bishop's Simplified Method and Janbu's Method are widely used for analyzing rotational failures by calculating the FOS for circular and non-circular surfaces (Donald and Chen, 1997, Zolkepli et al., 2019). Rotational failures in soft clays during monsoonal rainfalls are frequently reported in Southeast Asia, where saturated soils lose cohesion and exhibit significant deformation (Santoso et al., 2011).

2.6.3 Compound Failures

Compound failures involve a combination of translational and rotational mechanisms. These failures often occur in heterogeneous materials, where different zones within the slope exhibit distinct failure modes (Qi et al., 2016). A rotational slip may transition into a translational slide as the failure propagates across layers with varying shear strengths or material properties. Compound failures are highly unpredictable and require advanced numerical models for analysis (Puniya et al., 2023, Eberhardt et al., 2004). Seismic events, such as the Wenchuan earthquake, triggered compound failures in steep, stratified slopes, with rotational initiation transitioning into debris flows (Yin et al., 2009).

2.7 Analytical Methods in Slope Stability analysis

Analytical methods form the backbone of slope stability analysis, providing a means to estimate the FOS under various loading and environmental conditions. Among these, LEM is widely employed due to their simplicity and effectiveness. LEMs focus on evaluating the equilibrium of forces and moments

along a predefined failure surface, providing a measure of slope stability.

2.7.1 Limit Equilibrium Methods (LEM)

LEM assumes that a slope fails along a specific surface and divides the sliding mass into slices to calculate forces and moments acting on each slice. These methods use the Mohr-Coulomb failure criterion(Aleotti and Chowdhury, 1999, Michalowski, 1995). The following subsections discuss four prominent LEM techniques, each suited for different slope configurations and conditions.

(a) Fellenius Method: Also known as the Ordinary Method of Slices, the Fellenius Method is the simplest form of LEM. It assumes that interslice forces are negligible, making the calculations straightforward but conservative(Donald and Chen, 1997). This is simple and computationally inexpensive, provides a quick preliminary assessment of slope stability, ignores interslice forces, leading to conservative results. Not suitable for complex or irregular failure surfaces (Zolkepli et al., 2019). The Fellenius Method has been applied extensively in homogeneous soil slopes and initial stability evaluations.

(b) Bishop's Simplified Method: Bishop's Simplified Method improves upon the Fellenius Method by incorporating vertical interslice forces, making it more accurate for circular failure surfaces (Donald and Chen, 1997, Zhu et al., 2003b). This method is suitable for circular failure surfaces in homogeneous soils, moderately accurate for many practical applications, neglects horizontal interslice forces and requires iterative computations (Zhu, 2008). Widely used for embankments, earth dams, and homogeneous slopes (Firincioglu and Ercanoglu, 2021). Bishop’s Method is also utilized to assess slope stability in Himalayan terrains, highlighting its reliability under varying hydrological conditions (Kumar et al., 2017).

(c) Janbu's Method: Janbu's Method is a more generalized approach that can accommodate both circular and non-circular failure surfaces. It accounts for horizontal interslice forces, making it suitable for more complex geometries(Donald and Chen, 1997). This method is applicable to complex failure surfaces,

accommodates heterogeneous material properties and requires iterative procedures. Results are sensitive to the assumed interslice force distribution (Aleotti and Chowdhury, 1999). This method has been applied in the stability analysis of slopes in mining and infrastructure projects where irregular failure surfaces are common (Puniya et al., 2023). Janbu's Method is applied to analyze road-cut slopes in Northeast India, demonstrating its effectiveness in heterogeneous conditions (Malviya et al., 2024).

(d) Morgenstern-Price Method: The Morgenstern-Price Method is the most rigorous LEM, accounting for both horizontal and vertical interslice forces through a flexible force distribution function. It is suitable for highly irregular and complex failure surfaces (Zhu et al., 2003a). The method employs a force function to represent the interslice forces, ensuring both force and moment equilibrium. Applicable to both circular and non-circular surfaces. Offers higher accuracy than other LEMs. Computationally intensive. Requires assumptions about the interslice force function. The Morgenstern-Price Method is widely used in advanced slope stability software, such as GeoStudio and PLAXIS, for detailed stability analyses (Ansari et al., 2020). Its application is also demonstrated in 3D slope stability analyses, highlighting its precision in heterogeneous, large-scale slopes (Firincioglu and Ercanoglu, 2021). Comparison of various Limit Equilibrium methods is shown in Table 2.1.

Table 2.1: Comparison of various limit Equilibrium methods

Method	Complexity	Accuracy	Key Applications
Fellenius	Low	Conservative	Homogeneous slopes, preliminary assessments
Bishop's Simplified	Moderate	Suitable for circular surfaces	Embankments, earth dams
Janbu's	High	Suitable for irregular surfaces	Mining, heterogeneous slopes
Morgenstern-Price	Very High	Highly accurate	Complex geometries, detailed analyses

2.7.2 Finite Element Methods (FEM)

FEM has revolutionized slope stability analysis by allowing a detailed evaluation of stresses, strains, and displacements within the slope mass, offering a more realistic representation of failure mechanisms compared to the simplified force and moment equilibrium approach of LEM. FEM models the slope as a continuum divided into finite elements, where the stress–strain relationship of the material is defined through appropriate constitutive models, enabling simulation of both elastic and plastic behavior. This method can capture stress redistribution, progressive failure, and post-failure deformation, providing deeper insight into the failure mechanism and the influence of complex factors such as material heterogeneity, groundwater conditions, and seismic loading (Duncan, 1996; Fredlund, 1984; Eberhardt et al., 2004; Kanungo et al., 2013; Zhu et al., 2003a). FEM determines the Factor of Safety (FOS) by progressively reducing shear strength parameters (cohesion c and friction angle ϕ) until instability occurs, thus eliminating the need for predefined failure surfaces and offering an objective and comprehensive measure of slope stability. Although computationally intensive and dependent on accurate input parameters, FEM provides a powerful and versatile framework for analyzing slope deformation and failure under various static and dynamic conditions, and it is widely implemented in advanced software such as PLAXIS and GeoStudio for geotechnical stability assessments (Xie et al., 2011).

2.8 Advances in Slope Stability Analysis

Recent advances in computational techniques and geotechnical understanding have driven significant progress in slope stability analysis. Among these advances, the adoption of 3D Analysis represents a paradigm shift, offering greater accuracy and insight compared to traditional 2D methods. These innovations are crucial for complex geotechnical problems where the limitations of conventional methods become evident.

2.8.1 Three-Dimensional (3D) Analysis

3D slope stability analysis overcomes the limitations of 2D methods by incorporating the full spatial variability of slope geometry, material properties, and boundary conditions, providing a more realistic representation of slope behavior. This is particularly critical in cases involving irregular topography, anisotropic materials, or non-circular failure surfaces, as highlighted by (Xie et al., 2003, Firincioglu and Ercanoglu, 2021). While 2D methods, which assume planar or axisymmetric conditions, often oversimplify the problem by neglecting out-of-plane effects and assuming circular or planar failure surfaces, 3D methods account for the actual geometry and allow the evaluation of complex slope configurations (Hungr, 1987, Zhu et al., 2003a). This enables 3D analysis to model non-circular and irregular failure surfaces, better reflecting real-world conditions. Moreover, 3D methods capture spatial variations in stress and strength parameters, offering detailed insights into stress redistribution during failure, and provide a more accurate Factor of Safety (FOS) by incorporating out-of-plane forces and moments that 2D models ignore (Xie et al., 2003). Studies comparing 2D and 3D approaches demonstrate that 2D methods yield conservative results, particularly for slopes with irregular geometries or anisotropic conditions (Wines, 2016). It is also emphasized that 2D methods oversimplify failure mechanisms by assuming plane-strain conditions and neglecting lateral boundary effects, leading to inaccuracies in complex geological settings or under varying loading conditions (Bar et al., 2020). Conversely, 3D analysis captures the influence of lateral boundaries and heterogeneous material properties, providing critical insights into the progression of failure across the entire slope (Firincioglu and Ercanoglu, 2021).

Applications of 3D analysis are extensive, including the stability assessment of slopes near dams, tunnels, and roads, where 3D effects are pronounced (Ansari et al., 2020, Kumar et al., 2020), as well as large open-pit mines with complex geological conditions, where 3D modeling optimizes pit slopes and enhances safety (Lucas and de Graaf, 2013). Additionally, 3D methods have been employed in modeling landslides triggered by earthquakes or rainfall, where interactions between materials and topography are critical(Yin et al., 2009, Zhao et

al., 2020b). For instance, 3D analysis is used to assess the stability of a lava lobe at Unzen Volcano, Japan, identifying critical slip surfaces and stress distributions that were missed by 2D methods (Xie et al., 2003). Similarly 3D analysis in modeling pit slopes is demonstrated in Western Australia with complex geometries and anisotropic materials, underscoring the limitations of 2D methods (Firincioglu and Ercanoglu, 2021). Also, the effectiveness of 3D models is illustrated in analyzing the stability of slopes in the Lesser Himalayas, accounting for irregular topography and variable material properties (Ansari et al., 2020). These case studies underscore the enhanced accuracy and applicability of 3D methods in geotechnical engineering, making them indispensable for complex slope stability evaluations.

2.8.2 Integration of Geographic Information Systems (GIS)

Geographic Information Systems (GIS) have revolutionized slope stability analysis by providing a platform to manage, analyze, and visualize spatial data. The integration of GIS in geotechnical engineering allows for the efficient handling of complex terrain and geological datasets, enhancing the understanding of slope behavior and the identification of high-risk zones. GIS-based approaches are particularly valuable in large-scale studies, where traditional methods may be cumbersome or impractical (Bouajaj et al., 2016, Tiwari and Douglas, 2012).

(a) Spatial Data Analysis: GIS facilitates the integration and analysis of diverse spatial datasets, such as topography, geology, hydrology, and land use. These datasets are critical in evaluating factors influencing slope stability, including slope geometry, material properties, and external loads (Bouajaj et al., 2016). Digital Elevation Models (DEMs) generated through GIS provide detailed information on slope angles, aspects, and curvature, which are essential for stability assessments. GIS combines spatial and non-spatial data, such as soil properties, seismic activity, and rainfall patterns, enabling a holistic analysis of slope stability. GIS tools allow for automated processes, such as calculating slope angles and generating input parameters for analytical or numerical models (Tiwari and Douglas, 2012). Applications include identification of steep slopes and potential failure zones based on DEM-derived parameters, creating continuous spatial datasets from point

measurements, such as soil strength or groundwater levels, using interpolation techniques, simulating the impact of changes in hydrological or geological conditions on slope stability. (Gokceoglu et al., 2000)used GIS to generate probabilistic slope failure risk maps, incorporating spatial variability in discontinuity parameters. Landslide susceptibility maps are validated using GIS-based models, demonstrating the effectiveness of spatial data integration (Remondo et al., 2003).

(b)Hazard Mapping: Hazard mapping is a core application of GIS in slope stability analysis, providing spatial representations of areas susceptible to landslides or slope failures. These maps are essential for disaster risk reduction and land-use planning, offering a basis for prioritizing mitigation measures and resource allocation (Aleotti and Chowdhury, 1999). Methodology include integration of geological, hydrological, and topographical datasets into a GIS platform assigning weights to contributing factors, such as slope gradient, soil type, and proximity to water bodies, based on their influence on slope stability, employing methods like heuristic approaches, statistical models, or machine learning algorithms to predict susceptibility levels. Applications include mapping landslide-prone areas for regional disaster management strategies, identifying safe zones for infrastructure development, such as roads and buildings, guiding evacuation routes and emergency response plans in high-risk areas. GIS-based hazard mapping is utilised to analyze seismicity-induced landslides in Kashmir Himalaya, incorporating factors such as slope geometry and seismic intensity(Ray et al., 2009). Rainfall-induced landslide hazard maps are induced in Peninsular Malaysia, integrating historical rainfall data and terrain characteristics (Hassan et al., 2018).
GIS-based hazard maps typically present spatial variations in susceptibility or risk levels, with high-risk areas highlighted for focused interventions. Advantages of GIS-Based Hazard Mapping facilitates large-scale analyses that are impractical with traditional methods, provides an intuitive visualization of risk, aiding stakeholders in decision-making, allows for continuous updates as new data becomes available. Comparison of various GIS applications is shown in Table 2.2.

Table 2.2: Comparison of GIS Applications

Application	Key Features	Benefits	Limitations
Spatial Data Analysis	Terrain analysis, data integration, scenario modeling	Efficient handling of large datasets	Dependent on data quality and availability
Hazard Mapping	Susceptibility and risk mapping	Supports disaster risk reduction and planning	Requires accurate weighting and validation

2.8.3 Machine Learning and Artificial Intelligence Applications

AI and ML have brought transformative changes to slope stability analysis by enabling predictive modeling and advanced data-driven approaches. These techniques address the limitations of traditional methods by leveraging large datasets to identify patterns, predict slope failures, and provide data-driven decision-making tools. The adoption of ML and AI in geotechnical engineering has grown rapidly, supported by their capability to handle complex, multi-dimensional datasets and nonlinear relationships (Nanehkaran et al., 2023, Asteris et al., 2022).

(a) Predictive Modeling: Predictive modeling employs ML algorithms to forecast slope stability outcomes by analyzing input parameters such as soil properties, slope geometry, and external loads, enabling the identification of high-risk areas and providing early warnings for potential failures (Nanehkaran et al., 2023). Common algorithms include Decision Trees and Random Forests, where decision trees classify or regress data based on feature importance, and Random Forests, as ensembles of trees, enhance accuracy and mitigate overfitting, as demonstrated in the classification of landslide-prone areas using terrain features and rainfall patterns (Asteris et al., 2022). SVM are particularly effective for binary classifications, such as distinguishing stable from unstable slopes, by identifying optimal hyperplanes separating data classes. ANNs mimicking the neural structure of the human brain, excel in modeling complex nonlinear relationships in slope stability problems (Kanungo et al., 2013). Gradient Boosting Algorithms, such as XGBoost further

enhance predictive accuracy by sequentially refining weak learners, making them ideal for ranking slope stability risks in large datasets. Applications of these algorithms include landslide susceptibility modeling, which identifies landslide-prone zones based on geological, hydrological, and environmental factors, and risk assessment, forecasting the likelihood and impact of slope failures on infrastructure projects. A case study highlighted the effectiveness of RF and ANNs in accurately predicting high-risk slopes, showcasing their utility in practical scenarios (Nanehkaran et al., 2023). These techniques efficiently handle large and complex datasets, reduce dependency on predefined failure criteria, and enable data-driven pattern discovery, though challenges such as the need for extensive training data and interpretability issues, particularly with deep learning models, remain.

(b) Data-Driven Approaches: Data-driven approaches leverage empirical relationships derived from historical datasets to predict slope behavior and assess stability, complementing predictive modeling by enabling real-time analysis and decision-making (Asteris et al., 2022, Jiang et al., 2020). These methods integrate big data analytics by combining large-scale datasets such as remote sensing, historical landslide records, and real-time monitoring data to enhance stability assessments. Feature engineering extracts and transforms key parameters like slope angle, curvature, and precipitation intensity from GIS and sensor data to improve model performance (Tiwari and Douglas, 2012). Real-time monitoring systems, comprising sensors like inclinometers, piezometers, and accelerometers, provide continuous data streams that machine learning algorithms analyze to detect anomalies and predict failures. Applications include early warning systems that automate alerts based on critical thresholds, such as displacement rates monitored by sensors, and remote sensing integration, where satellite-based datasets are combined with machine learning models for mapping landslide-prone areas and monitoring slope movements (Yin et al., 2009). The use of tree-based intelligent techniques are showcased for slope stability classification under seismic conditions, integrating real-time data to improve predictive accuracy (Asteris et al., 2022). These approaches reduce the need for labor-intensive field investigations, support dynamic decision-making in rapidly changing conditions, and is often integrated with GIS to enhance spatial and

numerical analyses. However, they rely heavily on data quality and availability, and their high computational demands can pose challenges in resource-constrained environments. This multi-disciplinary integration provides a holistic framework for slope stability analysis (Tiwari and Douglas, 2012). Comparison of GIS Applications Predictive and Data-Driven Approaches in Table 2.3.

Table 2.3: Comparison of GIS Applications Predictive and Data-Driven Approaches

Aspect	Predictive Modeling	Data-Driven Approaches
Focus	Prediction based on input features	Analysis based on historical and real-time data
Strengths	Accurate forecasts, handles nonlinearities	Real-time monitoring, empirical insights
Weaknesses	Requires training data, less interpretable	Relies on data availability and quality
Applications	Landslide susceptibility, risk assessment	Early warning systems, dynamic analysis

2.8.4 Remote sensing techniques

Remote sensing techniques are integral to slope stability analysis, offering large-scale, high-resolution, and non-invasive data for monitoring, mapping, and assessing terrain characteristics over extensive areas, particularly in inaccessible regions. Advances in satellite imagery and LiDAR technology have significantly improved the precision and applicability of these methods in geotechnical engineering (Ray et al., 2009, Hassan et al., 2018). Satellite imagery, including optical imagery and SAR, provides critical insights into landslide-prone areas and slope deformations. Optical imagery captures high-resolution surface details for terrain mapping and post-failure assessments, while SAR, with its all-weather and day-night capabilities, measures ground deformation through InSAR techniques (Hassan et al., 2018). Applications include landslide mapping, deformation monitoring through time-series SAR analysis, and hazard assessment via GIS integration. For instance, satellite imagery is utilised to analyse landslides triggered

by the 2005 Kashmir earthquake, highlighting its role in post-disaster assessments (Ray et al., 2009). LiDAR, a laser-based remote sensing technology, generates precise three-dimensional (3D) representations of terrain, penetrating vegetation to provide accurate ground surface data (Bar et al., 2020). Airborne LiDAR facilitates large-scale topographic mapping, while terrestrial LiDAR offers high-resolution data for localized studies like rock slope analyses. Applications include DEM generation, change detection through temporal LiDAR datasets, and rock fall analysis by mapping discontinuities and failure surfaces. Also demonstrated the efficiency of LiDAR in rapidly appraising hazardous zones in mining areas using 3D models. Despite their advantages, such as large-scale coverage and high accuracy, limitations include weather and vegetation interference in optical imagery and high costs and computational demands for LiDAR data. The integration of remote sensing with GIS, numerical modelling, and machine learning provides a comprehensive framework for slope stability analysis, enhancing prediction accuracy and decision-making (Hassan et al., 2018).

2.9 Mitigation and Remediation Strategies

Effective slope mitigation and remediation require a comprehensive framework that integrates engineering measures, real-time monitoring, and policy-based management to enhance infrastructure resilience, minimize landslide risks, and ensure sustainable land use (Mizal-Azzmi et al., 2011; Sarkar et al., 2018). Engineering strategies remain central to this approach, focusing on site-specific reinforcement, drainage, and surface protection techniques that respond to local geological and hydrological conditions. Among these, drainage control is one of the most effective stabilization methods, as excess water increases pore pressure and reduces soil strength (Urciuoli and Pirone, 2013). Properly designed surface systems—such as catch drains, lined channels, and diversion trenches—prevent infiltration, while subsurface systems like horizontal and French drains or geosynthetic drainage layers lower groundwater levels and improve stability (Rahardjo et al., 2003; Arbanas and Arbanas, 2015).

Reinforcement and retaining methods are essential in resisting lateral earth pressure and improving slope integrity. Soil nailing, involving the insertion of grouted steel bars, provides internal tensile resistance and has been successfully applied in road cut slopes and retaining structures (Mizal-Azzmi et al., 2011; Rawat and Gupta, 2016; Mangnejo et al., 2019). Similarly, retaining systems such as concrete, gabion, or mechanically stabilized earth (MSE) walls resist soil movement and, when equipped with drainage provisions like weep holes and filter layers, effectively prevent hydrostatic buildup (Huang and Chen, 2004; Bathurst and Jones, 2001; Ansari et al., 2020; Hong et al., 2023). Geosynthetics—including geotextiles, geogrids, and geocells—further enhance soil reinforcement and drainage, offering flexible and durable stabilization for both natural slopes and embankments (Kristo et al., 2019; Niroumand et al., 2012; Mehdipour et al., 2020).

Surface protection plays a complementary role by reducing erosion and infiltration. Vegetative cover is an eco-friendly solution that improves shear strength through root interlocking and reduces runoff velocity, while bioengineering techniques like hydroseeding, brush layering, and vegetated geogrids combine natural and mechanical benefits (Suhatril et al., 2019; Kumarasinghe, 2021; Auty et al., 2024; Greenwood et al., 2004; Kokutse et al., 2016). In areas subject to high runoff, stone pitching or riprap provides additional protection. Other effective measures include slope grading, which modifies slope geometry to lower driving forces (Jeldes et al., 2013; Schor and Gray, 1995; Fay et al., 2012), and buttressing, which enhances resistance by adding compacted fill or rock at the toe (Gray and Sotir, 1992; Samson et al., 2024; Markiewicz et al., 2024). For deeper or more critical failures, ground anchors transfer tensile loads into stable layers (Hryciw, 1991; Liu and Geo, 2015), while grouting strengthens weak soils and reduces permeability using cementitious or chemical injections (Daraei et al., 2018; Winterkorn and Pamukcu, 1991).

In addition to engineering solutions, continuous monitoring and policy support are crucial for sustainable slope management. Monitoring instruments—such as inclinometers, piezometers, extensometers, and rain gauges—track key parameters

like displacement, pore pressure, and rainfall intensity, facilitating timely interventions (Ray et al., 2009; Hassan et al., 2018). Technological advancements, including IoT-enabled sensor networks and remote sensing systems, now enable near-continuous observation, early warning, and informed decision-making for hazard mitigation (Bar et al., 2020). On the governance front, effective risk management requires establishing and enforcing technical standards, building codes, and retrofitting protocols to ensure structural safety. Regular updates to risk and vulnerability assessments are also vital to reflect evolving geotechnical and climatic conditions. Ultimately, slope mitigation aims to either reduce driving forces such as gravity, pore pressure, and seismic effects or enhance resisting forces through drainage, reinforcement, and soil improvement. A coordinated integration of engineering innovation, real-time monitoring, and institutional frameworks offers the most robust pathway toward reducing slope instability and protecting vulnerable communities.

2.10 Summary of literature review

The literature review highlights that landslides are among the most frequent and destructive natural hazards, particularly in the geodynamically active Himalayan region, where steep slopes, intense rainfall, and tectonic activity contribute to instability. Kalimpong, located in the Lesser Himalayas, is highly susceptible to slope failures due to its fragile lithology, heavy monsoonal rainfall, and human interventions like road construction and urban expansion. Various types of landslides—falls, slides, flows, and complex movements—occur based on material composition and movement mechanisms. The integration of Artificial Intelligence (AI), Machine Learning (ML), Geographic Information Systems (GIS), and remote sensing technologies has further improved prediction accuracy and risk assessment. Key influencing factors include geological structure, hydrology, seismic activity, and human disturbances. Mitigation strategies emphasize engineering solutions such as soil nailing, drainage control, and retaining structures, supported by continuous monitoring and policy frameworks. Overall, the review underscores the necessity of combining geotechnical, computational, and data-driven approaches for sustainable landslide risk management in mountainous terrains like Kalimpong.

CHAPTER 3
MATERIALS AND METHODOLOGY

3.1 General

Situated on the border with Nepal, Kalimpong is a tiny peninsula town in the Indian state of West Bengal. It is well-known for its pleasant temperatures and stunning natural surroundings and is located 1,250 meters above sea level. Kalimpong is renowned for its tea plantations, flowers, and stunning views of the Himalayas. It is encircled by verdant hills. The Relli River encircles it on the east, while the Teesta River borders it on the west. This region's average temperature ranges from 27°C to 5°C. Every year, the powerful monsoons in this area cause terrible floods that block off Kalimpong from the rest of the state. Kalimpong is prone to landslides, much as many other mountainous locations, due to its position and natural feature. Because of the steep slopes and loose soil, the area experiences heavy rainfall throughout the summer, which frequently causes landslides. It still poses a serious threat to Kalimpong and the other towns in spite of several efforts. To avoid and lessen its consequences in the area, local authorities and citizens must exercise vigilance and adopt the necessary measures (Das et al., 2022).

Kalimpong, a hill station in West Bengal, is highly prone to landslides due to a combination of natural and human-induced factors.

- The region's heavy monsoon rainfall, which ranges from 2000 to 2500 mm annually, saturates the soil, reduces its shear strength, and increases pore water pressure, leading to slope failures.
- Human activities such as rapid urbanization and deforestation further destabilize slopes by removing vegetation cover, altering natural drainage patterns, and increasing surface runoff.
- Additionally, Kalimpong's location in a seismically active zone means that earthquakes frequently trigger landslides by inducing ground movement and reducing slope material strength.
- Effective mitigation strategies, including proper land use planning, afforestation, and improved slope stabilization and drainage, are crucial for reducing landslide risks in Kalimpong.

3.2 Remote sensing and GIS in landslide studies

Remote sensing data, including high-resolution satellite imagery and SRTM elevation data, provide critical terrain information such as slope, aspect, and elevation. SoI toposheets is used for base mapping and georeferencing. The spatial data are processed and analyzed within a GIS environment, where thematic layers representing landslide causative factors—such as slope, aspect, elevation, rainfall, proximity to roads and faults—are created and overlaid. The Frequency Ratio model is applied to calculate the likelihood of landslide occurrence for each class of these factors, based on their correlation with past landslide events. These past events are mapped through the creation of a landslide inventory, derived from satellite imagery interpretation and historical data. All spatial datasets are standardized and georeferenced to ensure consistent analysis. The influencing factors are grouped into physical (e.g., geology, slope) and environmental (e.g., land use, rainfall) variables, each of which can significantly affect slope stability. The study ultimately identifies critical landslide-prone zones and contributes to the development of mitigation strategies and land-use planning (Powers et al., 1996).

3.3 Landslide susceptibility mapping by Frequency ratio method

LSM is a critical tool in landslide risk assessment and mitigation planning, enabling the identification of areas that are potentially prone to slope failure. It involves the systematic analysis of various conditioning factors—such as geological, topographical, hydrological, and anthropogenic influences—that contribute to landslide occurrence. While LSM does not predict the exact timing of a landslide, it provides a spatial representation of the probability of future events, which is essential for land-use planning, infrastructure development, and disaster preparedness. Given the growing socio-economic impacts of landslides and the mounting pressure from urbanization in fragile mountainous environments, LSM has become increasingly important. Over the past three decades, numerous attempts have been made across various parts of India to delineate landslide-prone areas. One early effort employed photogrammetry and 3D GIS systems to enhance hazard zonation (Ramakrishnan et al., 2003). More recently, advanced techniques have been

introduced, including integrated models using GIS, remote sensing, and neural networks, such as in the eastern portion of the North Anatolian Fault Zone (Demir et al., 2015). Further, alternative frameworks have been proposed to better assess landslide consequences, considering past limitations and impacts (Alimohammadlou et al., 2013).

LSM employs a range of methodologies broadly categorized into heuristic, statistical, machine learning, and deterministic approaches. Heuristic techniques, such as the AHP, depend on expert knowledge to assign weights to conditioning factors like slope, geology, and land use, and are useful when data are scarce. Statistical methods establish mathematical relationships between historical landslides and causative factors. Among these, the FR model is a widely used bivariate statistical method that estimates the correlation between landslide occurrences and specific classes of conditioning variables. It calculates the ratio between the probability of landslides occurring within a particular class and the overall probability across the study area. Each conditioning factor—such as lithology, slope, aspect, rainfall, and proximity to roads or faults—is represented as a thematic layer in a GIS environment. Frequency ratios derived from these layers help compute the LSI**,** which reflects the cumulative effect of all contributing factors. The FR method has proven effective in various regional studies and is recognized for its simplicity, interpretability, and compatibility with remote sensing and GIS platforms (Lee and Talib, 2005).

The FR model has been successfully applied in diverse terrains for landslide susceptibility assessment. For example, it has been used to map the spatial distribution of landslides in south-west Calabria, Italy (Goswami, 2012), in Penang district, Malaysia (Lee and Pradhan, 2007). The model can be further strengthened through the integration of SRTM data, which provides high-resolution DEMs. These DEMs allow for the extraction of essential topographic parameters such as slope, aspect, and elevation—critical inputs for the FR model. These factors are classified and spatially correlated with historical landslide inventories to assess their relative influence on slope instability. In the present study, the FR model was selected to map

landslide susceptibility in the Kalimpong region of the Darjeeling Himalayas, owing to its computational efficiency and robustness in data-limited settings. Key advantages of the FR model include ease of application, straightforward interpretation of results, and the ability to generate reliable maps even when input data are of moderate quality. Overall, the integration of FR with remote sensing and GIS techniques provides an effective framework for identifying high-risk zones and informing disaster risk reduction and sustainable development efforts. For this study, six primary factors were selected based on their proven relevance in landslide occurrences: elevation, slope, aspect, distance to roads, distance to faults or lineaments, and annual rainfall. The integration of these factors was carried out in a GIS environment, ensuring spatial accuracy and analytical rigor.

3.3.1 Data Acquisition and Preprocessing

Understanding the geomorphological characteristics of terrain is fundamental to landslide susceptibility mapping, where slope instability is largely influenced by topography. The SRTM data plays a pivotal role in this context by offering high-resolution elevation data essential for analyzing landform attributes. In this study, SRTM1 data with a spatial resolution of 30 meters was used to derive a DEM that facilitated the extraction of critical topographic parameters. The 30 m SRTM elevation data is more than good enough for the vast majority of engineering-grade, regional analyses. It's a globally accepted baseline used by NASA/USGS and countless peer-reviewed studies. These features are essential for assessing terrain morphology and hydrological patterns associated with slope failure. For instance**,** slope gradient directly affects gravitational forces acting on the terrain, while slope aspect influences microclimatic conditions such as sunlight, vegetation, and moisture retention—all contributing to slope stability.

Beyond topographic characterization, the study integrated various ancillary datasets using advanced GIS-based preprocessing techniques**.** Landslide inventory data, comprising 126 landslide events, was acquired from the Bhukosh portal of the Geological Survey of India (GSI) in shapefile format. These points were processed in a GIS environment and served as ground-truth references for model

training and validation. Additional layers included road and fault proximity derived from infrastructure and geological vector datasets, as roads often act as destabilizing agents due to excavation, and faults signify structural weaknesses. Long-term rainfall data was interpolated to generate spatial distribution maps, which were overlaid with terrain and geological layers to assess their compounded effect on slope instability. Lineament analysis was also conducted to delineate fracture zones that enhance infiltration and reduce cohesion within slopes. Various GIS operations, such as buffer analysis for proximity calculations and raster-based analysis for topographic layers, were employed to standardize and reclassify all variables. Each contributing factor was assigned a weight based on expert judgment and statistical validation, allowing their integration into a robust LSM. This comprehensive approach underscores the effectiveness of SRTM data and geospatial tools in delineating landslide-prone zones and guiding mitigation planning. Sources from where different data was procured is mentioned in Table 3.1. A detailed methodological flowchart of this process is depicted in Figure 3.1.

Table 3.1 Different landslide conditioning factors and their source

Factors	Data source
DEM, Slope, Aspect,	SRTM Open Topography
Distance to Road, Lineament	Bhukosh Portal
Rainfall	CRU database

To ensure the statistical validity of the susceptibility model, the inventory data was divided into two subsets:

1. Training Dataset (75%): Comprising 94 points, this dataset was used to develop and calibrate the model.
2. Testing Dataset (25%): Containing 32 points, this dataset was reserved for validating the predictive accuracy of the model.

Testing and training division of dataset points are shown in Fig 3.2.

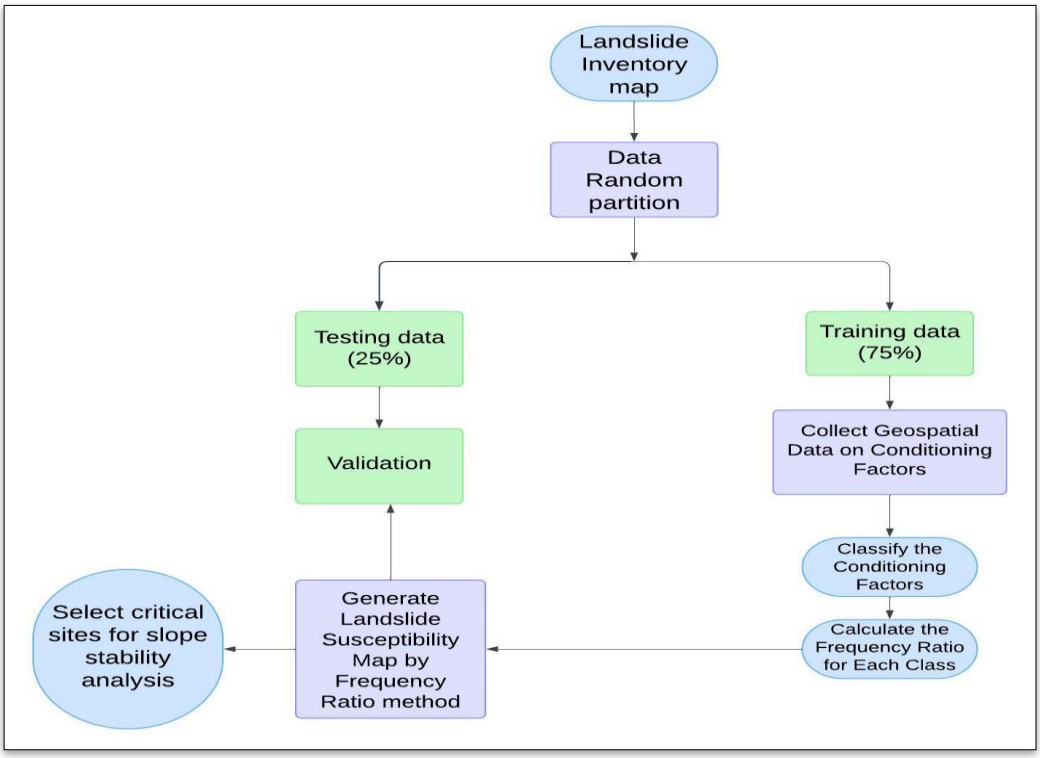

Fig 3.1 Flowchart for landslide susceptibility mapping

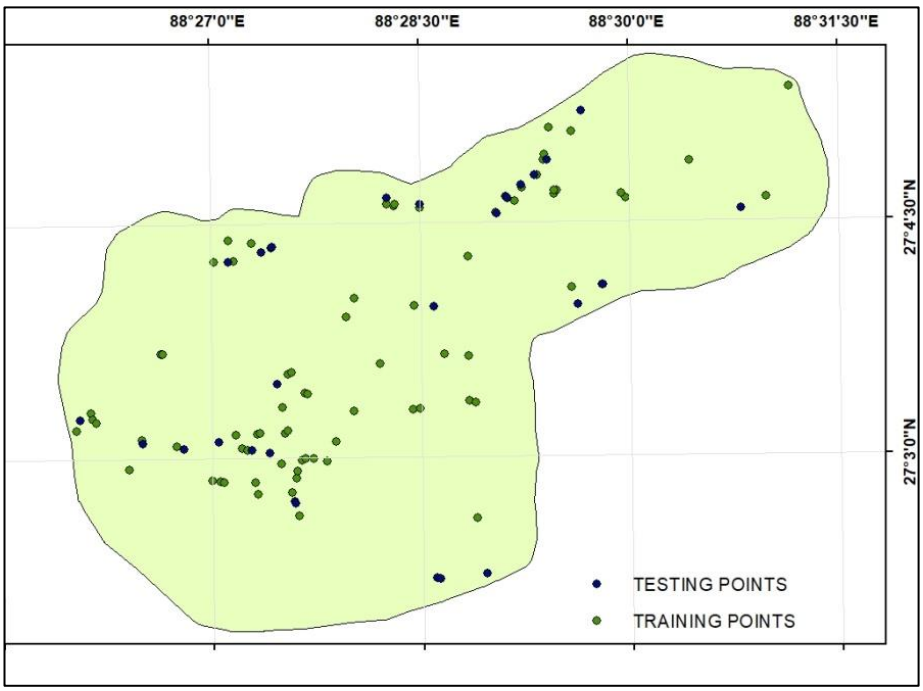

Fig 3.2 Map showing testing and training points in Kalimpong dataset

This division is critical in landslide susceptibility studies as it ensures the model is not overfitted to the training data, thereby maintaining its generalizability (Chung and Fabbri, 1999). The splitting process was performed using the Geostatistical Analyst tool in ArcGIS, ensuring a spatially consistent separation of data points. Each subset retained a representative distribution of the study area's landslide patterns.

3.3.2 Selection of Landslide-Conditioning Factors

Landslides are complex phenomena influenced by interplay of natural and human-induced factors. The selection of conditioning factors for this study was guided by their established significance in previous research and the availability of high-quality data. The six factors considered were processed using geospatial techniques, ensuring their compatibility with the analytical framework.

(a)Elevation: Elevation, derived from high-resolution DEMs, is a fundamental topographical variable. It influences slope stability, weathering processes, vegetation cover, and human activity patterns. For this research, elevation data was extracted and classified into five distinct categories ranging from 378.31 m to 1649.733 m shown in Fig 3.3. These classes were determined using natural breaks in the data distribution, a method that minimizes variance within each class while maximizing variance between classes. Elevation indirectly impacts landslide occurrences by influencing human habitation and infrastructure development. For instance, lower elevations are more likely to host settlements and roads, which can destabilize slopes, while higher elevations often have steeper gradients prone to natural failures. Studies such as those by Koukis et al. (1994) and Dai and Lee (2003) have highlighted the dual role of elevation in direct and indirect landslide susceptibility.

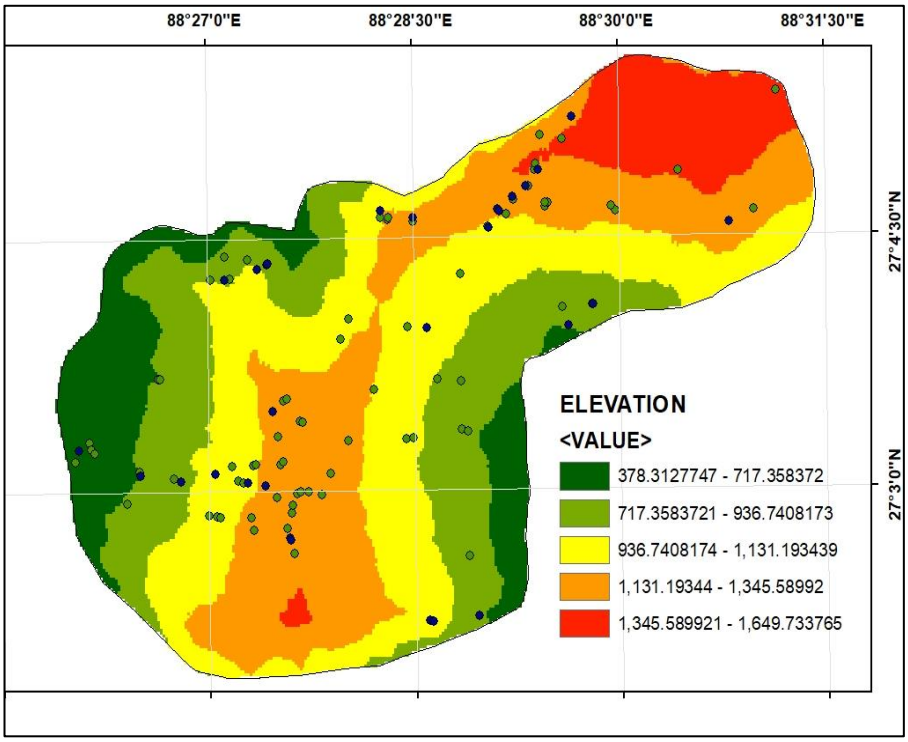

Fig 3.3 Thematic map for landslide causative factors: Elevation

(b) Slope: The slope angle is one of the most critical factors in landslide susceptibility, as it directly affects the gravitational force acting on soil and rock masses. Steeper slopes are inherently less stable, especially under conditions of intense rainfall or seismic activity. Using the Spatial Analyst tool in ArcGIS, the slope map was derived from the DEM shown in Fig 3.4 and categorized into five classes:

- 0°–13.88°
- 13.88°–20.36°
- 20.36°–27.77°
- 27.77°–36.87°
- 36.87°–61.53°

These classes capture the variability of slope angles across the study area, allowing for a detailed analysis of their influence on landslide occurrences. As noted by Nohani et al. (2019), higher slope angles typically correspond to a greater

likelihood of landslides, particularly in regions with loose or unconsolidated soils.

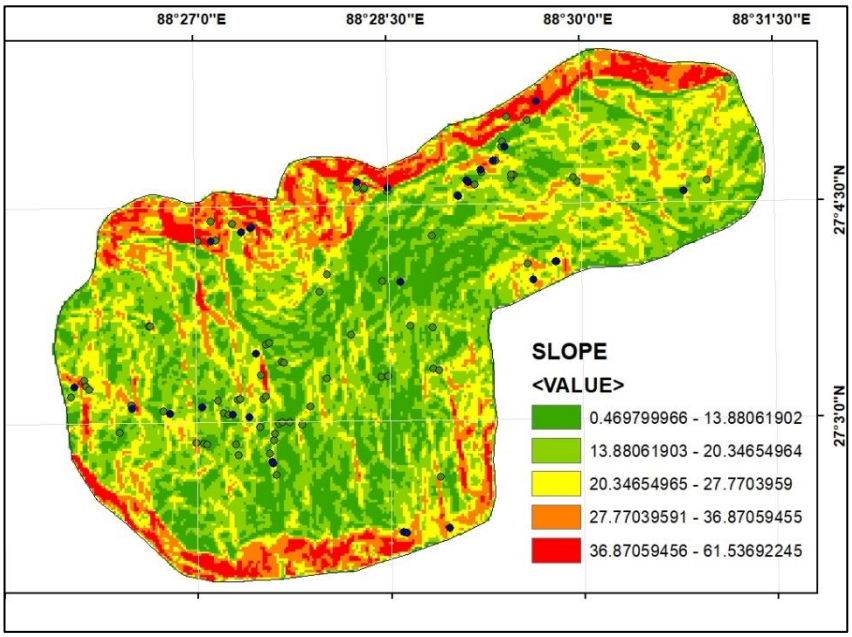

Fig 3.4 Thematic map for landslide causative factors: Slope

(c) Aspect: Aspect, or the orientation of slope faces, influences microclimatic conditions such as sunlight exposure, wind patterns, and precipitation distribution. These factors, in turn, affect soil moisture levels, vegetation cover, and erosion rates, all of which contribute to slope stability. The aspect map was generated using ArcGIS's Spatial Analyst tool, with orientations classified into 360° azimuth values as shown in Fig 3.5. The significance of aspect varies by region. In areas with predominant wind directions or uneven precipitation patterns, slopes facing these directions may experience greater instability. Similarly, slopes exposed to direct sunlight may undergo increased evaporation, reducing soil moisture and altering cohesion.

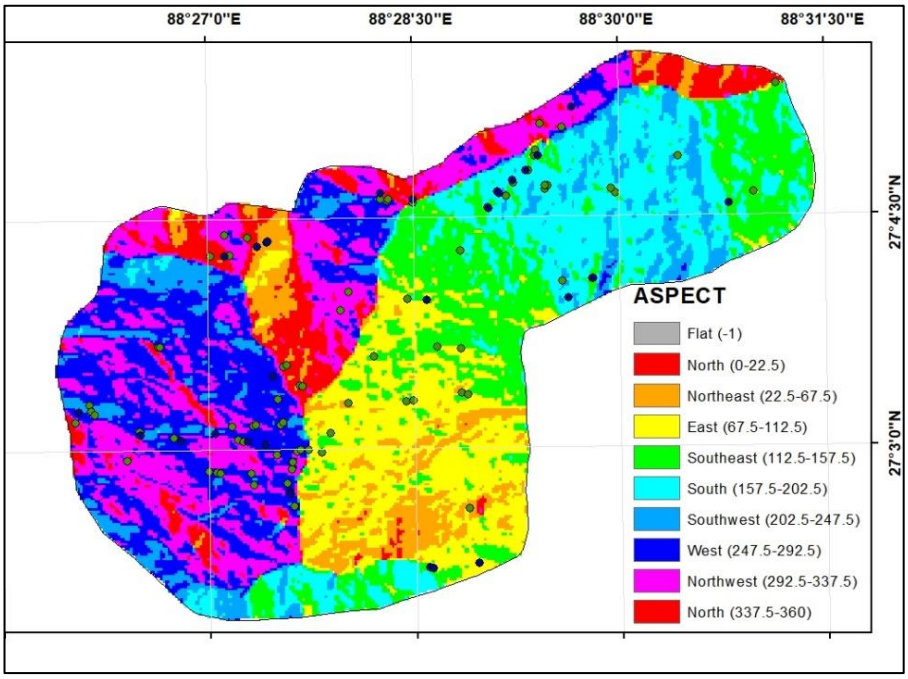

Fig 3.5 Thematic map for landslide causative factors: Aspect

(d) Distance to Roads: Road construction is a major anthropogenic factor contributing to landslide occurrences. Roads often involve cut-and-fill activities, drainage alterations, and vibrations from vehicular traffic, all of which destabilize natural slopes. For this study, road data was sourced from the Bhukosh portal and processed using the Euclidean Distance tool in ArcGIS to create a raster map with a 30-meter resolution. Distances were categorized into five classes, ranging from 0 to 2653.77 meters. Proximity to roads is a critical parameter in LSM as it reflects the extent of human intervention in natural terrains. Areas closer to roads are generally more susceptible to slope failures, particularly in hilly regions where road construction often involves extensive slope cutting. Map depicting distance to roads in Kalimpong for LSM is shown in Fig 3.6.

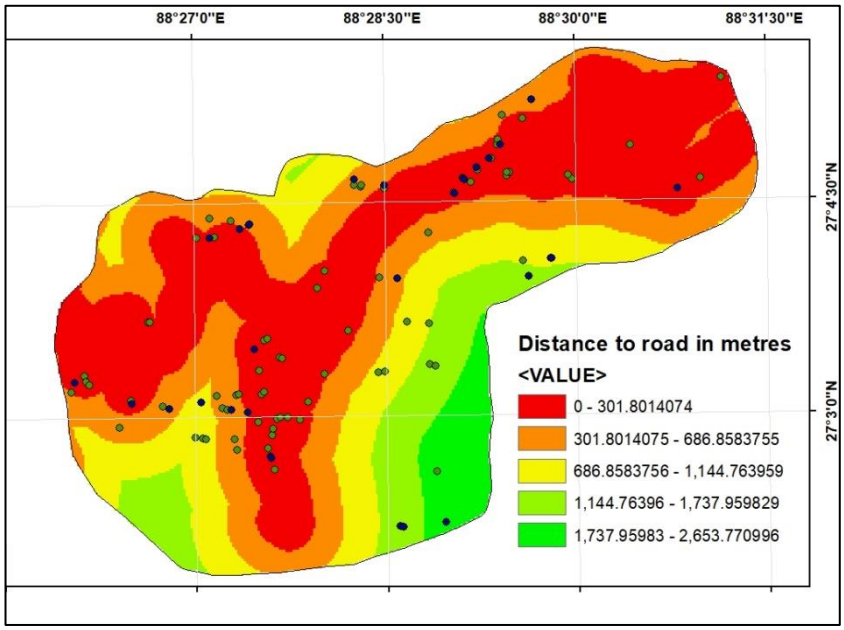

Fig 3.6 Thematic map for landslide causative factors: Distance to Roads

(e) Distance to Faults/Lineaments: Faults and lineaments are structural features that signify zones of weakness in the Earth's crust. These geological discontinuities make the surrounding areas more susceptible to landslides, especially under seismic activity. Vibrations generated during earthquakes can destabilize slopes by reducing shear strength and inducing soil or rock movement. Furthermore, faults often facilitate groundwater movement, which can lead to increased pore water pressure and reduced soil cohesion, further enhancing landslide potential. For this study, lineament data was sourced from the Bhukosh portal of the Geological Survey of India. The data was processed using the Euclidean Distance tool in ArcGIS to calculate distances from these geological features. The final raster output, with a 30-meter resolution, categorized the study area into five distance classes, ranging from 0 to 8414.77 meters. This classification was essential to identify how proximity to faults influences landslide occurrences. The results showed a higher concentration of landslides within close proximity to faults, consistent with findings in previous studies. This underscores the importance of incorporating geological factors into LSM to enhance predictive accuracy. Map depicting distance to lineamnents in Kalimpong for LSM is shown in Fig 3.7.

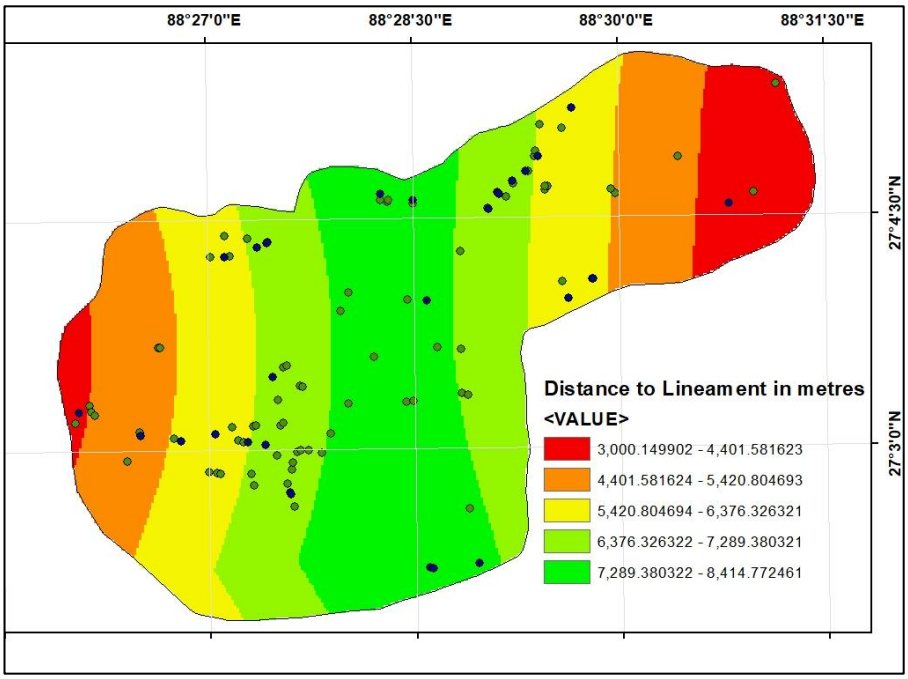

Fig 3.7 Thematic map for landslide causative factors: Distance to Faults/Lineaments

(f)Annual Rainfall: Rainfall is one of the most significant extrinsic factors influencing landslides, particularly in regions with tropical and subtropical climates. Precipitation directly impacts slope stability by saturating the soil, increasing pore water pressure, and reducing cohesion. Prolonged or intense rainfall can lead to slope failures, especially in areas with unconsolidated soils or steep gradients. For this research, annual rainfall data spanning the years 2011 to 2020 was acquired in NetCDF format from the CRU database. This dataset was processed using the IDW interpolation tool in ArcGIS, resulting in a high-resolution raster map. The map categorized annual rainfall values within the study area, ranging from 537.74 mm to 69612.55 mm as shown in Fig 3.8.

Rainfall-triggered landslides are common in the study area due to the region's susceptibility to intense monsoon rainfall. The integration of rainfall data into the LSM ensures that the model accounts for temporal and spatial variations in precipitation patterns. The inclusion of this factor aligns with the findings of

Rahardjo et al. (1995), who emphasized the critical role of rainfall in landslide initiation, especially in areas with residual soils and steep slopes.

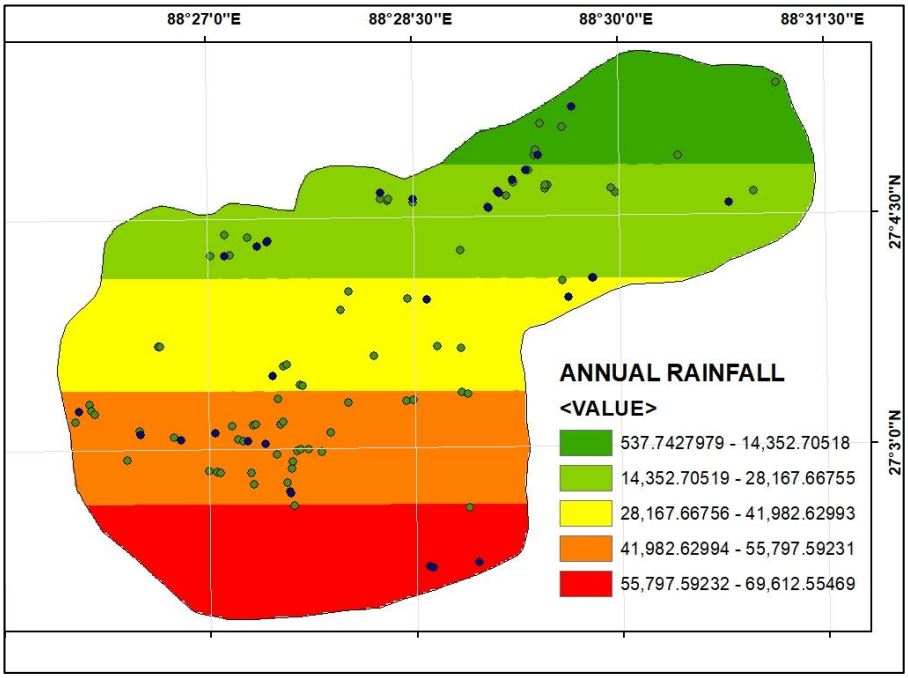

Fig 3.8 Thematic map for landslide causative factors: Annual Rainfall

3.3.3 Integration of Factors in Frequency Ratio (FR) Model

After processing and classifying the six conditioning factors, to create the landslip susceptibility map, they were incorporated into the FR model. By examining the ratio of landslide-prone to non-landslide-prone areas for each factor's class, the FR model determines the correlation between landslide occurrences and each conditioning factor. This statistical approach ensures that the relative contribution of each factor to landslide susceptibility is quantitatively assessed.

The FR technique is widely regarded as an effective method for identifying regions prone to landslide occurrences. Initially, FR values for each class within every influencing factor were calculated using Microsoft Excel. Following this, the RFV and PR for each factor were derived. The classes of individual factors were then reclassified by substituting their original values with the computed RF values. Subsequently, the Raster Calculator tool in ArcMap was employed to

multiply the PR values with the reclassified factor layers to produce a landslide susceptibility map for the study region. The FR and RF for each class of the causative factors were determined using Equations (3.1) and (3.2).

FR = (% Landslide Pixels÷ % Class Pixels)…….……...…. (3.1)

RFV = FR/Total sum of Frequency Ratios for that causative factor…… (3.2)

Then, prediction rate (PR) and LSM for all the six landslide causative factors can be calculated in Excel as mentioned in Eq. 3.3 and 3.4 respectively.

PR for a LCF = $\{RFV_{max} - RFV_{min}\} \div \{(RFV_{max} - RFV_{min})_{min}\}$ ……..…(3.3)

LSM=∑(PR for a LCF)∗(Corresponding LCF)……...……..….(3.4)

In this study, FR values were first computed for each class of every conditioning factor using Microsoft Excel and shown in Table 3.2 and 3.3 with corresponding prediction rate graph in Fig 3.9. The corresponding RF and PR values were then determined to assign appropriate weights. Using the raster calculator in ArcGIS, the weighted factor layers were integrated to produce the final landslide susceptibility map (LSM), which delineates areas with varying degrees of susceptibility based on the spatial relationship between landslide occurrences and conditioning factors.

Table 3.2 Calculation table for Frequency ratio model for all factors (FR and RF)

Factor	**Factor Classes**	**Landslide Pixels**	**% landslide pixels**	**Class Pixels**	**% class pixels**	**Frequency Ratio**	**Relative Frequency**
SLOPE	0.469799966-13.66061902	15300	22.37	8976	23.29	0.96	0.21
	13.88061903-20.34654964	23400	34.21	13371	34.70	0.99	0.21
	20.34654965-27.7703959	18900	27.63	8977	23.29	1.19	0.26
	27.77039591-36.87059455	9000	13.16	4731	12.28	1.07	0.23
	36.87059456-61.53692245	1800	2.63	2482	6.44	0.41	0.09

	TOTAL	68400	100.00	38537	100.00	4.61	1.00
ASPECT	-1	0	0.00	0	0.00	0.00	0.00
	0-22.5	2700	3.95	1240	3.22	1.23	0.14
	22.5-67.5	2700	3.95	2663	6.91	0.57	0.07
	67.5-112.5	9000	13.16	5720	14.84	0.89	0.10
	112.5-157.5	9900	14.47	5856	15.20	0.95	0.11
	157.5-202.5	7200	10.53	6199	16.09	0.65	0.07
	202.5-247.5	6300	9.21	3259	8.46	1.09	0.12
	247.5-292.5	12600	18.42	6124	15.89	1.16	0.13
	292.5-337.5	16200	23.68	5913	15.34	1.54	0.18
	337.5-360	1800	2.63	1563	4.06	0.65	0.07
	TOTAL	68400	100.00	38537	100.00	8.73	1.00
DISTANCE TO LINEAMENT	3000.149902-4401.581623	3600	5.26	3674	9.53	0.55	0.12
	4401.581624-5420.804693	7200	10.53	7056	18.31	0.57	0.12
	5420.804694-6376.326321	16200	23.68	8083	20.97	1.13	0.24
	6376.326322-7289.380321	27900	40.79	9675	25.11	1.62	0.35
	7289.380322-8414.772461	13500	19.74	10049	26.08	0.76	0.16
	TOTAL	68400	100.00	38537	100.00	4.64	1.00
DISTANCE TO ROAD	0-301.8014074	43200	63.16	15470	40.14	1.57	0.44
	301.8014075-686.8583755	15300	22.37	10521	27.30	0.82	0.23
	686.8583756-1144.763959	6300	9.21	6769	17.56	0.52	0.15
	1144.76396-1737.959829	2700	3.95	3912	10.15	0.39	0.11
	1737.95983-2653.770996	900	1.32	1865	4.84	0.27	0.08
	TOTAL	68400	100.00	38537	100.00	3.58	1.00
ELEVATION	378.3127747-717.358372	6300	9.21	5016	13.02	0.71	0.15
	717.3583721-936.7408173	9900	14.47	8688	22.54	0.64	0.14
	936.7408174-1131.193439	16200	23.68	11530	29.92	0.79	0.17
	1131.19344-1345.58992	32400	47.37	9961	25.85	1.83	0.40
	1345.589921-1649.733765	3600	5.26	3342	8.67	0.61	0.13
	TOTAL	68400	100.00	38537	100.00	4.58	1.00

RAINFALL	537.7427979-14352.70518	6300	9.21	5915	15.35	0.60	0.12
	14352.70519-28167.66755	18000	26.32	10000	25.95	1.01	0.21
	28167.66756-41982.62993	10800	15.79	7836	20.33	0.78	0.16
	41982.62994-55797.59231	31500	46.05	7690	19.95	2.31	0.48
	55797.59232-69612.55469	1800	2.63	6999	18.16	0.14	0.03
	TOTAL	68400	100	38440	99.748 29385	4.84346 5059	1

Table 3.3 Calculation table for Frequency ratio model for all factors (PR)

Feature	PR	Net PR
Aspect	1.05	105
Slope	1	100
Distance From Lineament	1.35	135
Elevation	1.59	159
Distance From Road	2.12	212
Annual Avg Rainfall	2.65	265

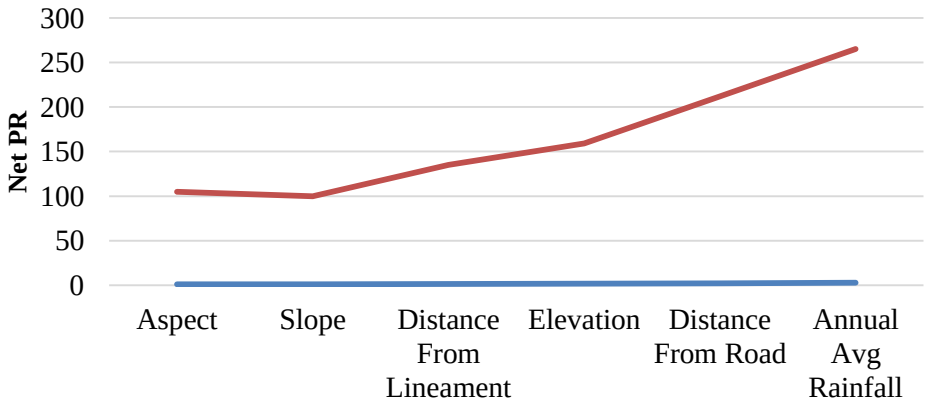

Fig 3.9 Prediction rate graph of various factors

The resulting LSI values were classified into susceptibility zones—high, moderate, and low—using natural breaks. This classification ensures that areas with similar susceptibility levels are grouped together, facilitating their identification and prioritization for mitigation efforts. The landslide susceptibility map shown in Fig

3.10 provides a spatial representation of areas categorized into high, moderate, and low susceptibility zones. This map serves as a crucial tool for various applications:

1. Disaster Risk Reduction: By identifying high-risk areas, the map enables targeted interventions, such as slope stabilization, afforestation, and drainage improvement.
2. Infrastructure Planning: The map informs the siting of roads, buildings, and other infrastructure to minimize exposure to landslide risks.
3. Land-Use Planning: Policymakers can use the map to enforce land-use regulations, restricting development in high-susceptibility zones.
4. Community Awareness: The map can be disseminated to local communities to raise awareness of landslide risks and promote preparedness.

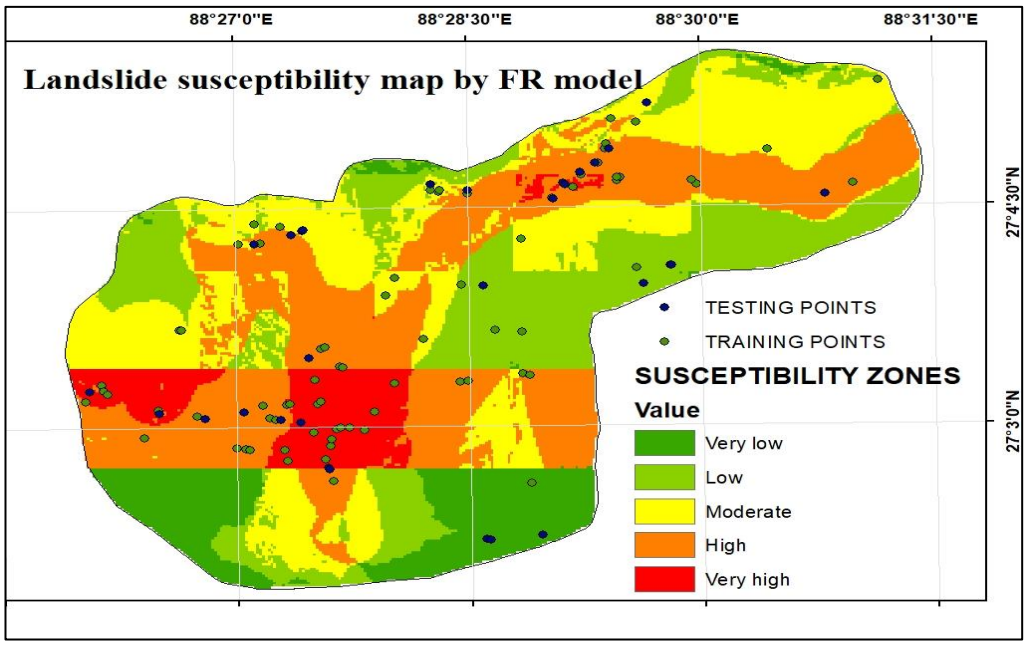

Fig 3.10 Landslide susceptibility map of Kalimpong by FR model

Following the landslide susceptibility mapping, three locations classified as very high susceptibility, and one location each from high, moderate, and low susceptibility areas, were selected for further study. These selections shown in Fig. 3.11 were based on actual site visits and information gathered from locals regarding recurring landslides. Post landslide images of critical locations with latitudes and longitudes have been shown in Fig 3.12.

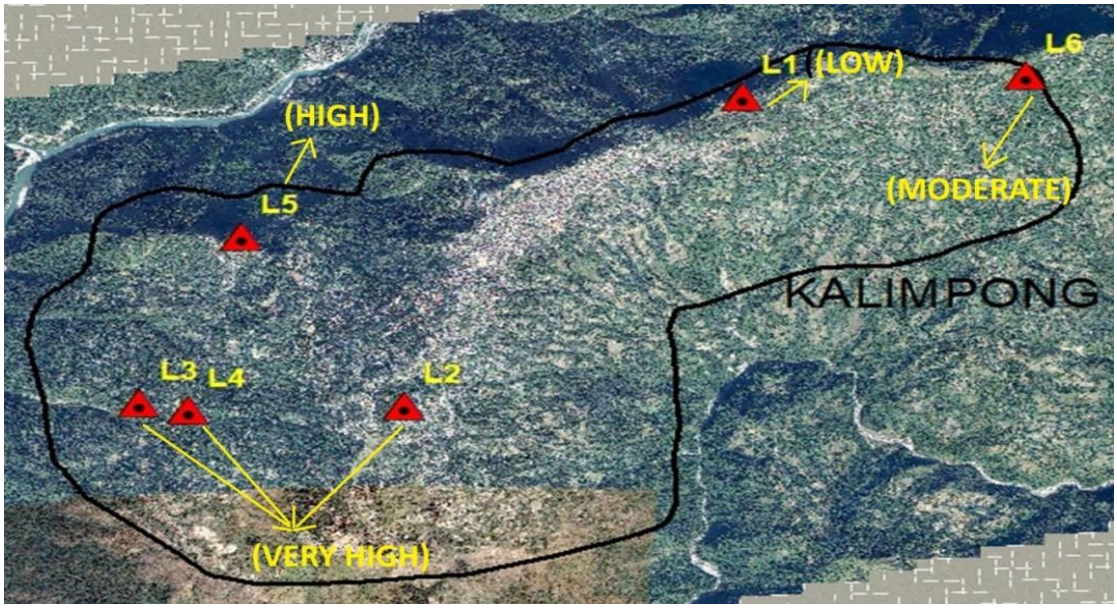

Fig.3.11 Critical locations selected in Kalimpong

Location 1 (27.08681,88.49431)

Location 2 (27.0518, 88.46469)

Location 3 (27.05211, 88.4415)

Location 4 (27.05141, 88.44572)

Location 5 (27.07102, 88.45036) Location 6 (27.089218, 88.519134)

Fig. 3.12 Post landslide images of critical locations with latitudes and longitudes

3.4 Geo-mechanical Properties of Soil Sample

The experiment was conducted for the mechanical analysis tests of samples taken from the soil slope in the field. The geomechanical characteristics of the slope-forming materials were investigated in the laboratory collected from the failure zones of the debris slope. Disturbed samples were collected to perform the following basic soil tests such as Grain Size Distribution (GSD) as per IS 2720 Part 4(1985), Proctor Compaction Test as per IS 2720 Part 8(1983), and Atterberg Limit tests as per IS 2720 Part 5 are essential for understanding soil behavior in slope stability analysis. The GSD test determines the proportion of different particle sizes in a soil sample, helping classify the soil and assess its permeability and shear strength characteristics. The Proctor Compaction test establishes the optimum moisture content and maximum dry density, which are vital for evaluating soil strength and stability under field conditions. The Atterberg Limit test identifies the liquid limit, plastic limit, and plasticity index, indicating the soil's consistency, compressibility, and potential for volume change.

3.4.1 Estimated through the triaxial test

The primary goal of triaxial testing is to look into strength properties for stability designs. The natural effective stress conditions can be replicated in the triaxial test to get important soil strength parameters. The strength characteristics and stress-strain behavior of cylindrical soil specimens—either “undisturbed” or “remolded”—are evaluated through CD triaxial tests. In this procedure, specimens are first isotropically consolidated and subsequently sheared under drained conditions at a controlled axial strain rate. CD tests are applicable to a wide range of soil types. During both the consolidation and shearing phases, drainage is permitted, allowing for pore water dissipation throughout the test. The specimen is initially consolidated under a specified confining pressure, and following full consolidation, shear strength is mobilized by gradually applying deviator stress at a slow, constant rate of strain while maintaining drainage. Due to the time-intensive nature of complete drainage at every stage, CD tests require significantly longer durations to complete compared to CU tests. For this reason, they are often referred to as "slow" tests and are typically reserved for detailed research applications. The experimental setup is illustrated in Fig. 3.13. Different confining pressures were applied to the same type of soil in four tests to calculate shear strength parameters. The test results are recorded using axial displacement, load cells, and pressure transducers. According to the relationship given by Kezdi (1980), the strain rates were checked within the recommended limit.

Furthermore, during consolidation and shearing, the volume of the specimen area may change due to compression shown in Fig 3.14 before and after shearing. As a result, the initial area was corrected to account for both the change in the cross-section area and the rubber membrane's restricting impact. The shear strength parameters (c and ϕ) were determined using the adjusted axial, and radial forces applied to the specimen from the modified Mohr circle failure envelope of the effective shear stress vs. normal stress relationship graph (Fig 3.15-3.20). Also final geotechnical parameters of all soil samples have been shown in Table 3.4.

Fig 3.13 Triaxial shear test apparatus

Before failure After failure

Fig 3.14 Soil specimen before and after failure

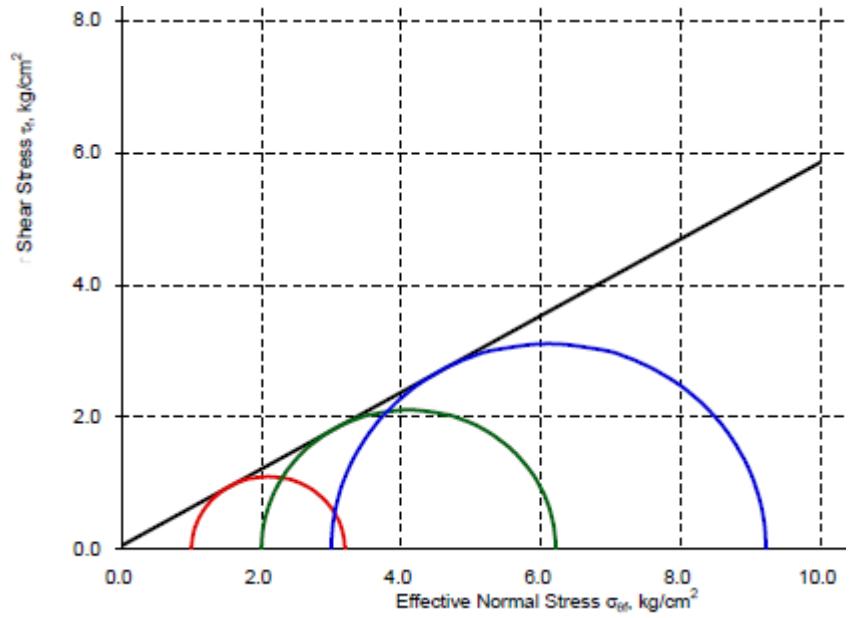

Fig 3.15 Mohr- Coulomb failure envelope for sample L1

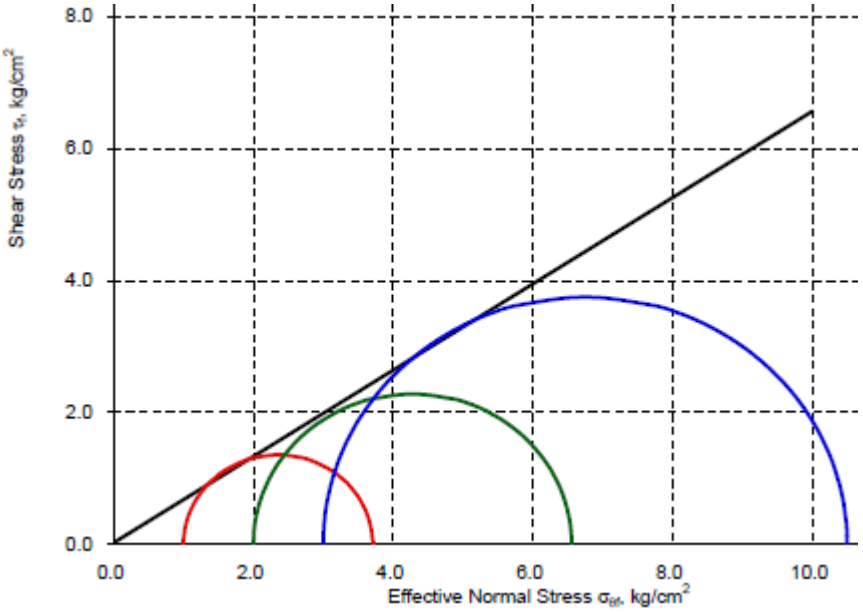

Fig 3.16 Mohr- Coulomb failure envelope for sample L2

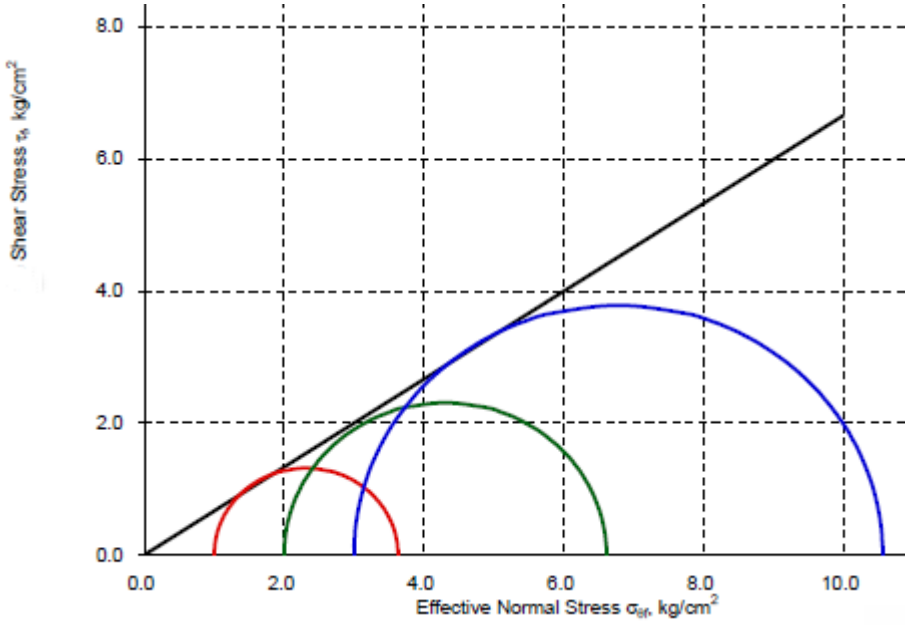

Fig 3.17 Mohr- Coulomb failure envelope for sample L3

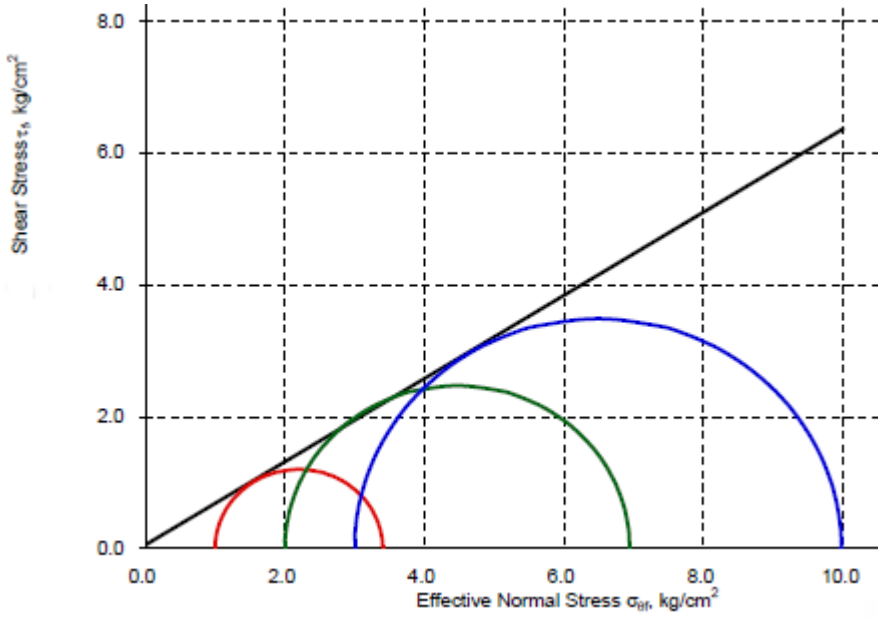

Fig 3.18 Mohr- Coulomb failure envelope for sample L4

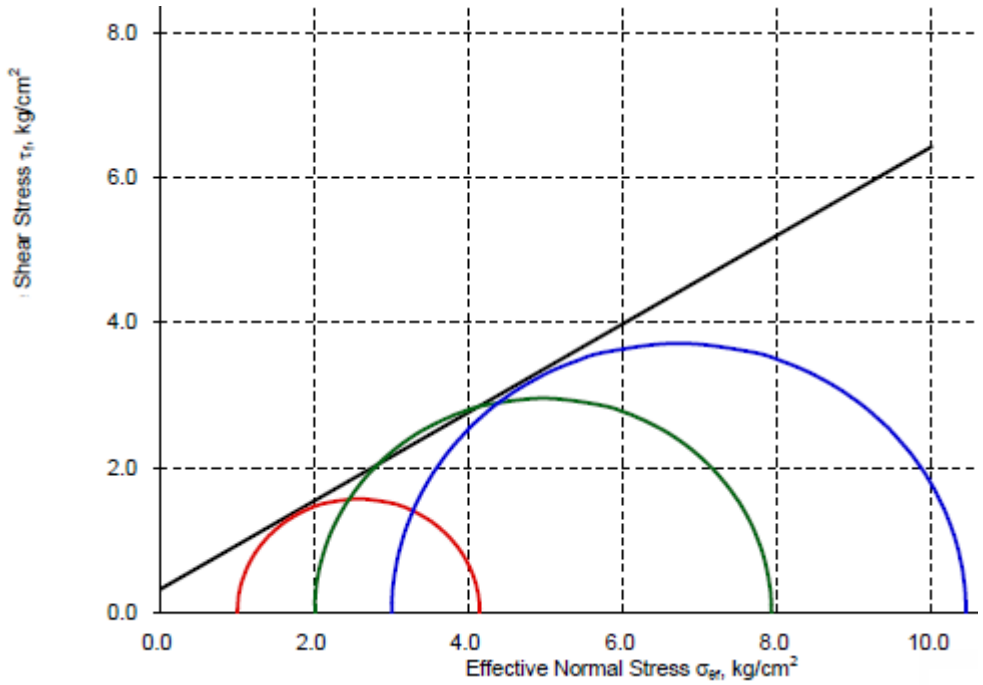

Fig 3.19 Mohr- Coulomb failure envelope for sample L5

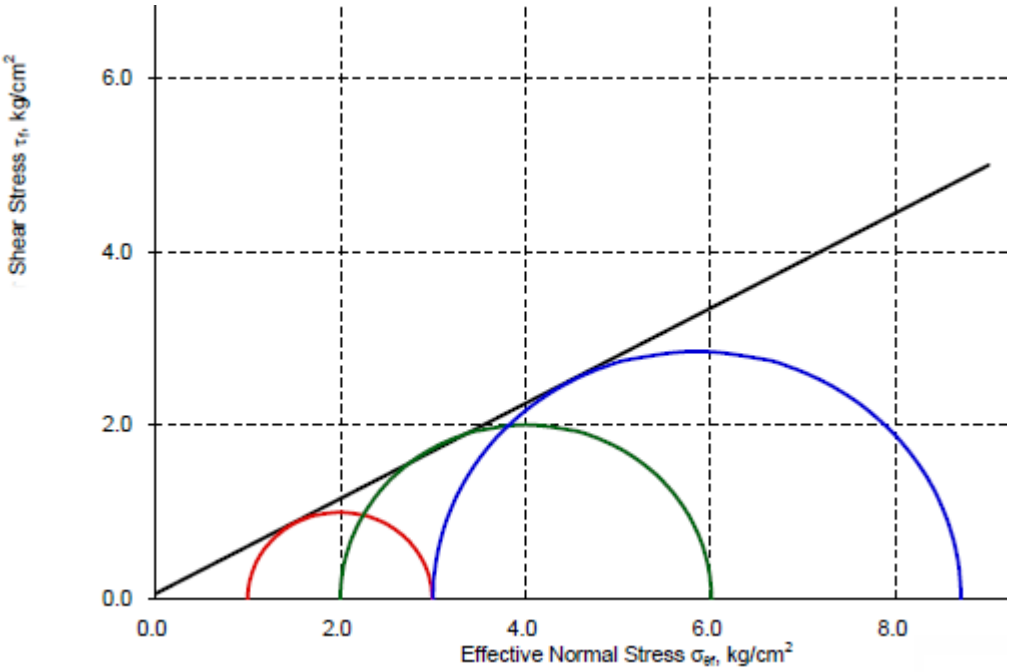

Fig 3.20 Mohr- Coulomb failure envelope for sample L6

Table 3.4 Geotechnical properties of soil samples

Site/State	% of sand	% of Silt	% of Clay	Liquid Limit (L.L)	Plastic Limit (P.L)	Plasticity Index (P.I.)	Soil Classification	Unit weight (kN/m^3)	Cohesion (kg/cm^2)	Internal Friction angle($^\circ$)
L1 Dry	73	11	16	22.9	11.3	11.6	Clayey sand	20	0.05	33
L1 Sat.	73	11	16	22.9	11.3	11.6	Clayey sand	21	0.05	33
L2 Dry	54	22	24	38.3	27.9	10.4	Clayey sand	18.5	0.02	33.2
L2 Sat.	54	22	24	38.3	27.9	10.4	Clayey sand	20	0.02	33.2
L3 Dry	70	26	4	23.7	N.P	-	Silty fine sand	15	0.01	33.6
L3 Sat.	70	26	4	23.7	N.P.	-	Silty fine sand	17	0.01	33.6
L4 Dry	85	15	0	24.9	N.P.	-	Silty fine sand	19.7	0.05	32.3
L4 Sat.	85	15	0	24.9	N.P.	-	Silty fine sand	21.8	0.05	32.3

L5 Dry	54	20	26	38.4	27.7	10.7	Clayey sand	19.9	0.32	31.5
L5 Sat.	54	20	26	38.4	27.7	10.7	Clayey sand	22	0.32	31.5
L6 Dry	73	10	17	24.2	N.P.	-	Silty fine sand	19	0.05	28.8
L6 Sat.	73	10	17	24.2	N.P.	-	Silty fine sand	20	0.05	28.8

3.5 Geostudio SLOPE/W Program- Slope stability analysis

SLOPE/W is an advanced geotechnical analysis software that applies the LEM to evaluate the stability of slopes. It is capable of simulating a wide variety of soil behaviors, accommodating complex stratigraphic profiles, diverse slip surface configurations, and spatially variable pore-water pressure distributions through the use of multiple constitutive soil models. These capabilities render SLOPE/W highly effective for comprehensive slope stability assessments, which justifies its selection for this study. The software supports multiple analytical approaches, including the Ordinary/Fellenius method, Bishop's Simplified method, Janbu's Simplified method, Spencer's method, Morgenstern-Price method, the GLE method, and finite element-based stress analyses. Among these, only the M-P and GLE methods account for both interslice normal and shear forces, thereby satisfying conditions of both force and moment equilibrium. In contrast, the remaining methods simplify the problem by neglecting interslice shear interactions. The M–P method is used in this work to measure the FOS for a range of critical cut slopes in Kalimpong with various soil parameters.

3.5.1 Approach for static conditions

In this study, the Limit Equilibrium Method (LEM) was selected over the Finite Element Method (FEM) due to its computational efficiency, lower data

dependency, and suitability for regional-scale slope assessments. While FEM allows detailed stress–strain simulations, it requires complex constitutive models and precise parameter calibration, which can introduce uncertainty in large-scale applications. LEM, on the other hand, effectively estimates the Factor of Safety (FOS) by analyzing the equilibrium of forces and moments along potential slip surfaces using readily available geotechnical parameters. The static slope stability assessment was carried out using GeoStudio's SLOPE/W software, which applies LEM to evaluate slope stability under defined conditions. Slope profiles were prepared using field survey data and Digital Elevation Models (DEMs) to accurately represent terrain geometry. The Morgenstern-Price method was adopted as it provides a rigorous framework by considering both force and moment equilibrium between slices, offering more reliable results than simplified methods such as Bishop's or Janbu's. Soil parameters including unit weight, cohesion, and angle of internal friction were assigned based on laboratory test outcomes and validated through literature values specific to the Kalimpong region. Analyses were performed under both dry and saturated conditions to capture the influence of pore-water pressure variations. The software iteratively identified the most critical slip surface and computed the corresponding FOS and stress distribution profiles, highlighting the zones of potential instability. Furthermore, the FOS values and model outputs were integrated with previously published datasets and subjected to machine learning techniques for coherence evaluation, statistical correlation, and predictive modeling. This integration allowed for the development of advanced data-driven models aimed at improving the accuracy and reliability of future slope stability assessments under similar geological and environmental conditions.

3.5.2 Approach for dynamic conditions

The analysis of slope stability under dynamic conditions was carried out using a pseudo-static approach within GeoStudio's SLOPE/W framework to simulate the influence of seismic loading on slope performance. This method was preferred for its simplicity and effectiveness in incorporating earthquake-induced forces into conventional static analysis, making it suitable for preliminary and regional-scale stability evaluations. In this approach, dynamic effects were represented by

equivalent static forces characterized through horizontal and vertical seismic coefficients, which were determined in accordance with the provisions of IS 1893 (Part 1): 2016 for seismic design considerations. These coefficients were assigned based on the seismic zoning of the Kalimpong region, which falls under Zone IV of the Indian seismic map, ensuring that the seismic loading conditions reflected realistic ground motion intensities. The slope geometry and material properties used in the static analysis were retained, while the additional inertial forces were introduced to simulate earthquake acceleration acting on the potential sliding mass. The Morgenstern-Price method was again employed to achieve comprehensive force and moment equilibrium between slices, allowing for accurate estimation of the Factor of Safety (FOS) under pseudo-static conditions. Analyses were performed for both dry and saturated states to account for the combined influence of seismic excitation and pore-water pressure on slope stability. The results provided insight into how seismic loading alters the location of the critical slip surface and reduces the FOS compared to static conditions. Subsequently, the dynamic FOS values and related parameters were incorporated into the machine learning framework alongside static results and existing datasets to perform statistical analyses, pattern recognition, and predictive modeling. This integration enabled the development of a robust data-driven system capable of forecasting slope performance under future seismic events with improved precision.

3.6 Stabilization Technique adopted- Soil Nailing

Soil nailing is a superior technique for slope stabilization compared to geogrids and retaining walls due to its specific advantages and applications. Geogrids are generally used for land leveling and ground improvement, providing reinforcement for the soil but primarily functioning in flatter terrains or gentle slopes. They are less effective in stabilizing steep or highly unstable slopes where higher shear strength is required. Retaining walls, on the other hand, often face issues such as soil settlement behind the wall, which can lead to wall failure over time. The rigid nature of retaining walls can make them susceptible to such failures, especially in areas with significant soil movement or water infiltration. Soil nailing, by contrast,

involves inserting steel bars into the slope, which increases the shear strength and provides immediate and continuous support(Mangnejo et al., 2019). This method is particularly effective for steep and complex slopes where conventional retaining methods might fail. It allows for incremental stabilization, meaning nails can be installed progressively as excavation or construction advances, ensuring ongoing support and minimizing the risk of collapse.

In addition to its comparative advantages, soil nailing is widely regarded as one of the most effective and reliable methods for stabilizing soil slopes due to its versatility, deep reinforcement capability, and minimal disturbance to the existing terrain. Unlike surface-based treatments such as vegetative cover or terracing, soil nailing provides internal stabilization by reinforcing the soil mass with closely spaced steel bars that are drilled and grouted into the slope. This technique significantly improves the shear strength of the slope and enhances its resistance to both shallow and deep-seated failures. One of the primary advantages of soil nailing is that it preserves the existing slope geometry, making it highly suitable for space-constrained areas such as urban developments, road cuts, and steep embankments where extensive excavation or slope flattening is impractical. Moreover, it is cost-effective and allows for relatively fast installation, without the need for large retaining structures or heavy fill. Construction can proceed in a top-down manner, enabling immediate support to excavated sections and enhancing safety throughout the process. Soil nailing also performs well under both static and dynamic loading conditions, making it highly suitable for landslide-prone and seismically active areas. Its compatibility with other stabilization methods, such as shotcrete, geosynthetics, and drainage systems, further strengthens its applicability. With a strong track record in critical infrastructure projects and the ability to customize designs for varying site conditions, soil nailing stands out as the most dependable and flexible method for ensuring long-term slope stability.

CHAPTER 4
RESULTS AND DISCUSSIONS

4.1 SLOPE/W Results for static loading

With the use of Slope/W software and the M–P method (Morgenstern and Price 1965), the current study calculates the FOS for a range of critical cut slopes in Kalimpong with different soil characteristics. This is verified by a field survey. This section gives details about the results related to slope failures, factor of safety at different locations including mathematical modelling.

4.1.1 Location 1 in Mahakal Dara Bhalukhop (static)

Mahakal Dara in Bhalukhop, Kalimpong, is a geologically active region characterized by steep slopes and a fragile geomorphic setup, making it highly susceptible to landslides. The area experiences significant seasonal rainfall, contributing to high pore water pressures in the soil strata. In this study, the slope stability analysis was conducted using the soil parameters specific to the site, where c and ϕ were determined from site-specific geotechnical investigations. For saturated conditions, a water table was modeled at a depth of 5 meters from the ground surface as per "Report on the Dynamic Ground Water Resources of West Bengal as on 31-03-2022" to simulate the effects of infiltration and increased pore pressure during monsoons. Conversely, for dry conditions, the water table was considered absent to evaluate slope stability under normal circumstances. The presence of high pore pressures during saturated conditions reduces the effective stress and shear strength of the soil, significantly increasing the likelihood of slope failure. Combined with Kalimpong's seismic vulnerability and its history of rainfall-induced landslides, the region around Mahakal Dara remains at high risk for landslide occurrences, necessitating detailed risk mitigation and stabilization measures. Fig. 4.1 and 4.2 shows the SLOPE/W results for the location L1 under dry and saturated situations, respectively.

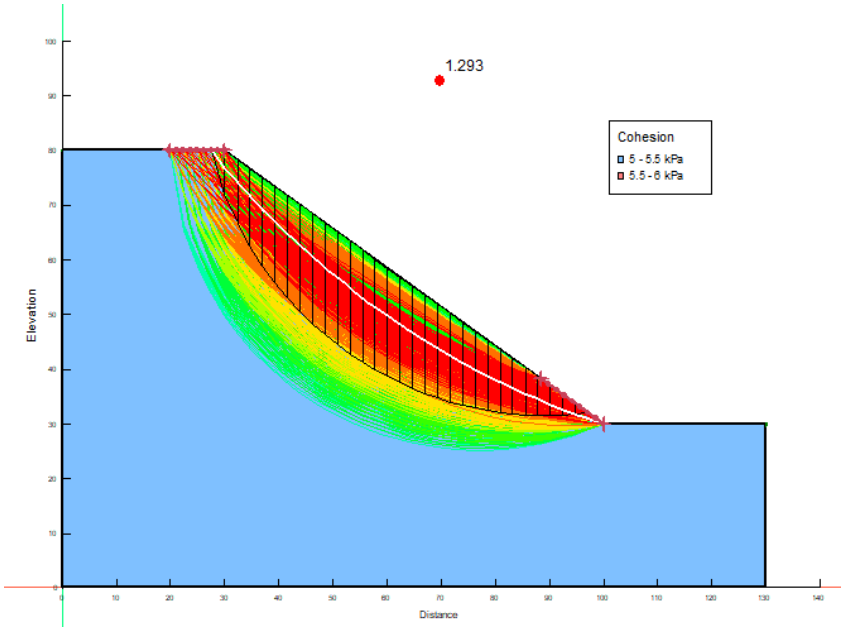

Fig 4.1 SLOPE/W results for L1 in dry condition under static loading

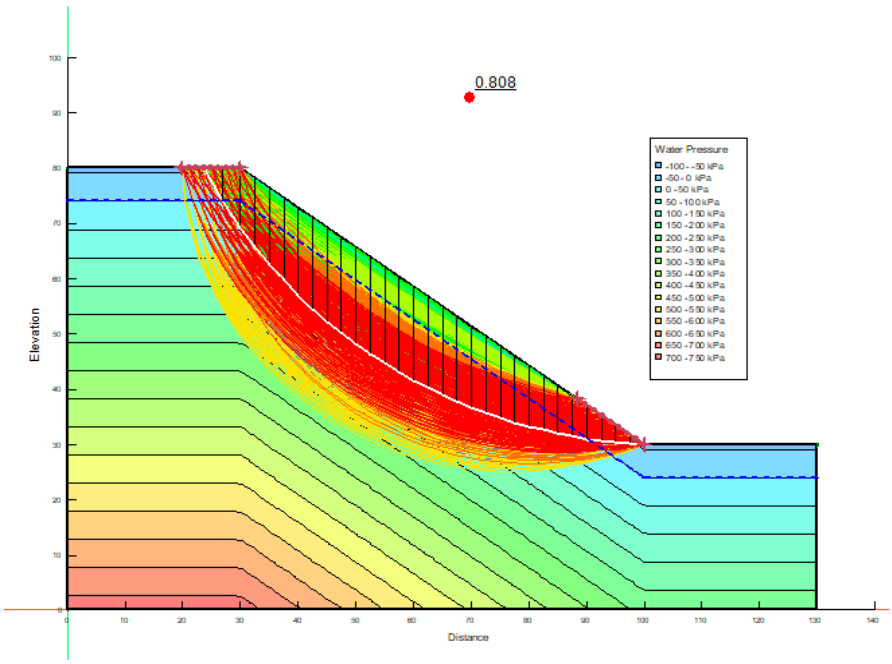

Fig 4.2 SLOPE/W results for L1 in saturated condition under static loading

4.1.2 Location 2 in Chandraloke (static)

Chandraloke in Kalimpong is a region of hilly terrain with steep slopes

and a history of instability due to its geological and hydrological characteristics. This site, like much of Kalimpong, is highly vulnerable to landslides, exacerbated by heavy rainfall during monsoons and the area's seismic activity. For the slope stability analysis of this location, the soil parameters, including cohesion (c) and internal friction angle (ϕ), were obtained from detailed geotechnical studies. The water table was modeled at a depth of 5 meters below the surface to simulate the saturated conditions that typically occur during peak rainfall periods, while no water table was considered for dry conditions to represent stable weather periods. Under saturated conditions, elevated pore water pressures significantly reduce the effective stress and shear strength of the soil, increasing the potential for slope failure. The combination of steep slopes, variable water levels, and the region's propensity for heavy rainfall makes Chandraloke particularly susceptible to rainfall-triggered landslides, emphasizing the need for effective slope stabilization techniques and proactive risk management. Fig. 4.3 and 4.4 shows the SLOPE/W results for the location L2 under dry and saturated situations, respectively.

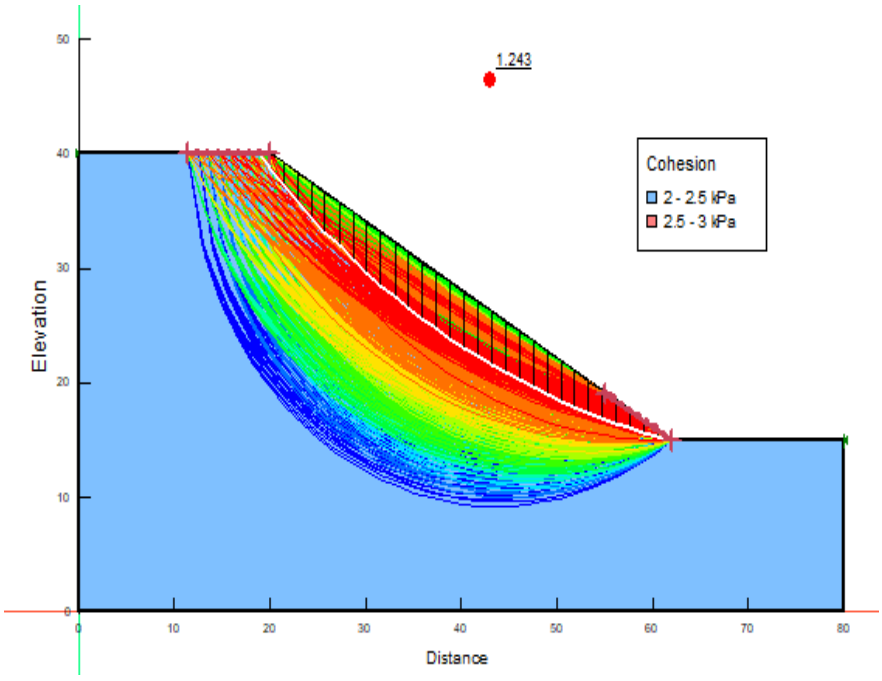

Fig 4.3 SLOPE/W results for L2 in dry condition under static loading

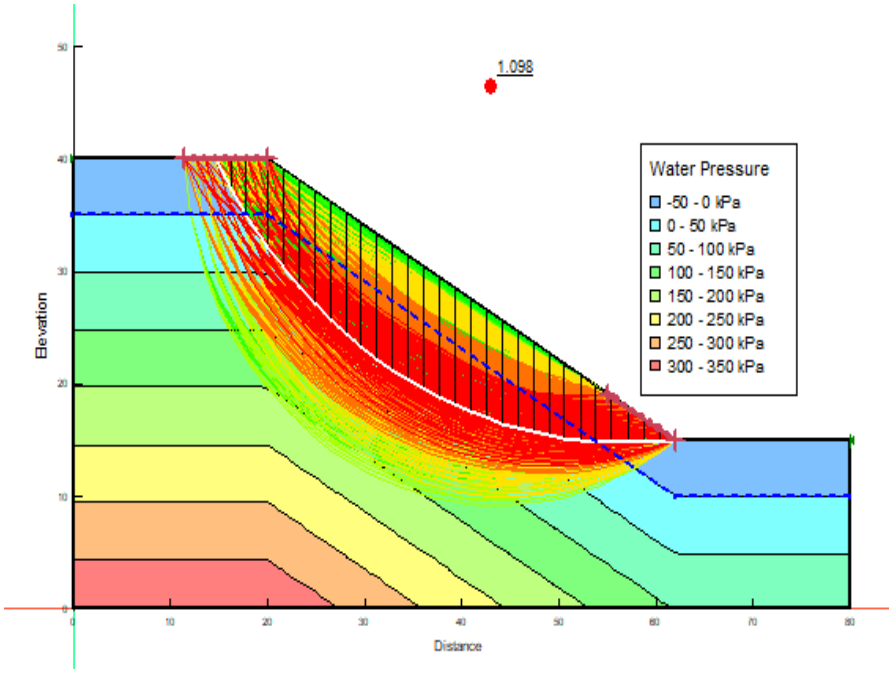

Fig 4.4 SLOPE/W results for L2 in saturated condition under static loading

4.1.3 Location 3 in Upper Tashiding (static)

Upper Tashiding in Kalimpong is a region with a complex terrain marked by steep gradients and loosely consolidated soil, making it highly vulnerable to slope instability. The area is characterized by frequent heavy rainfall during the monsoon, leading to significant changes in groundwater levels and an increase in pore water pressure. For the slope stability analysis at this site, geotechnical parameters, including the c and ϕ, were evaluated to assess soil strength under varying conditions. A water table was considered at a depth of 5 meters from the surface to account for saturated conditions, reflecting the effects of prolonged rainfall, while dry conditions were modelled without any water table to simulate non-monsoon scenarios. The increase in pore water pressure under saturated conditions drastically reduces the soil's shear strength, making the slopes more prone to failure. Given the area's geological sensitivity and the dynamic hydrological influences, Upper Tashiding is highly susceptible to landslide events, particularly during intense rainfall, necessitating targeted mitigation measures and continuous monitoring to ensure slope stability. Fig. 4.5 and 4.6 shows the SLOPE/W results for the location

L3 under dry and saturated situations, respectively.

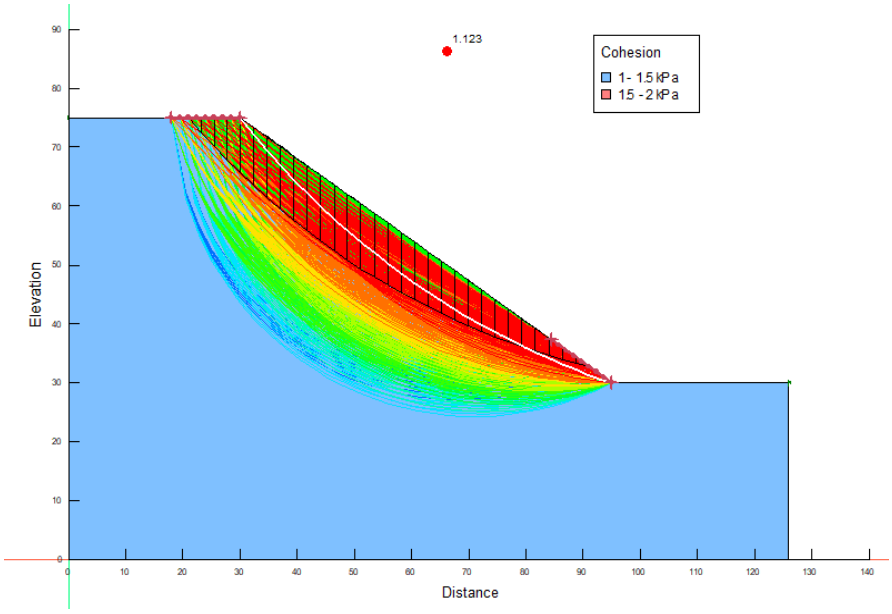

Fig 4.5 SLOPE/W results for L3 in dry condition under static loading

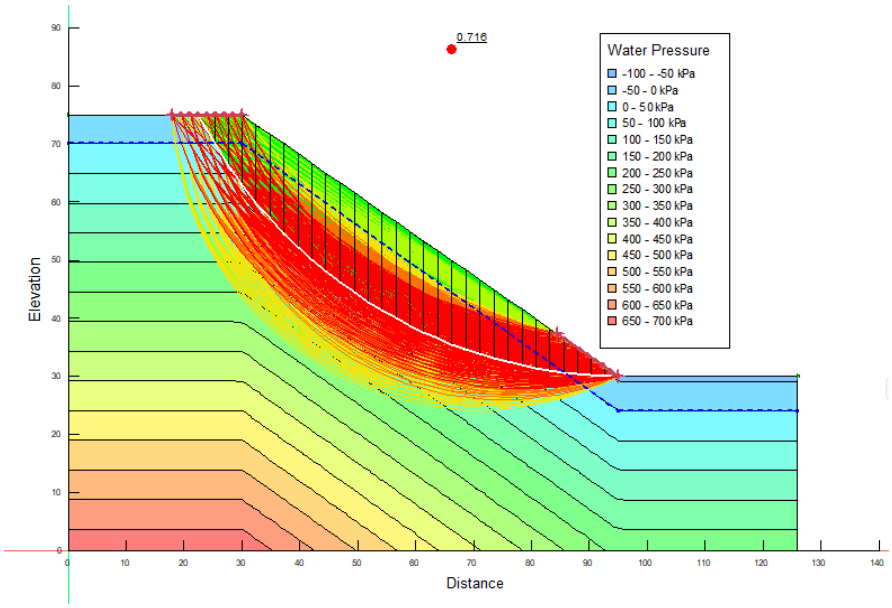

Fig 4.6 SLOPE/W results for L3 in saturated condition under static loading

4.1.4 Location 4 in Upper Tashiding (static)

Ngassey Busty, located in the hilly terrain of Kalimpong, is a region with slopes that are highly sensitive to environmental and geotechnical factors, making it prone to landslides. The area experiences significant monsoonal rainfall, which plays

a critical role in destabilizing the slopes. The slope stability analysis for this site incorporated detailed soil parameters, including c and ϕ, derived from geotechnical investigations. For scenarios simulating saturated conditions, a water table was placed 5 meters below the surface, representing the typical impact of prolonged rainfall and infiltration. Under dry conditions, no water table was considered to reflect normal circumstances. Saturated conditions substantially weaken the soil structure by increasing pore water pressures, reducing shear strength, and elevating the risk of slope failure. Coupled with the steep topography and high precipitation levels, the site exhibits a heightened susceptibility to rainfall-induced landslides, underlining the necessity for robust monitoring systems and slope reinforcement strategies to mitigate risks effectively. Fig. 4.7 and 4.8 shows the SLOPE/W results for the location L4 under dry and saturated situations, respectively.

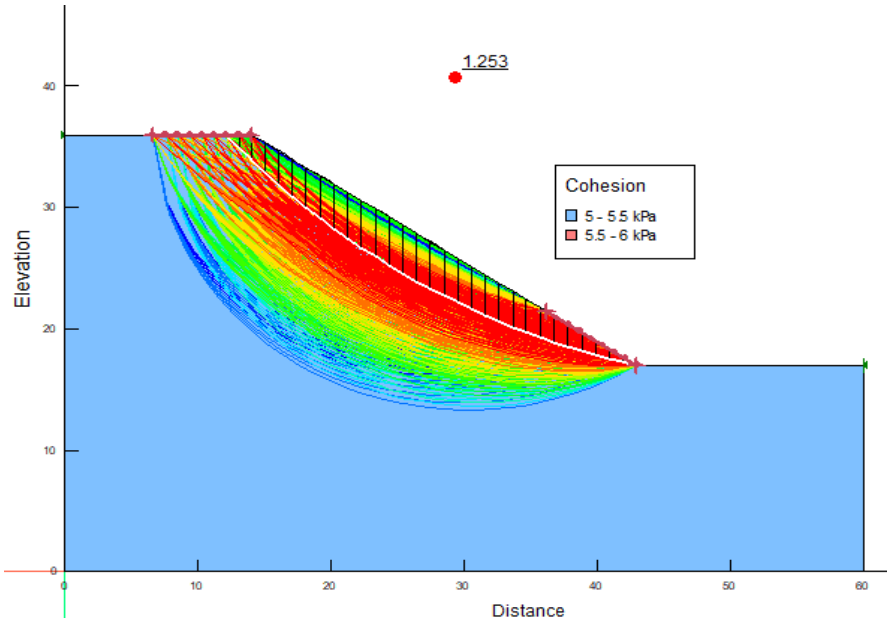

Fig 4.7 SLOPE/W results for L4 in dry condition under static loading

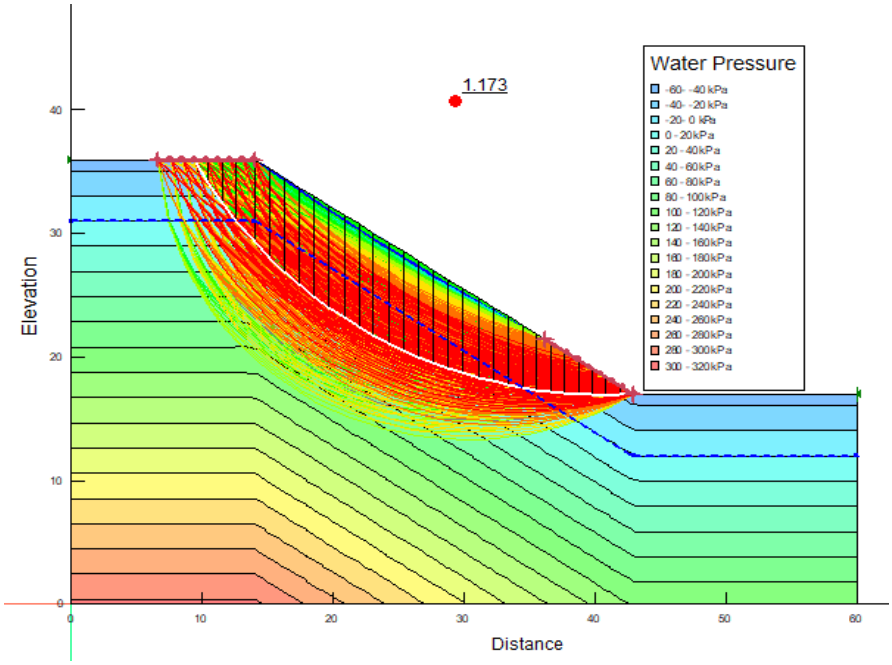

Fig 4.8 SLOPE/W results for L4 in saturated condition under static loading

4.1.5 Location 5 in Mongbol Road (static)

Mongbol Road in Kalimpong presents a challenging terrain where slope stability is a critical concern due to the interplay of steep gradients, soil characteristics, and climatic conditions. This area experiences frequent and intense rainfall during the monsoon, a key factor influencing slope failure. For this study, soil parameters such as c and ϕ were utilized to assess stability under varying hydrological scenarios. Saturated conditions were modeled with the water table positioned at 5 meters below the surface to reflect typical monsoonal impacts, whereas dry conditions excluded the presence of a water table to represent normal weather. Saturation during heavy rainfall significantly elevates pore water pressure, undermining the effective stress and thereby reducing the soil's ability to resist shear forces. Given the dynamic hydrological environment and steep topography, Mongbol Road is highly susceptible to landslides, especially during periods of intense rainfall. Proactive slope stabilization measures and consistent geotechnical monitoring are essential to mitigate these risks and ensure the safety of this area. Fig. 4.9 and 4.10 shows the SLOPE/W results for the location L5 under dry and saturated situations, respectively.

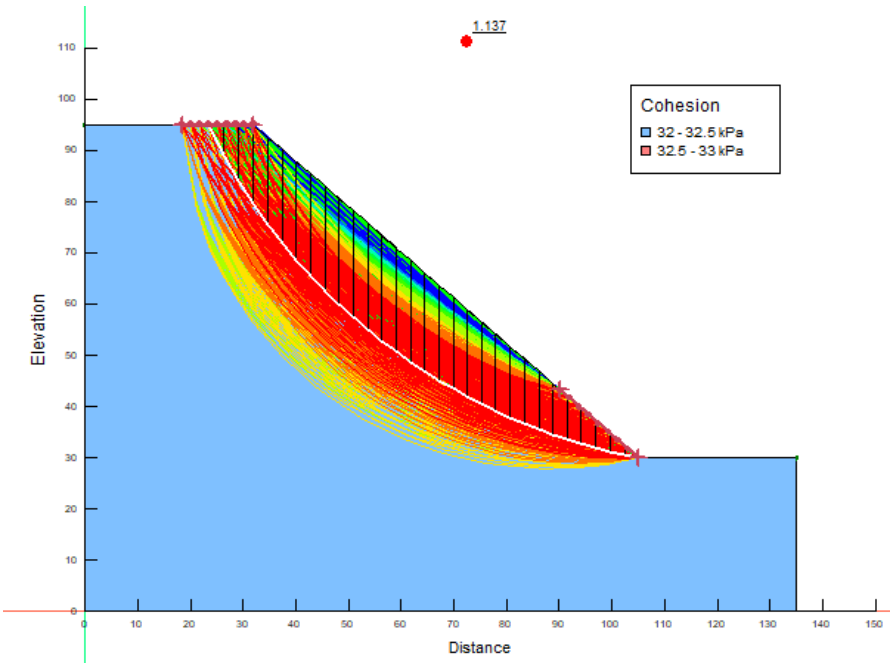

Fig 4.9 SLOPE/W results for L5 in dry condition under static loading

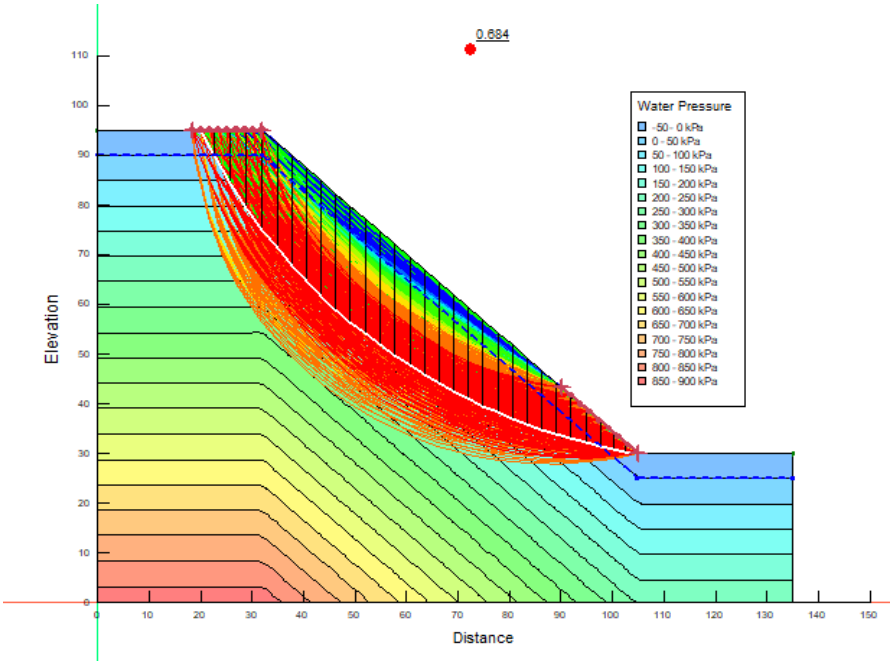

Fig 4.10 SLOPE/W results for L5 in saturated conditions under static loading

4.1.6 Location 3 in Deolo (static)

Deolo, a prominent location in Kalimpong known for its elevated terrain and scenic landscapes, faces significant challenges related to slope stability. The site

is characterized by steep slopes and a combination of loose and weathered soils, which are particularly susceptible to external triggers such as heavy rainfall. To analyze slope stability, key geotechnical parameters, including c and ϕ were considered. For saturated conditions, a water table was modeled at a depth of 5 meters below the surface to simulate the effects of water infiltration during monsoon rains. In dry conditions, the absence of a water table was assumed to evaluate stability under normal circumstances. The saturated condition increases pore water pressures, reducing effective stress and weakening the soil's shear resistance, thus amplifying the likelihood of slope failure. Deolo's combination of steep gradients, variable hydrological conditions, and susceptibility to rainfall-triggered instability underscores the need for thorough monitoring and the implementation of slope reinforcement techniques to ensure safety and minimize landslide risks. Fig. 4.11 and 4.12 shows the SLOPE/W results for the location L6 under dry and saturated situations, respectively.

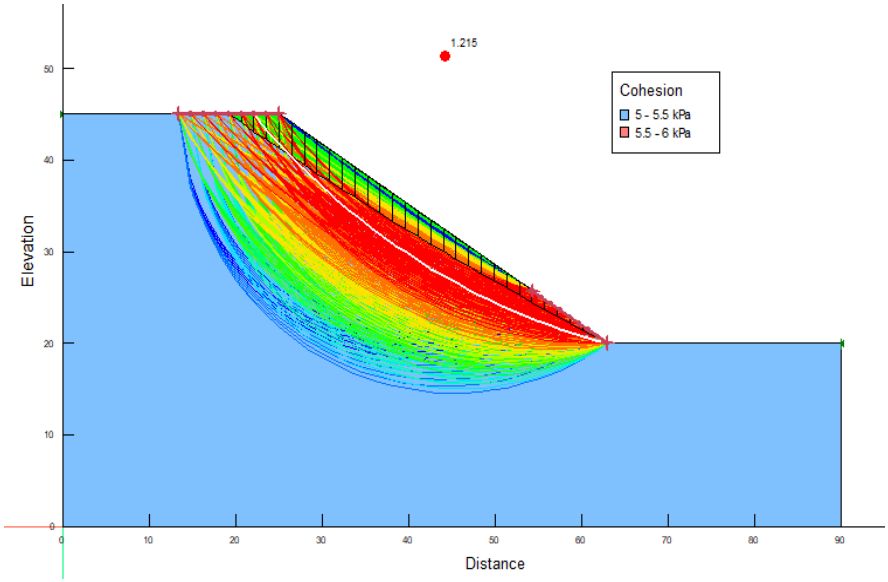

Fig 4.11 SLOPE/W results for L6 for dry conditions under static loading

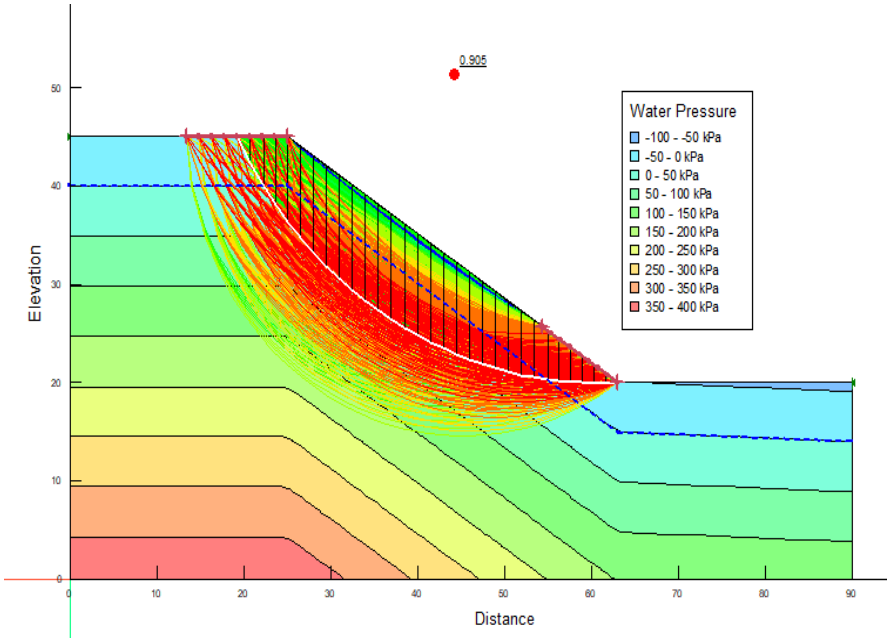

Fig 4.12 SLOPE/W results for L6 for saturated conditions under static loading

4.2 Sanity of the data (static)

In the present investigation, a total of 97 slope stability case studies were analyzed. This dataset includes 85 documented cases sourced from existing literature (Sah et al. 1994; Zhou and Chen 2009; Li and Wang 2010) focused on slope stability evaluation along with 12 additional cases derived from critical locations within the Kalimpong region. The outcomes of the Kalimpong site analyses have been detailed in the preceding sections. Every sample represents a slope engineering field study that includes five input parameters, or independent components. After that, a signal with one dependent component is utilized to determine whether the slope is stable or not. For the purpose of prediction, slope conditions were encoded numerically—assigning a value of 0 to "failure" cases and 1 to "stable" cases. This binary classification was subsequently standardized to ensure compatibility with ML model input requirements. Each group of data was matched based on five independent variables, resulting in one dependent outcome. Because the data has been integrated, each sample property is significant, distinct, and provides an accurate indicator. Among the 97 dataset rows, 41 are classified as "stable," while the remaining 56 are classified as "failure." There is a 1:1.36 ratio between these two groupings, showing

that the indications are dispersed almost evenly. A violin chart (a strip plot that reveals underlying data via points) is used to quickly assess the data's authenticity. Figure 4.13(a-e) depicts the violin plots for UW, C, Phi, SA, and SH in both the "Stable" and "Failure" categories. Each plot's median is represented with a white circle in the centre. The box's range contains both the first and third quartiles. The 95% confidence level is represented by a narrow black line in each violin plot. The silhouette or boundary of each violin approximates the normal kernel density for the given feature. The findings show that the data is stable and has a normal distribution.

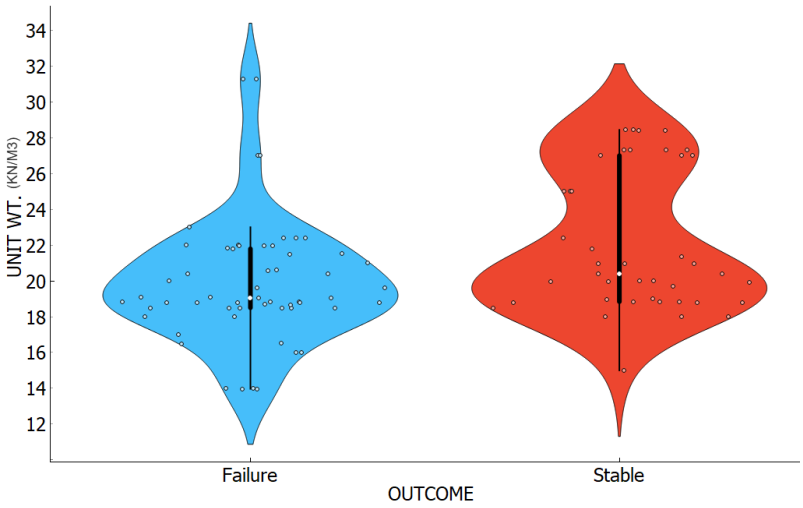

(a) UW

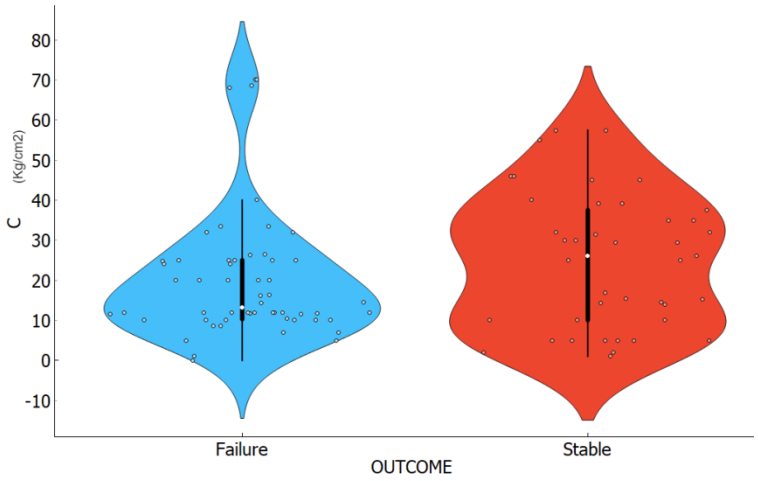

(b) C

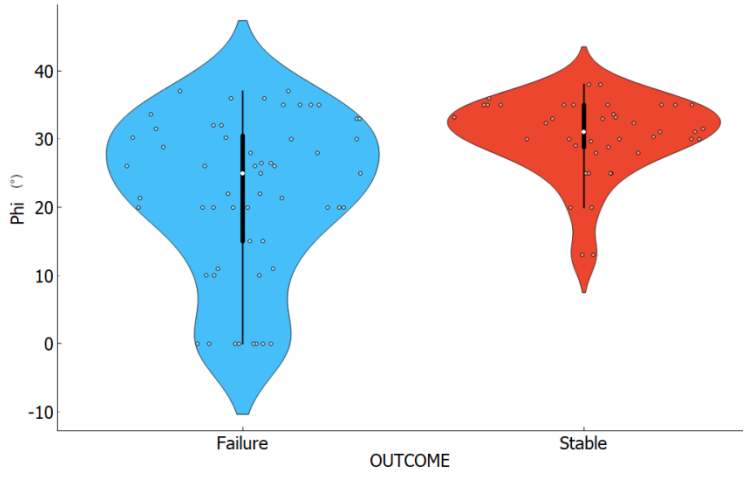

(c) Phi

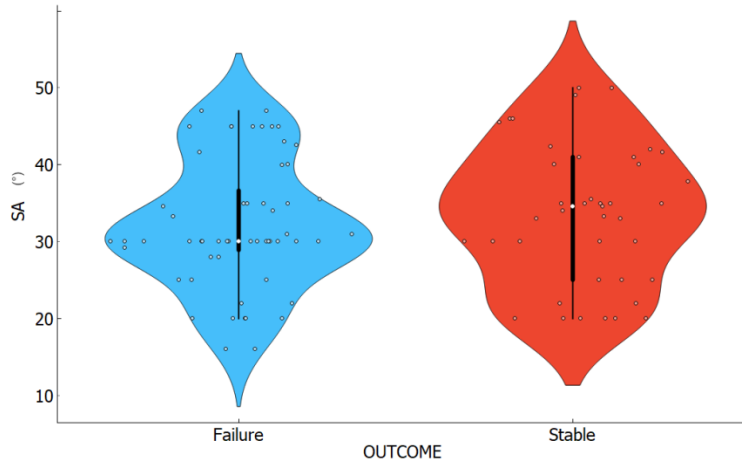

(d) SA

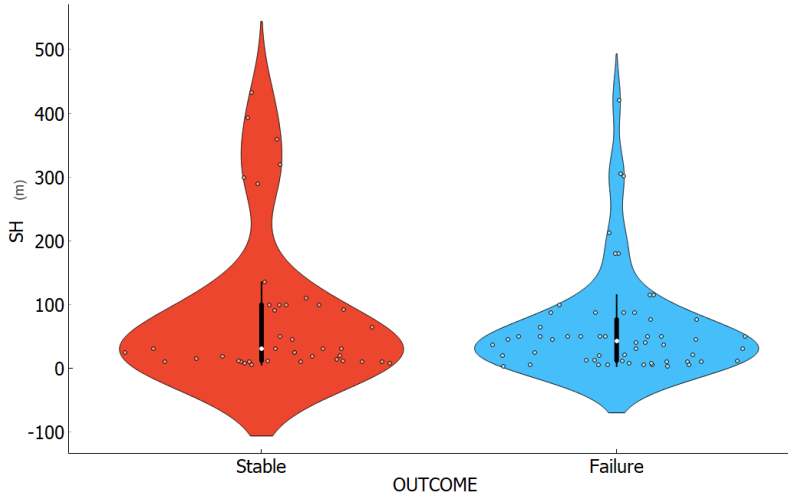

(e) SH

Fig. 4.13 Normal kernel density Violin plots for different input parameters

4.3 Statistical summary of the simulated dataset for static modeling

In order to determine whether the data or parameters have a "skewness" distribution, this section examines various statistics for each feature. Each of the five sources is assessed separately due to their different SI units and meanings. All statistical data values, including mean, median, mode, min, max, standard deviation, and dispersion, are also shown in Table 4.1. A parametric distribution is shown in Fig. 4.14, along with the rate parameter (lambda) for an exponential distribution and the mu and sigma for a normal distribution. In contrast to the normal distribution in other indices, the slope height in Fig. 4.14 (d) shows that it fits the exponential distribution better. The rate parameter lambda=0.01379 is the inverse of the mean and standard deviation. However, because slope height fits the distribution better if the rate parameter (lambda=0.01379) is present, it shows that this component has a relatively exponential distribution. Additionally, the exponential distribution's mean and standard deviation, which equal 72.49, are the inverse of the rate parameter. The distribution of the remaining parameters, UW, C, Phi, and SA, is normal.

Table 4.1 Statistical characteristics of dataset for static modeling

Indices	Mean	Mode	Median	Maximum	Minimum	Dispersion	Standard Deviation
UW	20.827	18.5	19.97	31.3	13.97	0.1811	3.79
C	22.161	5	16.28	70.07	0	0.7417	16.52
Phi	25.389	0	28.8	38	0	0.4078	10.4
SA	32.799	30	31	50	16	0.2629	8.66
SH	72.499	50	37	432	3.6	1.353	72.499

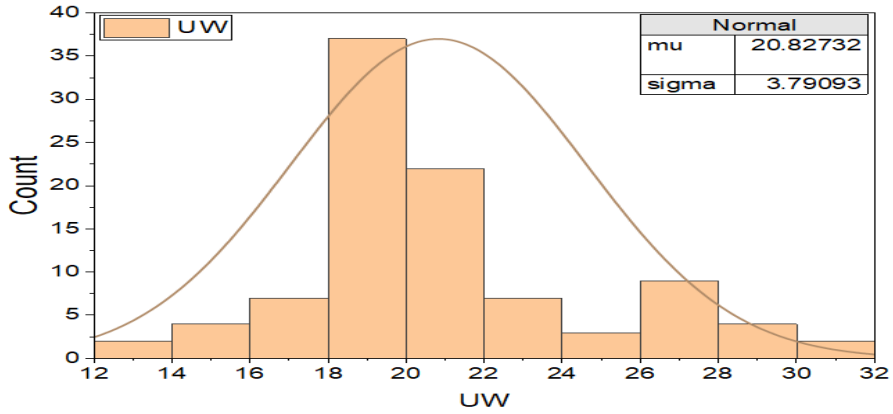
UW
Normal
mu 20.82732
sigma 3.79093
Count
UW

(a) UW

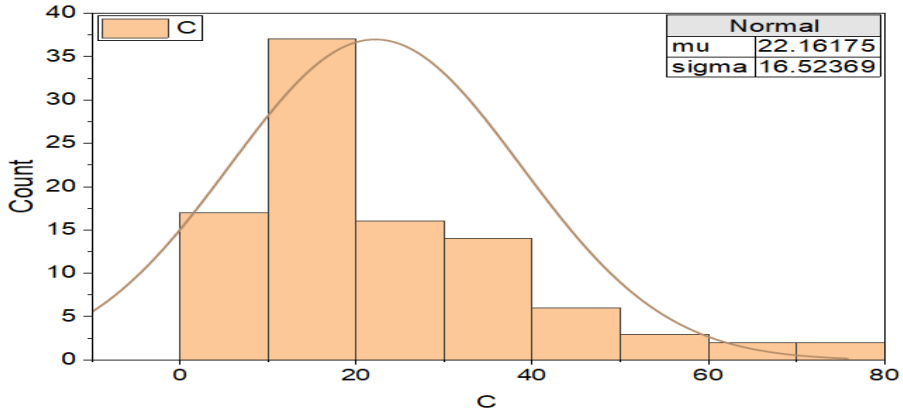
C
Normal
mu 22.16175
sigma 16.52369
Count
C

(b) C

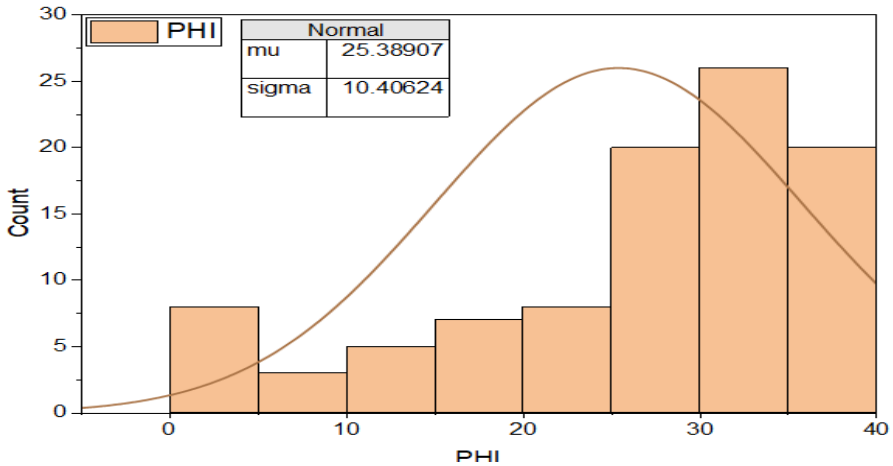
PHI
Normal
mu 25.38907
sigma 10.40624
Count
PHI

(c) Phi

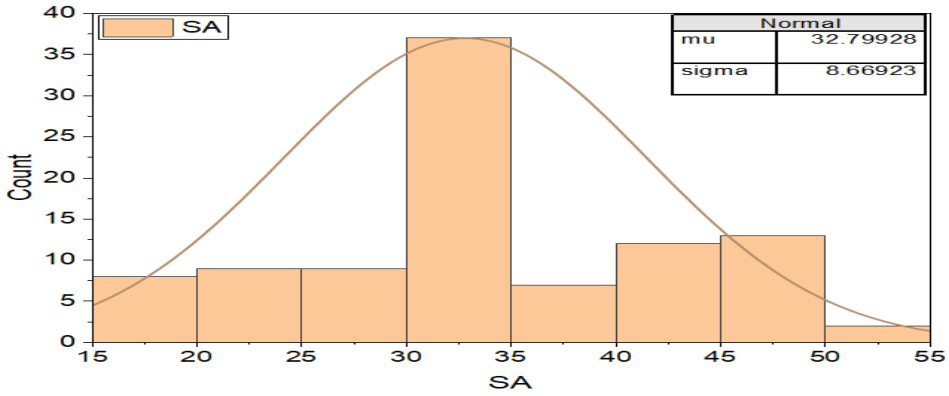

(d) SA

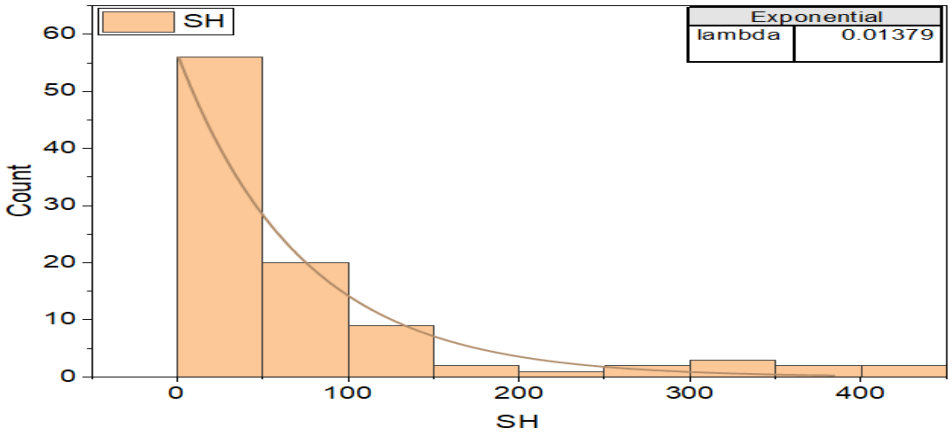

(e) SH

Fig. 4.14 Distribution histogram of different indexes UW, C, Phi, SA and SH

4.4 Assessment of correlations among parameters for static modeling

Before drawing any conclusions about prediction models, it is imperative to first examine the relationship between the five qualities, or variables. The strong correlation between these characteristics may affect the forecast accuracy of the models and result in derogatory conclusions that contradict reality. Eq. 4.1 shows the equation to determine "Pearson's correlation coefficient" for any two items (Cohen et al., 2009).

$$(r) = \frac{\sum(x_i-\bar{x})(y_i-\bar{y})}{\sqrt{\sum(x_i-\bar{x})^2 \sum(y_i-\bar{y})^2}} \quad \text{..... (4.1)}$$

where y_i is the value of the y variable, x_i is the value of the x variable, $\bar{x}$ is the mean of the x values, $\bar{y}$ is the mean of the y values, and r is the coefficient of

correlation of x and y (range -1 to 1). A matrix containing the association values for each of the five attributes can be found in Fig 4.15. Two components are considered to have a strong correlation if their correlation values are close to one. If not, there is little connection between these two components. The correlation between cohesiveness and internal friction angle is -0.22, indicating a negative relationship between the materials. With an r value of 0.522, the slope angle and friction have the most positive correlation. Nonetheless, two entities are not inexorably linked if their correlation coefficient is less than 0.5. The five attributes so show an ignorable relationship. The correlation matrix illustrating the interrelationships among the factors affecting slope stability is presented in Fig. 4.15. It was generated by integrating graphical elements using specialized drawing software to enhance the interpretation of interactions among the five selected parameters. This visual representation aids in clarifying the variable ranges and the degree of association between the influencing factors considered in this study.

Unit Weight	C	Phi	SA	SH	
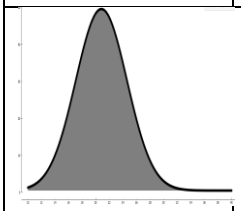	0.023	0.505	0.279	0.283	Unit Weight
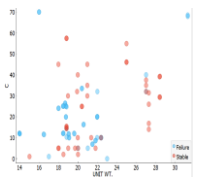		-0.22	0.107	0.153	C
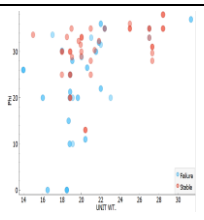	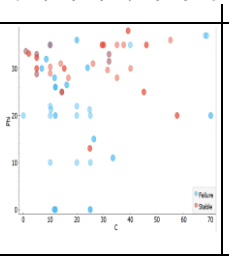	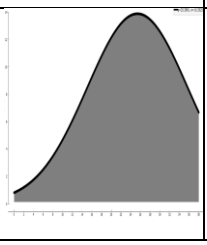	0.522	0.201	Phi

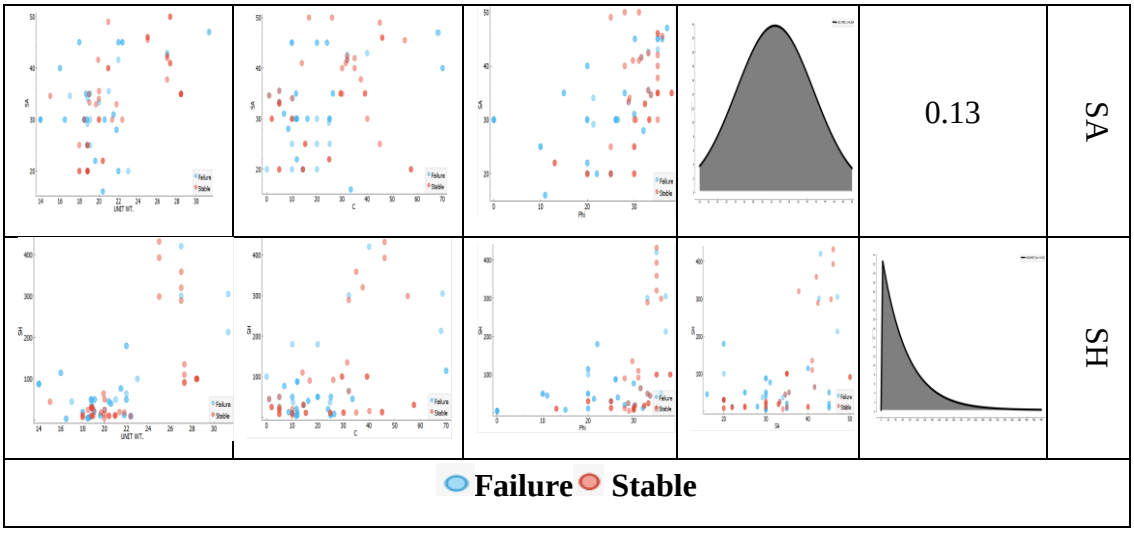

Fig. 4.15 Correlation matrix for parameters undergoing static modeling

4.5 Prediction from models

4.5.1 Conventional ML Models

This study uses one probabilistic model NB, and seven supervised models: SVM, DT, KNN, LR, RF, and AdaBoost. SVM is a supervised machine learning technique that can be used for outlier identification, regression, and classification. This type of linear classifier looks for the best hyperplane to use while classifying the data. By selecting the hyperplane in this way, the difference between the two classes is maximised (Samui, 2008). Decision Trees are supervised machine learning techniques for regression analysis and categorisation. It is a visual depiction of every option for a decision depending on specific criteria. Every node in a decision tree denotes a choice, and every edge shows how that choice turned out (Hwang et al., 2009). As a non-parametric approach, kNN does not assume any particular distribution of the data. It just looks at a data point's k nearest neighbours to determine its categorisation or regression value (Cheng and Hoang, 2016). The likelihood that the output variable will belong to a certain class is represented by a logistic function in the logistic regression linear model (Bhagat et al., 2022).

The final prediction is obtained by averaging the forecasts of each individual decision tree, which is trained in Random Forest using arbitrary subsets of the training data (Xie et al., 2022). For regression analysis and classification, a

supervised machine learning method known as AdaBoost is used. To improve the model's performance and accuracy, a number of weak learners are combined in this ensemble learning technique (Lin et al., 2021). One probabilistic machine learning approach for categorisation is called Naive Bayes. It assumes that the input qualities are conditionally independent of each other and is based on the Bayes theorem (Feng et al., 2018). The first step in using ML for geotechnical analysis is gathering and preprocessing geotechnical data, which includes data normalisation and missing value correction. Finding the elements required for predicting slope stability and possibly even engineering them is the next stage. The particular problem at hand and the available data will determine which machine learning model is best. The hyperparameters of the model are then adjusted for best results using a portion of the training data. An extra data set is then used to ensure that the model has good generalisation capabilities. In the end, criteria like accuracy and precision are used to assess the model. After validation, it is put into use and then regularly checked to adapt to fresh information and evolving circumstances. Additionally, the full procedure employed for this investigation is depicted in the flowchart in Fig. 4.16 below.

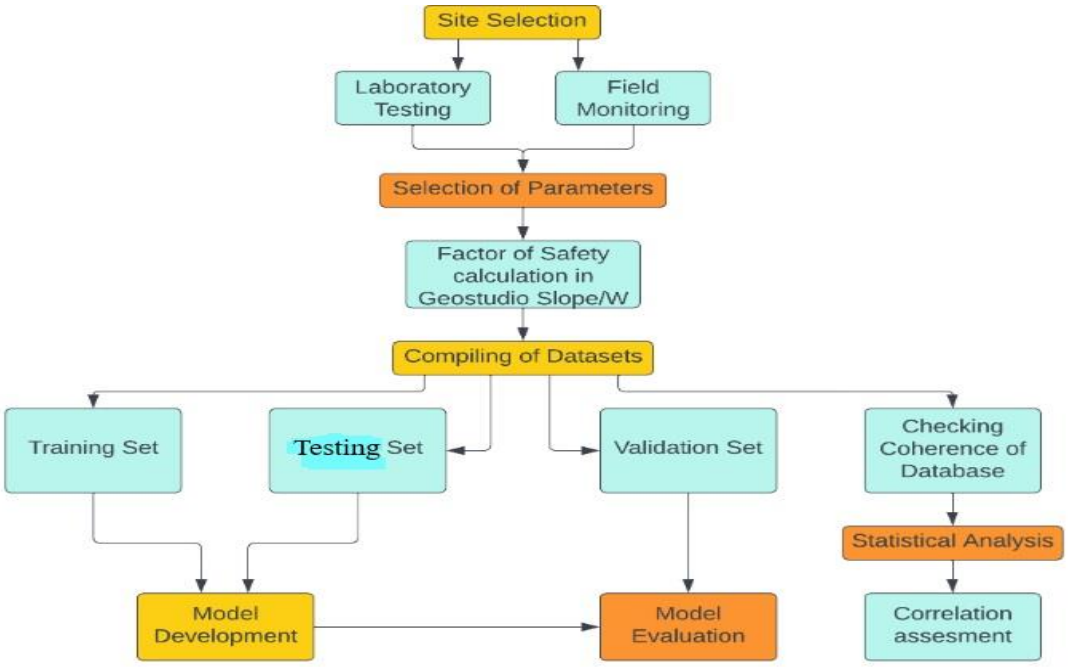

Fig 4.16 Methodology flowchart

4.5.2 Consideration of impacting parameters on slope stability (static)

Both quantitative and qualitative factors affect slope stability. Cohesiveness, slope height and angle, pore water pressure, unit weight, internal friction angle, and other factors are among the numerical parameters. Failure patterns, the physical attributes and quality of rocks and soil, subsurface water, and more are examples of qualitative factors. Here, the goal is to use numerical computations to ascertain whether a slope is stable or failing. The largest problem, though, is translating qualitative traits into numerical values when field data is insufficient. The dependent component pertaining to the evaluation of slopes is therefore categorised as "stable" or else "failure" when ML algorithms are utilised to create prediction models based on the following five indicators: C, SA, SH, Phi, and UW. Since value assignment is based on a variety of criteria and interstitial water pressure is frequently ambiguous in field situations, it is excluded from the prediction models. The five selected variables correctly depict slope stability, according to this study, which focuses on 99 slope data case sets. In order to guarantee adequate precision and dependability in the prediction models, interstitial water pressure is thus eliminated.

4.5.3 ML models analysis (static)

On the initial test data, standard cross validation methods like 2, 3, 5, 10, and 20 fold are used. 29 randomly chosen samples are used as a testing set and rest of the data is used as the training set to build the slope stability predicting model. The model's final outcome is the mean of the five prediction outcomes following five iterations of the previously specified random option. Randomized cross validation is carried out in this article utilizing the Python programming language for convenience. Due to space constraints, this article only shows the "scatter plots" and "linear fitting curves" between unit weight on the horizontal axis (x) and different parameters on the vertical axis (y). The fitting line equation, its slope and intercept, Pearson's coefficient (r), and the COD are also shown in Fig. 4.17.

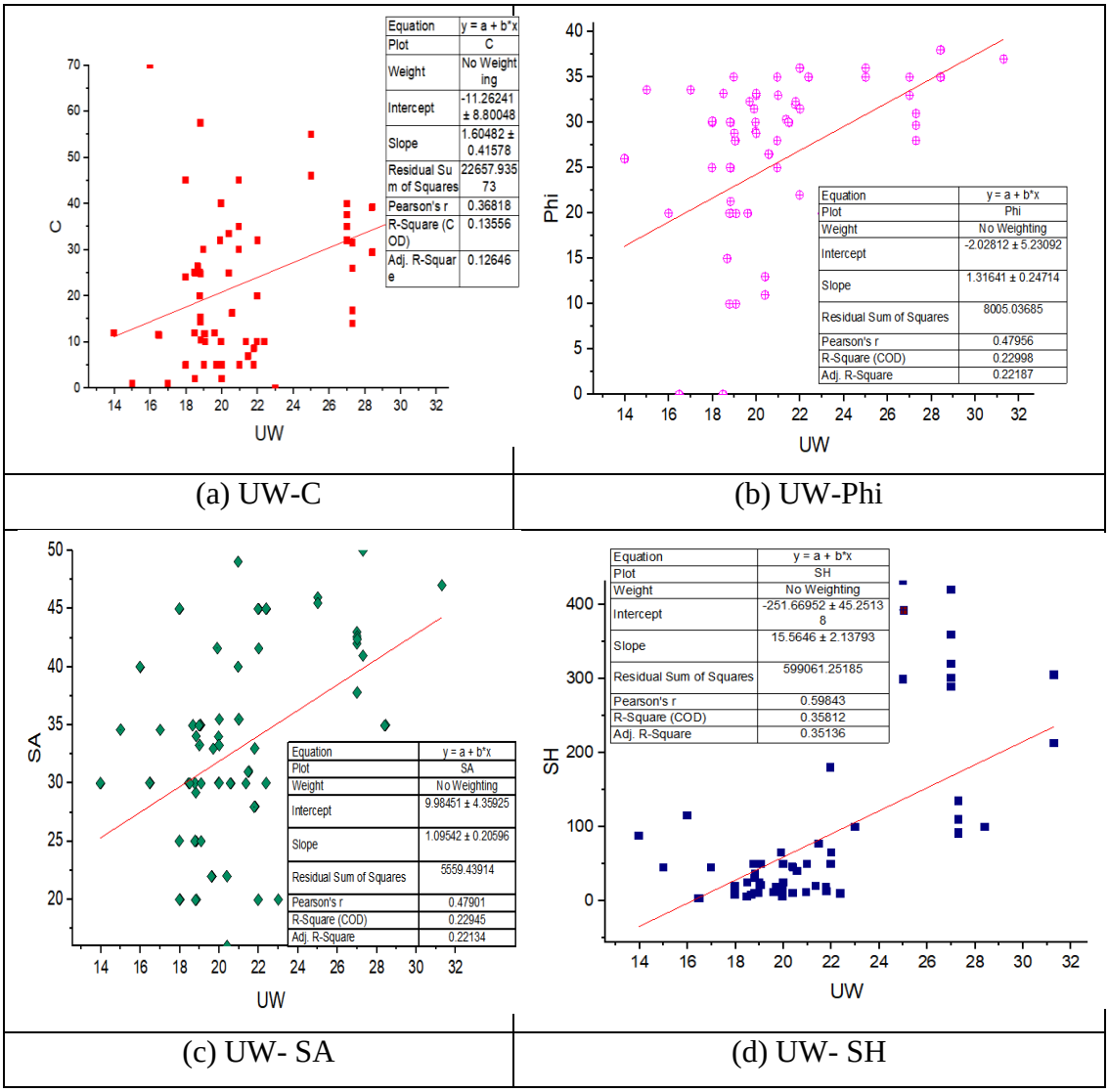

(a) UW-C (b) UW-Phi

(c) UW- SA (d) UW- SH

Fig. 4.17 Regression fitting line and scatter plots of different parameters

4.5.4 Valuation of Models (static)

Common performance evaluation metrics for classification models include CA, P, R, F1 and AUC shown in Fig 4.18. The comparison between predicted and actual outcomes is categorized into four outcomes: TP, TN, FP, and FN. Classification Accuracy represents the overall correctness of the model in predicting both positive and negative outcomes (Begum et al., 2021). Precision quantifies the proportion of correctly predicted positive instances among all instances predicted as positive (Chen et al., 2022). Recall, conversely, measures the model's

ability to identify all actual positive instances. The F1 Score, which is the harmonic mean of Precision and Recall, provides a more balanced performance measure, especially under imbalanced class distributions or when both false positives and false negatives incur similar costs. A higher F1 Score signifies improved model performance in distinguishing between positive and negative classes. When Recall is plotted on the x-axis and Precision on the y-axis, the Precision-Recall curve is obtained. The ROC curve, on the other hand, graphically represents the relationship between the TPR and the FPR across different classification thresholds. The AUC serves as an aggregate measure of model performance, where higher values indicate greater classification effectiveness.

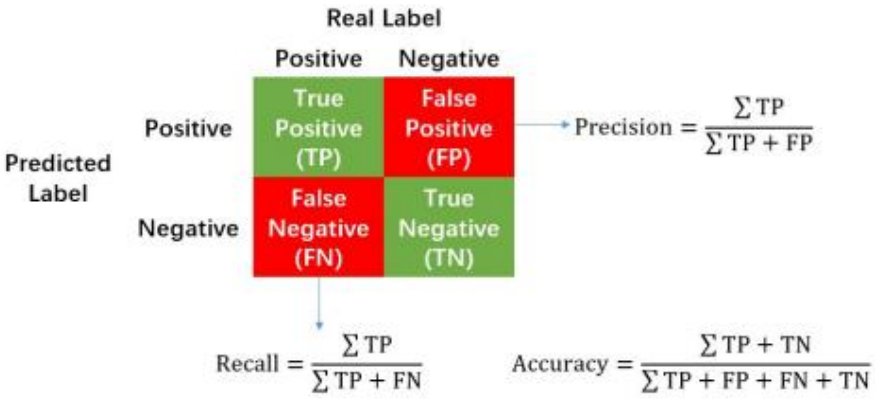

Fig 4.18 Performance indicators

4.6 Examination of results from predictions (static)

4.6.1 Model assessment based on the unprocessed data (static)

To perform the random cross assessment, seven different machine learning techniques are presented, along with one stacking technique of Random Forest and AdaBoost, or R-Boost. The classification accuracy, precision, recall, F1, and AUC values obtained are displayed in Table 4.2. AUC is a crucial machine learning metric because it offers a trustworthy and understandable assessment of a model's performance in binary classification tasks, particularly in cases where the dataset is unbalanced. R-Boost has an AUC of 0.798, followed by LR with a value of 0.74, while RF shows an average value of 0.81. With an average of 0.725, R-Boost

also has the best forecasting ability in terms of CA. After this AdaBoost and RF had an average accuracy of 0.723. Additionally, AdaBoost generates excellent results because it transforms a high bias low variance model into a low bias low variance model, which helps create the optimal machine learning model that yields an extremely accurate estimate. In comparison to methods like SVM, it is also easier to use and requires less modification.

However, in this case, the R-Boost algorithm produces the highest CA since it generates an initial array of decision trees by applying random forest to the dataset. AdaBoost is then applied to the decision trees to improve their accuracy and efficiency. This technique can improve the model's accuracy and reduce its variance, increasing its dependability and capacity to manage complex datasets with a wide range of features. to more clearly describe each model's soundness. One sign that the model's behaviour is erroneous for skewed data is accuracy. It is possible to create effective prediction models when both F1 and AUC values are considered. The results in Table 4.2 show that R-Boost, AdaBoost, and RF are the forecast models with F1 values more than 70%. Additionally, the AUC values for LR, R-Boost, and RF are higher than 74%. According to AUC and CA, RF and R-Boost are therefore thought to be the most accurate predictor, which further enhances the novelty factor of this study.

Table 4.2 Evaluation metrics for different ML methods

Evaluation Metrics	Folds	AdaBoost	kNN	Logistic Regression	Naive Bayes	Random Forest	SVM	Decision Tree	Stack (R-Boost)
Area under the curve	2	0.719077	0.695557	0.684016	0.726916	0.772648	0.667465	0.652657	0.752178
	3	0.643946	0.6777	0.736934	0.726916	0.858449	0.72561	0.789416	0.801829

F1 Score	Classification Accuracy									
2	Average	20	10	5	3	2	Average	20	10	5
0.719257	0.7237	0.762887	0.752577	0.701031	0.670103	0.731959	0.7337	0.783972	0.797256	0.724085
0.663267	0.6784	0.701031	0.690722	0.71134	0.618557	0.670103	0.7350	0.777657	0.761542	0.762413
0.621176	0.6742	0.680412	0.71134	0.659794	0.690722	0.628866	0.7412	0.768728	0.779617	0.736716
0.620605	0.6330	0.639175	0.628866	0.618557	0.659794	0.618557	0.7236	0.714939	0.733667	0.71581
0.714843	0.7237	0.752577	0.71134	0.71134	0.721649	0.721649	0.8141	0.794861	0.84473	0.799652
0.621176	0.6845	0.670103	0.701031	0.71134	0.71134	0.628866	0.7329	0.756533	0.78027	0.734538
0.579084	0.6784	0.659794	0.690722	0.690722	0.762887	0.587629	0.6545	0.704268	0.74412	0.718206
0.681634	0.7258	0.762887	0.742268	0.701031	0.721649	0.701031	0.7983	0.815767	0.832317	0.789199

Precision										
Average	20	10	5	3	2	Average	20	10	5	3
0.7241	0.763089	0.751637	0.698838	0.665886	0.741123	0.7179	0.758795	0.749101	0.699254	0.663267
0.6804	0.711892	0.699566	0.71134	0.613393	0.665886	0.6769	0.702823	0.692512	0.71134	0.614323
0.6708	0.677929	0.708963	0.657021	0.687917	0.622227	0.6709	0.678513	0.708916	0.657772	0.688124
0.6374	0.640407	0.634505	0.622695	0.663693	0.625917	0.6344	0.639724	0.630624	0.620039	0.661116
0.7226	0.751383	0.7098	0.71134	0.71942	0.721248	0.7213	0.751655	0.710264	0.71134	0.71856
0.6815	0.665886	0.698838	0.71134	0.708963	0.622227	0.6808	0.663267	0.699254	0.71134	0.708916
0.6746	0.655111	0.687715	0.687715	0.76377	0.578569	0.6730	0.653924	0.684313	0.684313	0.763247
0.7275	0.76183	0.740654	0.698838	0.723568	0.712435	0.7189	0.760255	0.740736	0.699254	0.712534

Recall	2	0.731959	0.670103	0.628866	0.618557	0.721649	0.628866	0.587629	0.701031
	3	0.670103	0.618557	0.690722	0.659794	0.721649	0.71134	0.762887	0.721649
	5	0.701031	0.71134	0.659794	0.618557	0.71134	0.71134	0.690722	0.701031
	10	0.752577	0.690722	0.71134	0.628866	0.71134	0.701031	0.690722	0.742268
	20	0.762887	0.701031	0.680412	0.639175	0.752577	0.670103	0.659794	0.762887
	Average	0.7237	0.6784	0.6742	0.6330	0.7237	0.6845	0.6784	0.7258

4.6.2 Sensitivity Analysis for static analysis

The importance factor is calculated for each input parameter in this section, which focusses on the sensitivity analysis using weight determination criteria. This task is carried out using the CRITIC approach, which uses the coefficient of variation, which is equal to (Standard Deviation/Average) for each individual parameter provided by I_j. Equation 4.2 is used to calculate the objective weight (Wj) of any given criterion j (Krishnan et al., 2021)

$W_j = I_j \div \sum_{j=1}^{n} I_j$ ..... (4.2)

In accordance with the five input criteria, weightage plays a vital function. The values of weightage in percentage comes out to be 2.7, 12, 7.5, 6.3 and 71.5 for UW, C, Phi, SA and SH correspondingly. According to the data, slope height has a bigger influence on slope stability than cohesiveness while unit weight has the least demonstrated in Fig 4.19.

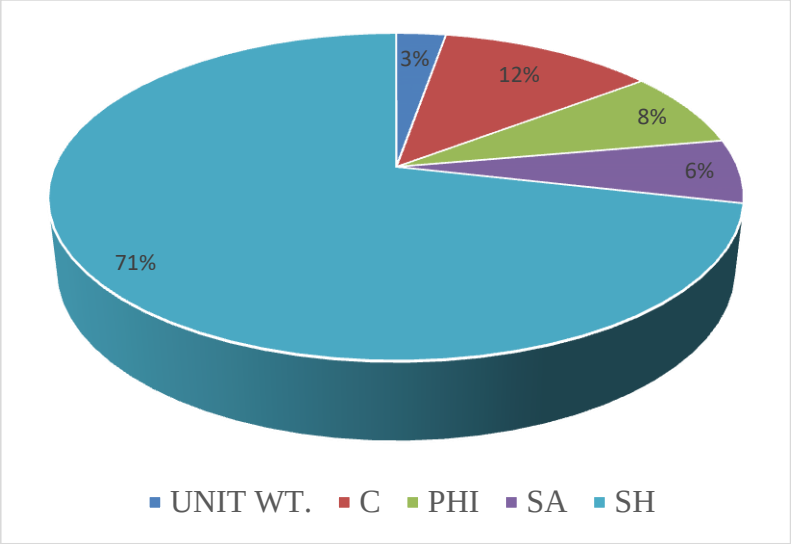

Fig. 4.19 Weightage indicator of each parameter

4.6.3 Receiver Operating Characteristic (ROC) Curve for static analysis

The ROC curve is a graphical representation used to evaluate the performance of binary classification models. The AUC-ROC serves as a quantitative measure of a model's discriminative ability. In the present study, as illustrated in Fig. 4.20 and 4.21 for failure and stable classes respectively, the RF algorithm demonstrated the highest overall classification accuracy among all evaluated models. Both RF and R-Boost, being robust ensemble learning techniques, exhibited strong predictive capabilities for estimating the Factor of Safety (F.S) across various slope conditions, as inferred from the ROC analysis. SVM also yielded reliable and consistent results, making it a viable alternative classifier. Among the models assessed, RF achieved the highest AUC value of 0.81, followed by R-Boost with an AUC of 0.798, and LR with 0.74. In contrast, the Naïve Bayes classifier recorded the lowest AUC value of 0.654. These findings underscore the superior predictive accuracy and reliability of RF and R-Boost models, aligning well with results obtained through conventional LEMs. Consequently, the application of these machine learning approaches holds significant promise for the development of efficient slope stability assessment frameworks and the formulation of appropriate stabilization strategies.

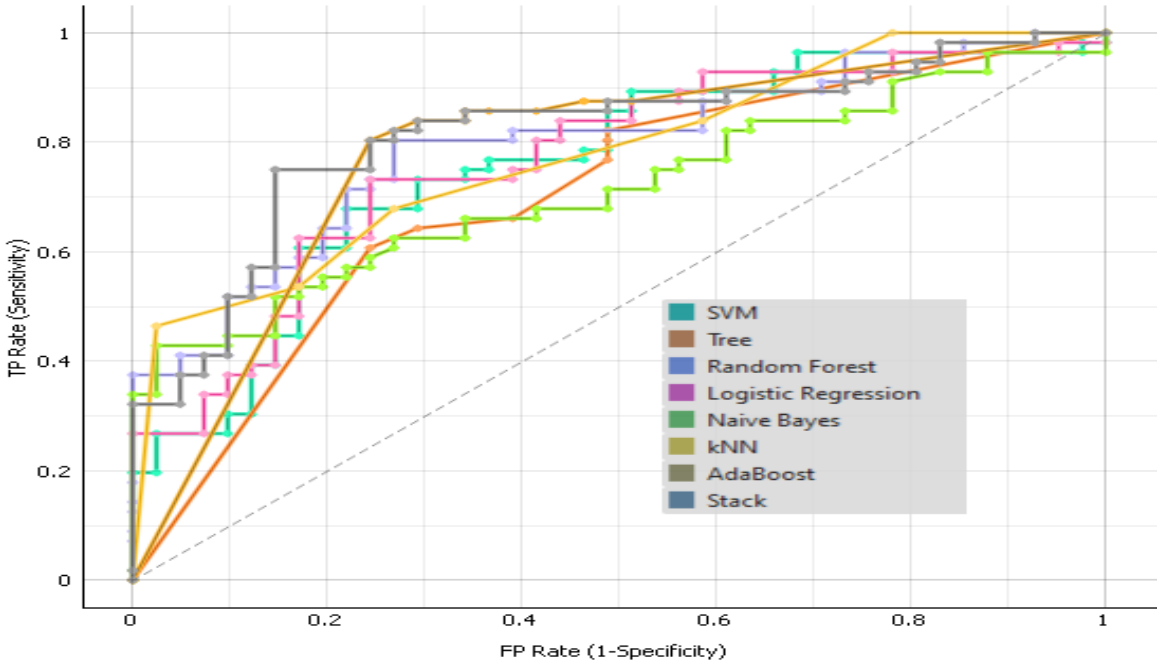

Fig. 4.20 ROC Curve (Failure)

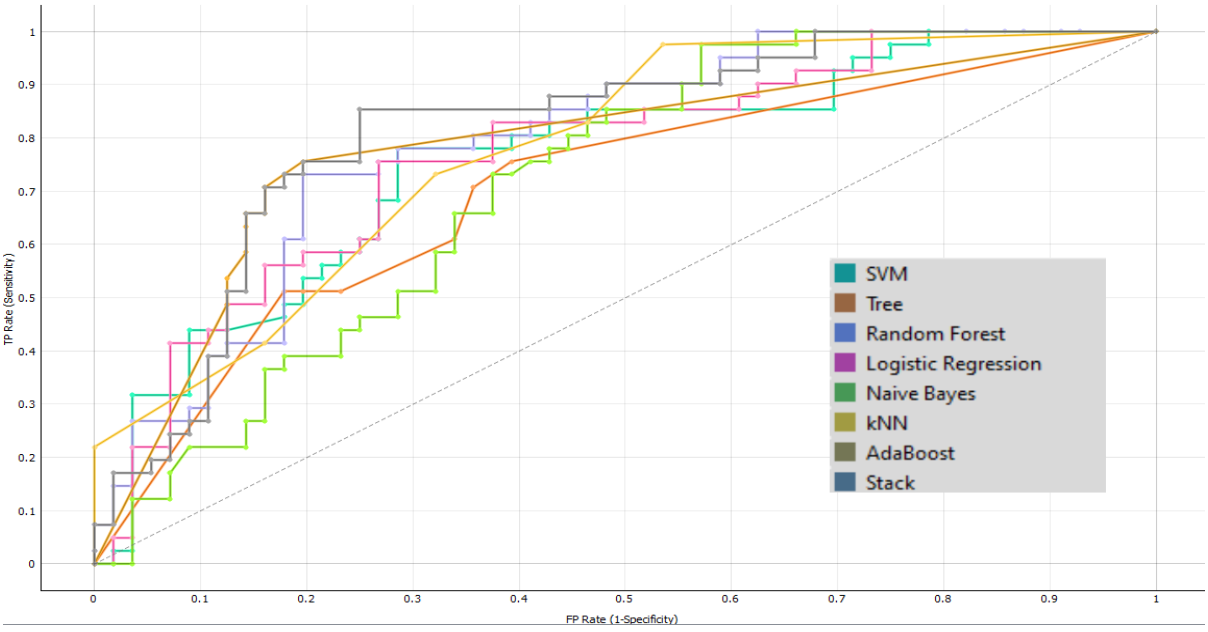

Fig. 4.21 ROC Curve (Stable)

4.6.4 Comparison with GeoStudio results for static loading

As per the above results, in Table 4.3 author has presented the slope stability assessment outcomes, derived from both the best-performing machine learning models and the SLOPE/W simulation outputs. Among the predictive

models, R-Boost, followed closely by RF, demonstrated high reliability by producing results that closely align with the stability outcomes observed in the numerical analysis.

Table 4.3 Testing results on stability condition criteria for Kalimpong (static condition)

Site/State	UNIT WT.	C	Phi	SA	SH	Prediction from SLOPE/W	RF	AdaBoost	LR	Stack (R-Boost)
L1 Dry	20	5	33	35.5	50	S	S	S	F	S
L1 Sat.	21	5	33	35.5	50	F	F	F	F	F
L2 Dry	18.5	2	33.2	30	25	S	F	S	S	S
L2 Sat.	20	2	33.2	30	25	S	S	F	S	S
L3 Dry	15	1	33.6	34.6	45	S	S	S	S	S
L3 Sat.	17	1	33.6	34.6	45	F	F	F	S	F
L4 Dry	19.7	5	32.3	33	19	S	S	S	S	S
L4 Sat.	21.8	5	32.3	33	19	S	S	S	S	S
L5 Dry	19.9	32	31.5	41.6	65	S	S	S	F	S
L5 Sat.	22	32	31.5	41.6	65	F	F	F	F	F
L6 Dry	19	5	28.8	33.3	25	S	S	S	S	S
L6 Sat.	20	5	28.8	33.3	25	F	S	S	F	S

4.7 Slope/W results for dynamic loading

For a variety of critical slopes in Kalimpong with variable soil parameters, such as seismic loading for dry and saturated conditions, the current study employs the M-P approach to measure the FOS using the "Slope/W" software under GeoStudio 2021.4, which is confirmed by field survey (Morgenstern and Price, 1965). The entire procedure, including mathematical models and field validation, is covered in this section.

4.7.1 Location 1 in Mahakal Dara, Bhalukhop (dynamic)

Mahakal Dara in Bhalukhop lies in a seismically active region with steep terrain and loose soil strata, making it particularly vulnerable to dynamic loading factors. In this slope stability analysis, pseudo-static loading was introduced to simulate seismic conditions, reflecting the additional forces generated during earthquakes. Key soil parameters, such as c and ϕ, were analyzed for both dry and saturated conditions. In saturated scenarios, a water table was placed 5 meters below the surface to represent post-rainfall infiltration. The seismic forces act as an added destabilizing factor, increasing the shear stress within the slope while reducing the effective stress, particularly under saturated conditions where pore water pressure is already elevated. This combined impact significantly lowers the factor of safety, emphasizing the critical need for earthquake-resistant slope reinforcement measures, such as retaining walls, soil nailing, and drainage systems, to prevent potential catastrophic slope failures in this area. SLOPE/W results are shown in Fig. 4.22 and 4.23 for L1 soil specimens under dry and saturated conditions, respectively.

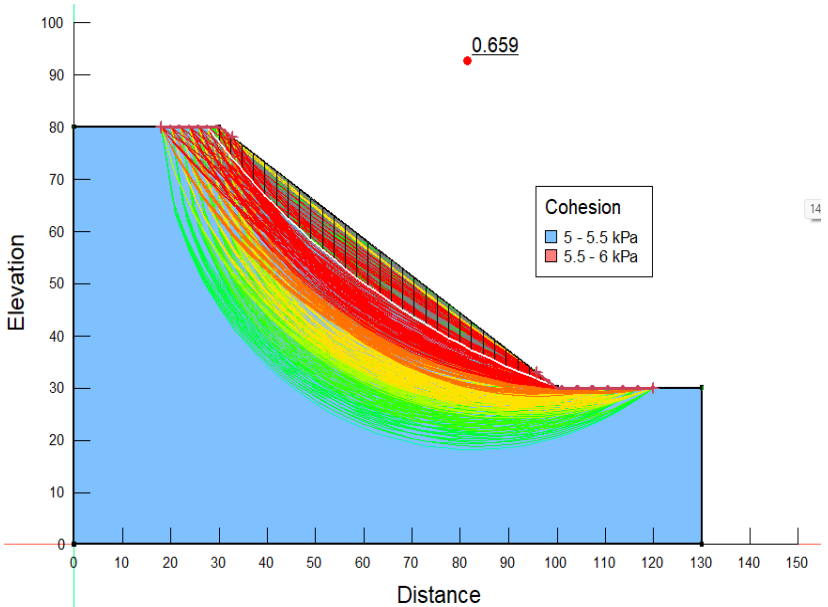

Fig 4.22 SLOPE/W results for L1 in dry conditions under dynamic loading

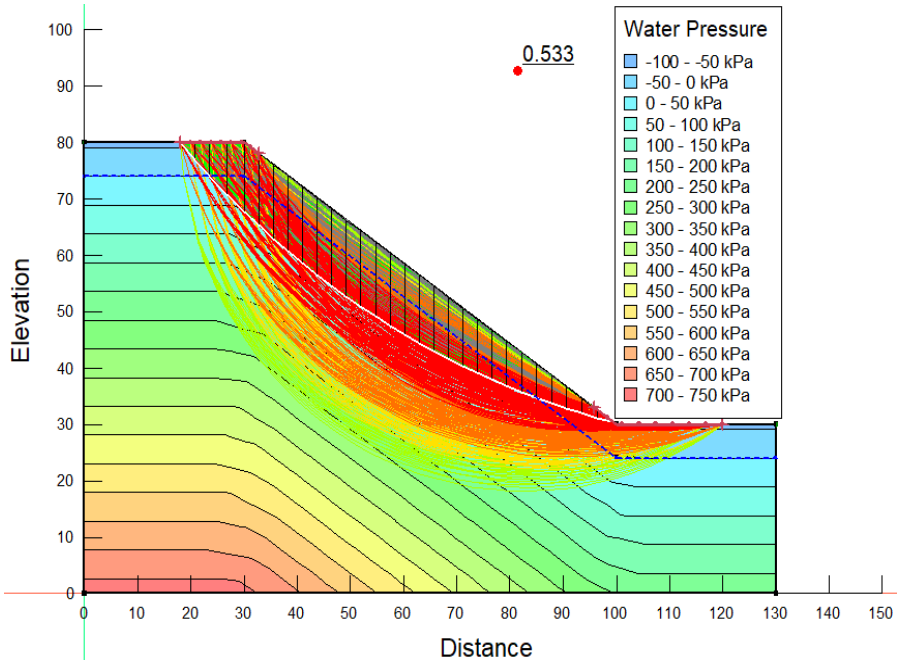

Fig 4.23 SLOPE/W results for L1 in saturated conditions under dynamic loading

4.7.2 Location 2 in Chandraloke (dynamic)

The terrain of Chandraloke, with its steep inclines and proximity to seismic zones, poses a substantial risk of landslides under dynamic conditions. Pseudo-static analysis was utilized to assess the stability of the slope under seismic forces. Soil properties, including c and ϕ were measured to evaluate the resistance of the soil mass against these forces. Saturated conditions, modeled with a water table at 5 meters below the surface, significantly weaken the soil due to increased pore water pressure. When combined with dynamic forces, the destabilization is further amplified, as the inertial effects of seismic loading increase the likelihood of slope failure. This analysis underscores the necessity for advanced mitigation techniques, such as shock-absorbing barriers, geosynthetic reinforcements, and seismic slope drainage systems, to enhance the stability of Chandraloke's vulnerable slopes. SLOPE/W results are shown in Fig. 4.24 and 4.25 for L2 soil specimens under dry and saturated conditions, respectively.

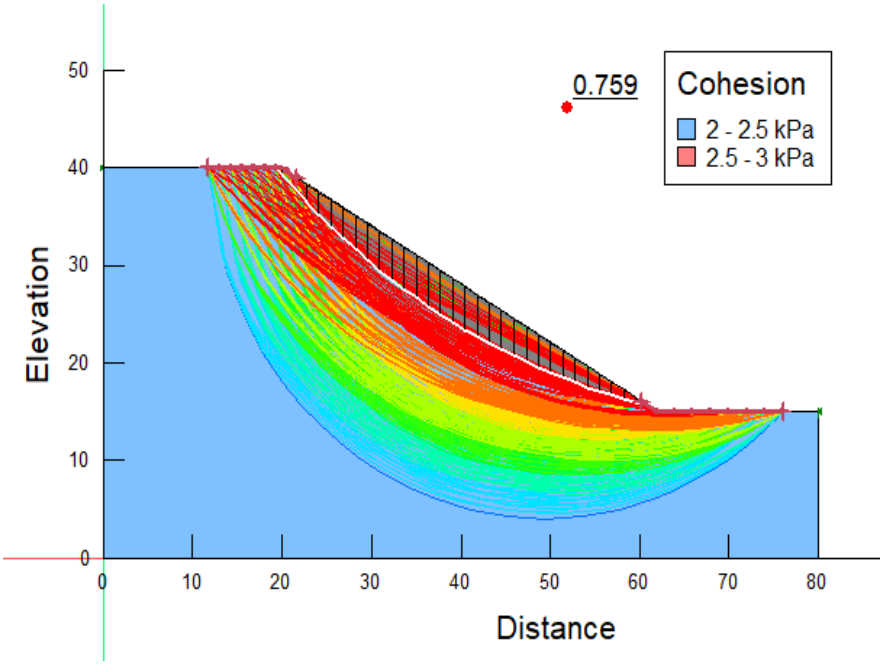

Fig 4.24 SLOPE/W results for L2 in dry conditions under dynamic loading

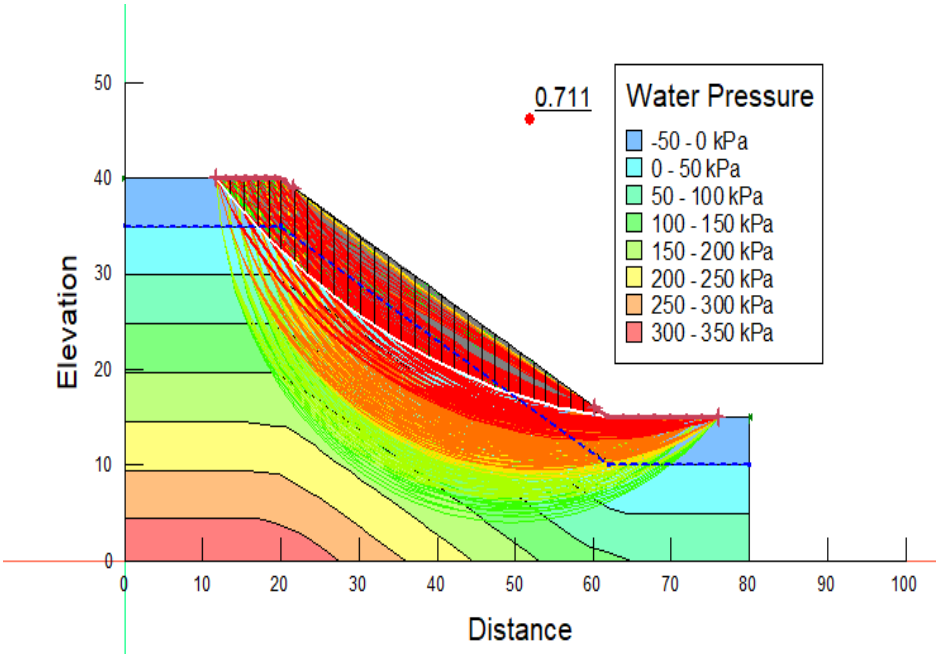

Fig 4.25 SLOPE/W results for L2 in saturated conditions under dynamic loading

4.7.3 Location 3 in Upper Tashiding (dynamic)

Upper Tashiding is characterized by steep slopes and loose, weathered soils, making it extremely susceptible to seismic activity and associated landslide risks. The slope stability analysis incorporated pseudo-static factors to model the

impact of dynamic loading during seismic events. The geotechnical parameters, including c and ϕ were evaluated under both dry conditions and saturated scenarios, the latter featuring a water table at 5 meters depth to reflect post-rainfall effects. Dynamic loading introduces additional shear stresses and reduces the soil's ability to resist failure, particularly in water-saturated conditions where pore water pressures compromise soil stability further. This compounded risk highlights the importance of integrated stabilization strategies, such as anchored retaining systems, slope reinforcement using geogrids, and earthquake-resistant infrastructure, to mitigate the seismic and hydrological vulnerabilities of the site. SLOPE/W results are shown in Fig. 4.26 and 4.27 for L3 soil specimens under dry and saturated conditions, respectively.

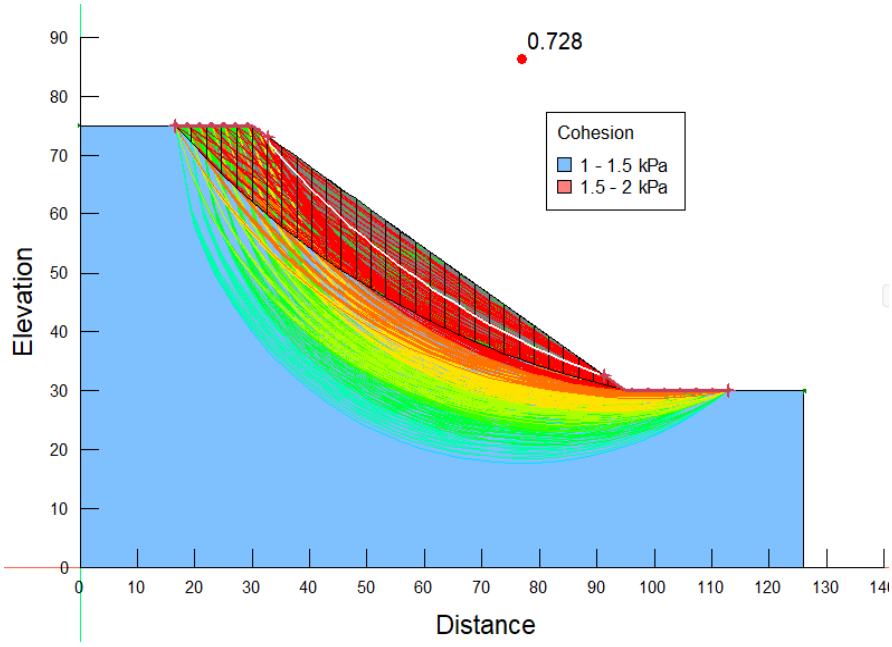

Fig 4.26 SLOPE/W results for L3 in dry conditions under dynamic loading

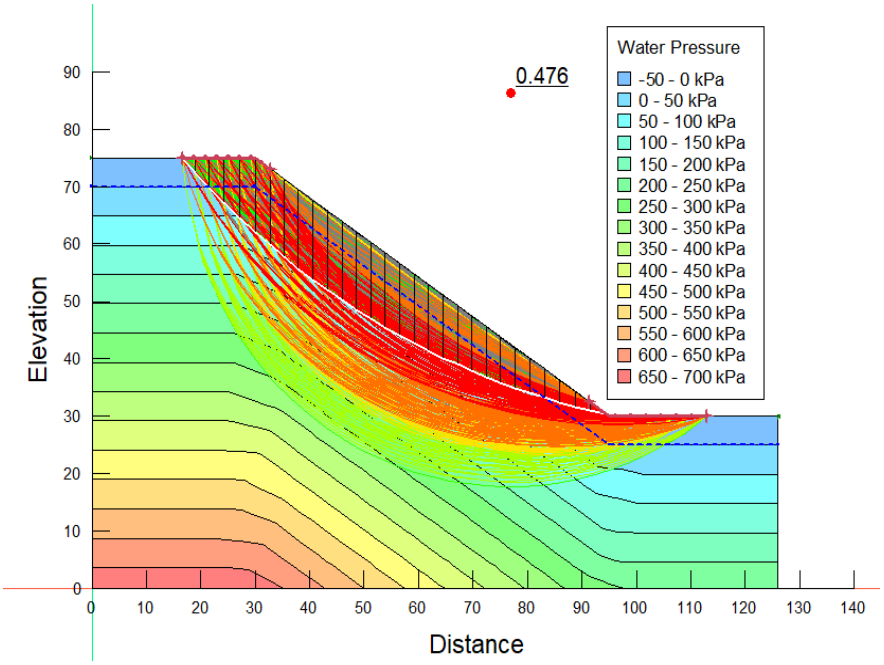

Fig 4.27 SLOPE/W results for L3 in saturated conditions under dynamic loading

4.7.4 Location 4 in Ngassey Busty (dynamic)

The slopes of Ngassey Busty are notably steep, with a geologically fragile soil structure that is highly sensitive to dynamic influences. Pseudo-static slope stability analysis was performed to assess the effects of seismic accelerations, representing the potential impact of earthquakes. Soil parameters c and ϕ were crucial parameters in evaluating the soil's strength. Saturated conditions were modeled with a water table positioned at 5 meters below the surface, simulating the hydrological impact of intense rainfall. During seismic events, the added inertial forces generated by ground shaking interact with pore water pressures in saturated soils, further decreasing the shear strength and increasing the likelihood of slope failure. The findings highlight the need for robust interventions, such as earthquake-resilient slope stabilization, efficient subsurface drainage systems, and the use of energy-dissipating retaining structures to safeguard this area against potential dynamic slope failures. SLOPE/W results are shown in Fig. 4.28 and 4.29 for L4 soil specimens under dry and saturated conditions, respectively.

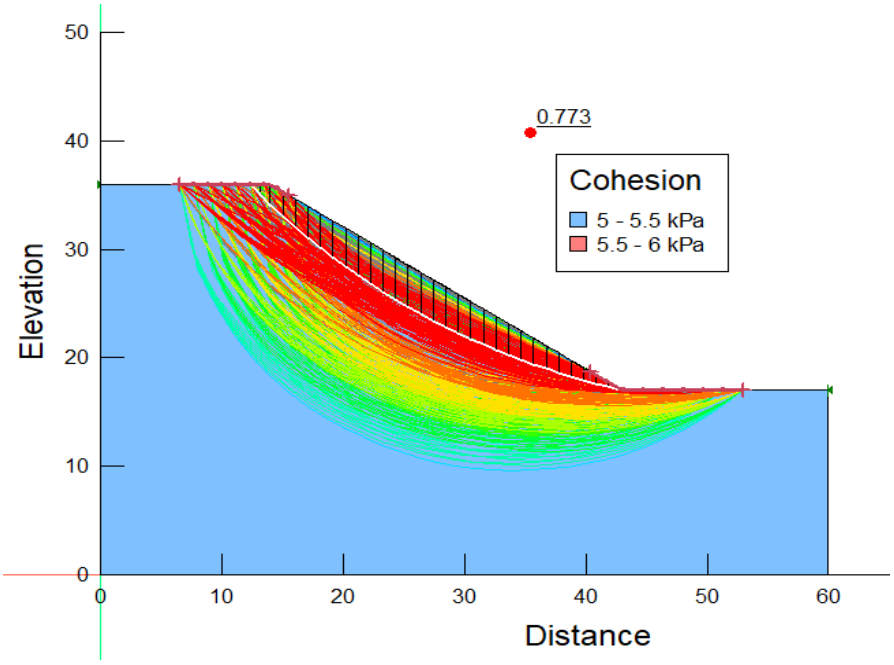

Fig 4.28 SLOPE/W results for L4 in dry conditions under dynamic loading

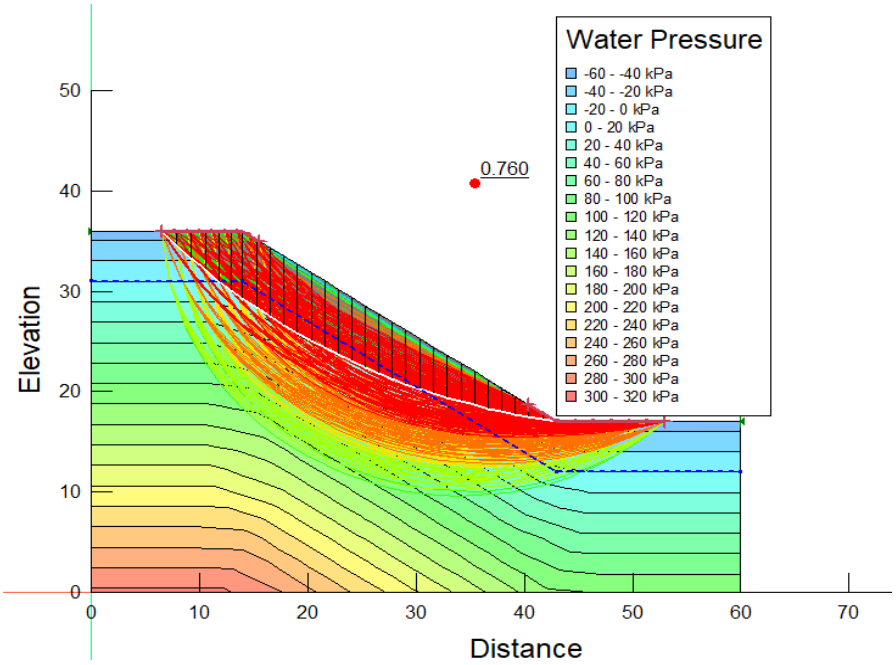

Fig 4.29 SLOPE/W results for L4 in saturated conditions under dynamic loading

4.7.5 Location 5 in Mongbol Road (dynamic)

Mongbol Road traverses a region with steep gradients and loose soil, making it highly susceptible to the compounded effects of seismic activity and hydrological changes. In this study, a pseudo-static approach was adopted to simulate

seismic loading, allowing for an assessment of slope stability under dynamic conditions. The soil's c and ϕ were analyzed under both dry conditions and saturated scenarios, with the latter featuring a water table at 5 meters to reflect monsoonal influences. Seismic forces intensify the destabilizing shear stresses while reducing the effective stress within the slope, particularly in water-saturated soils. This combined impact significantly lowers the safety margin, highlighting the urgent need for dynamic slope stabilization measures. Recommended interventions include the installation of flexible retaining walls, reinforcement with soil nails or geogrids, and slope drainage improvements to mitigate the risk of landslides along Mongbol Road. SLOPE/W results are shown in Fig. 4.30 and 4.31 for L5 soil specimens under dry and saturated conditions, respectively.

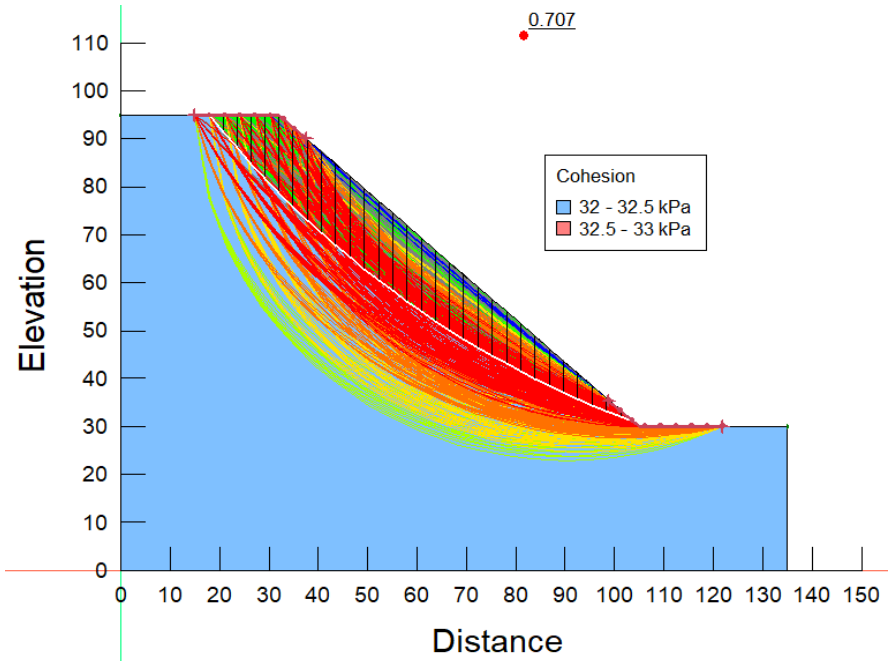

Fig 4.30 SLOPE/W results for L5 in dry conditions under dynamic loading

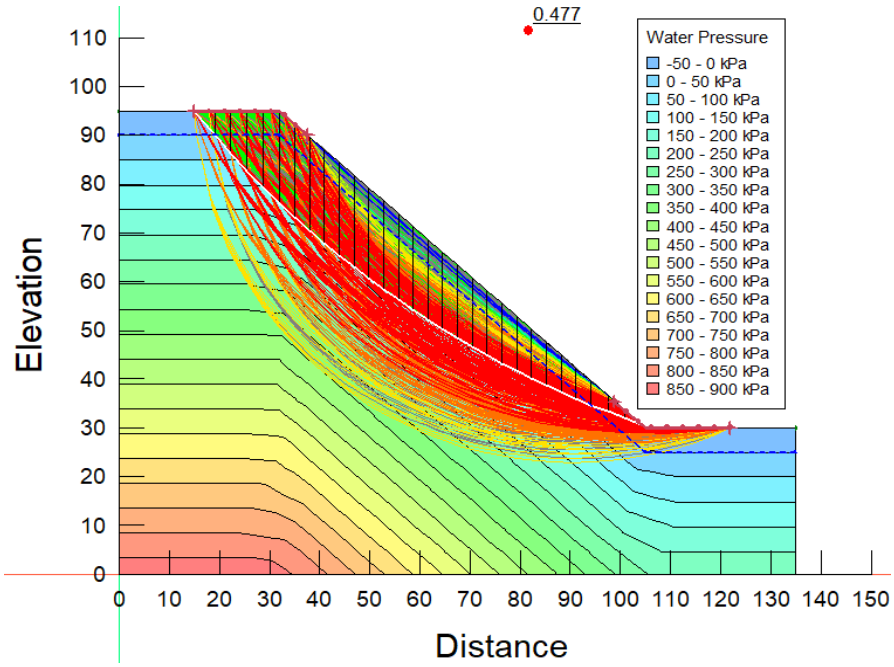

Fig 4.31 SLOPE/W results for L5 in saturated conditions under dynamic loading

4.7.6 Location 6 in Deolo (dynamic)

Deolo, a high-altitude location in Kalimpong with steep and scenic terrain, is highly vulnerable to dynamic slope instability. Pseudo-static slope stability analysis was undertaken to evaluate the effects of seismic forces on this already fragile terrain. The study incorporated soil c and ϕ as key parameters and analyzed stability under dry and saturated conditions. For saturated scenarios, the water table was modeled at 5 meters from the surface to represent monsoonal conditions. Dynamic loading due to seismic forces further destabilizes the slope by increasing the shear stresses acting on the soil mass, especially in conditions where pore water pressures are elevated. These findings indicate a pressing need for earthquake-resistant stabilization strategies, including reinforced earth embankments, the use of shock-absorbing geosynthetics, and efficient drainage systems, to manage the combined risks posed by seismic and hydrological factors in Deolo. SLOPE/W results are shown in Fig. 4.32 and 4.33 for L6 soil specimens under dry and saturated conditions, respectively.

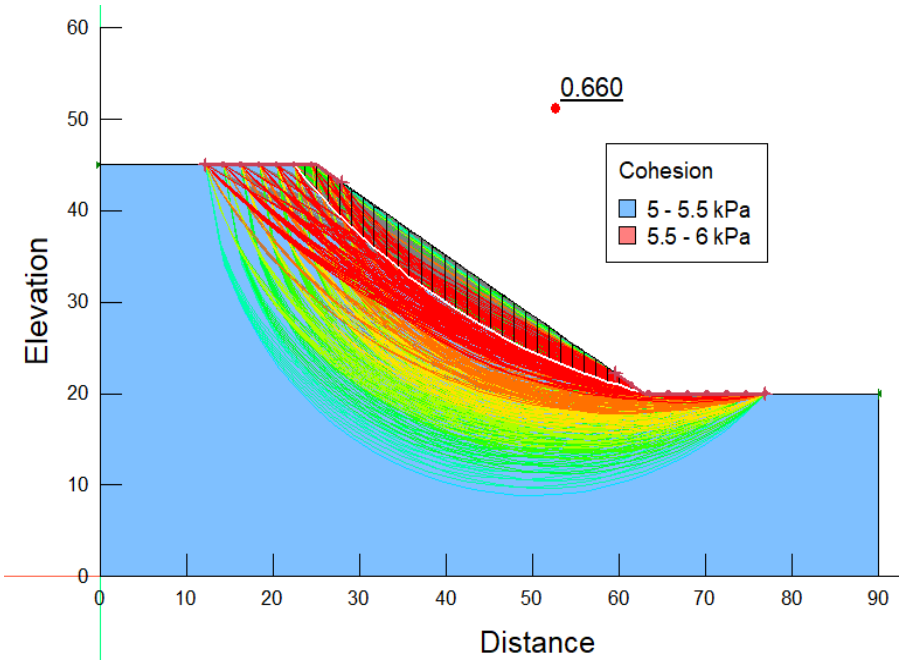

Fig 4.32 SLOPE/W results for L6 in dry conditions under dynamic loading

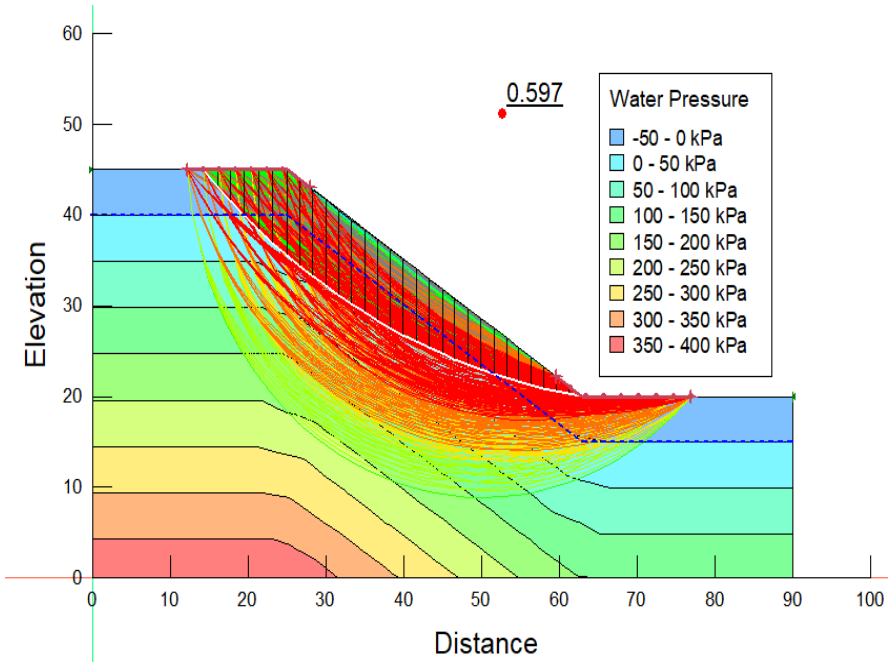

Fig 4.33 SLOPE/W results for L6 in saturated conditions under dynamic loading

4.8 Coherence of database (dynamic)

This study looked at 92 field examples of slope stability analysis,

including 80 cases with slope cases that were previously described in the literature and 12 cases with significant locations in the Kalimpong region whose outcomes had already been published. The database contains information about the geometry, stability condition, slope location, and geological conditions that were found during fieldwork and that consider seven input parameters (i.e., seven independent factors). After the creation of the primary database, its features were classified and given labels. If the evaluated FOS values were less than 1.00, they were categorised as unstable; if they were more than or equal to 1.00, they were categorised as stable. This well-known and experimentally proven classification technique offers adaptability in a variety of contexts. Next, a signal with one dependent component that may be categorised as "stable" or "failure" will be used to assess the slope's stability. To make the application of ML models simpler, the terms "failure" and "stable" were represented as 0 and 1 during prediction and subsequently transformed to these values. Seven different factors were used to harmonize each and every data set. The geometric and geological requirements of slopes were characterized by seven parameters (UW, C, Phi, SA, SH, K_h, and K_v) with a single dependent outcome. These seven characteristics were then used to generate the input features for the classification models. Slope occurrences were classified as either S or F based on their stability state. Because of the data integration, every specimen attribute is distinct, contains valuable information, and exhibits precise signs. 45 of the dataset's 92 rows are categorised as "stable," while the remaining 47 are categorised as "failure" The 1:1.04 ratio between these two clusters indicates that the signals are dispersed nearly evenly. The violin charts for each parameter are shown in Figs. 4.34(a-g). The median is shown by the white circle in the middle of each figure. Summary statistics that provide more information about the data, such as the median, quartiles, and possible outliers, are usually shown inside each violin as a box plot or horizontal line. All things considered, the violin plot provides a straightforward and educational way to show how data is distributed and fluctuates over multiple groups or categories. The box spectrum is a statistical representation of a variable's quartile distribution. The box's ends represent the lower and higher degrees of variance, while the body represents the data concentration. In each violin plot, a thin black line indicates the 95% confidence level. In addition to providing a visual depiction of the

data's distribution, the violin plot's border or silhouette offers details on the data's density, range, central tendency, and symmetry. The findings demonstrate the data's stability and normal distribution.

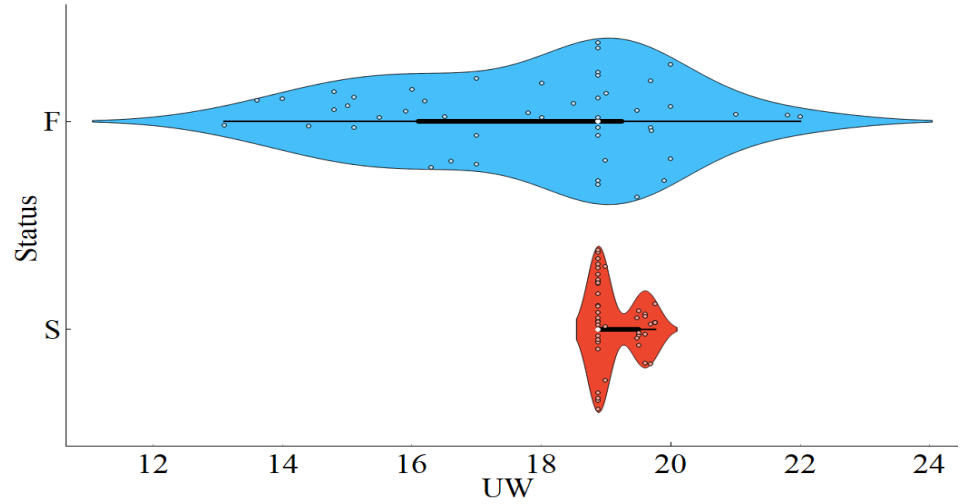

(a) UW

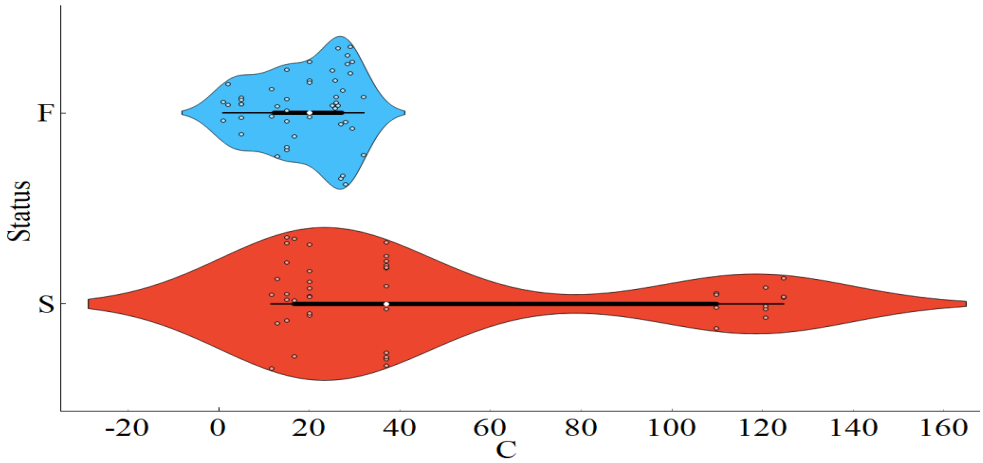

(b) C

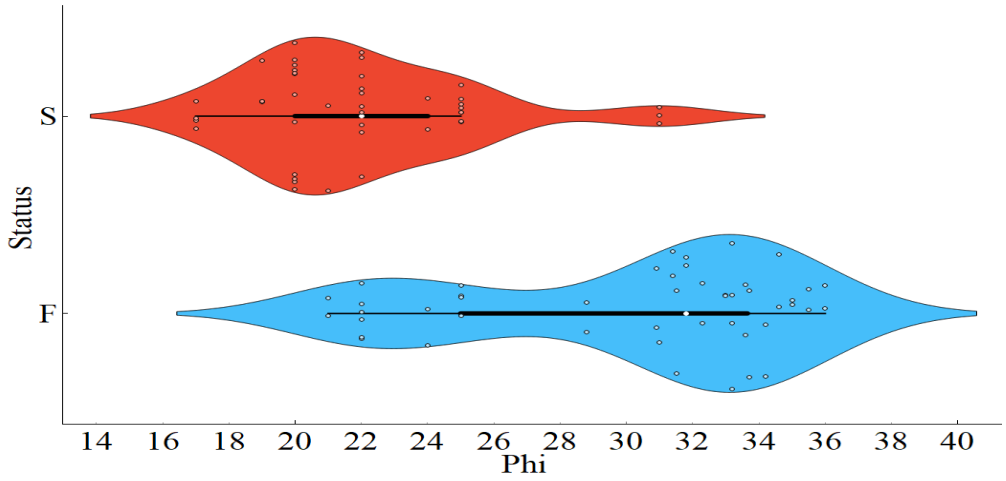
S
F
Status
14 16 18 20 22 24 26 28 30 32 34 36 38 40
Phi

(c) Phi

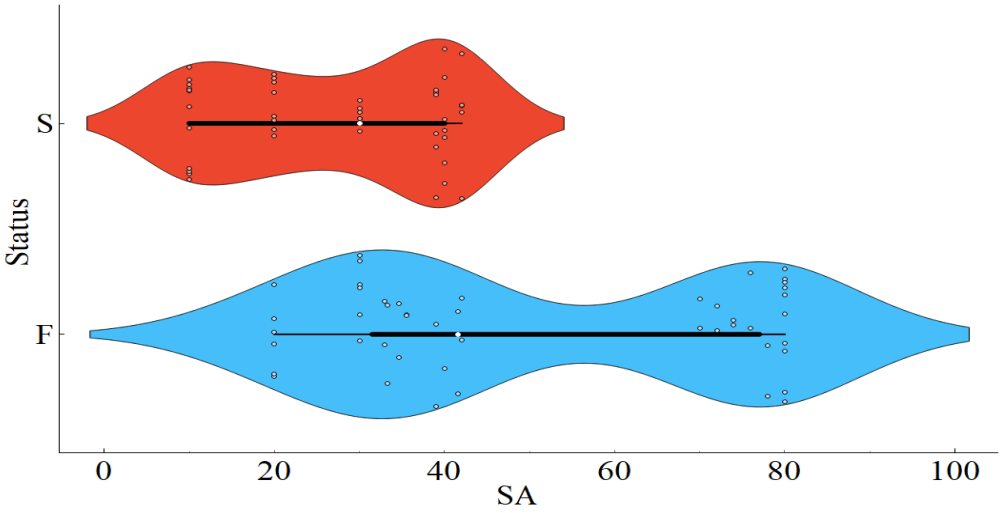
S
F
Status
0 20 40 60 80 100
SA

(d) SA

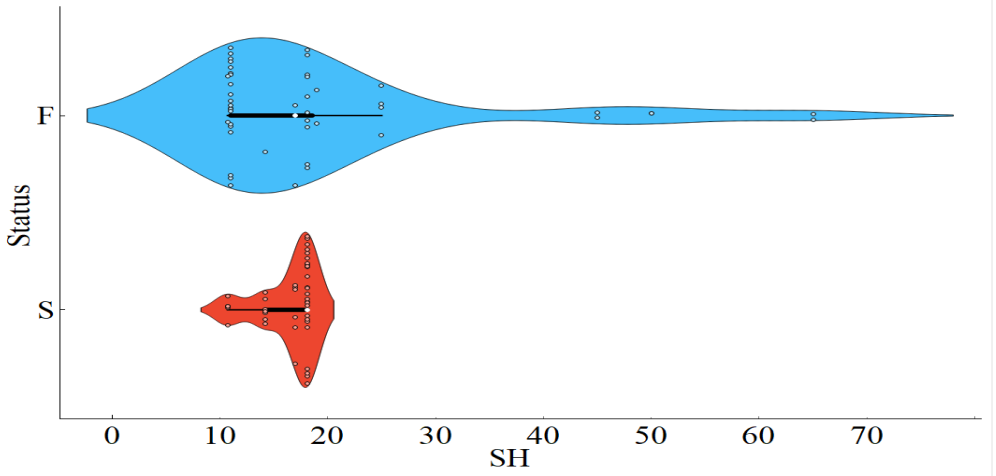
F
S
Status
0 10 20 30 40 50 60 70
SH

(e) SH

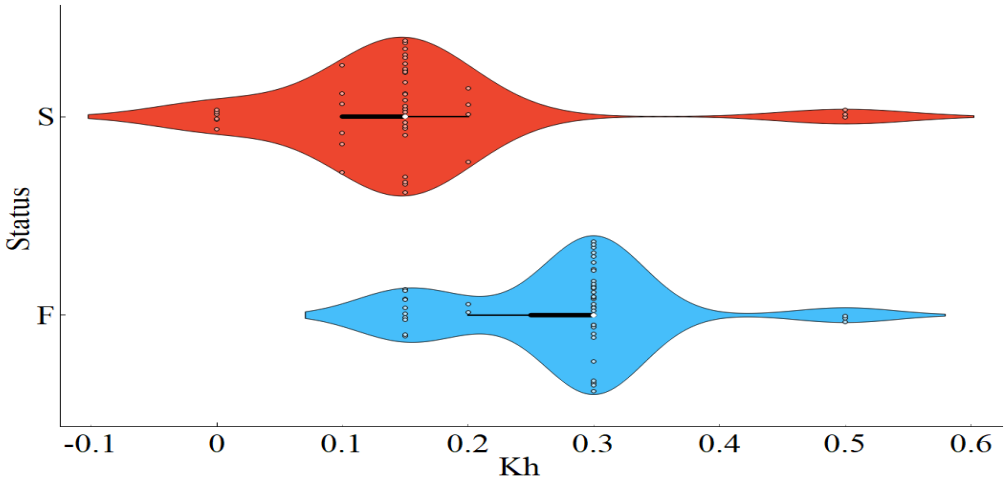

(f) K_h

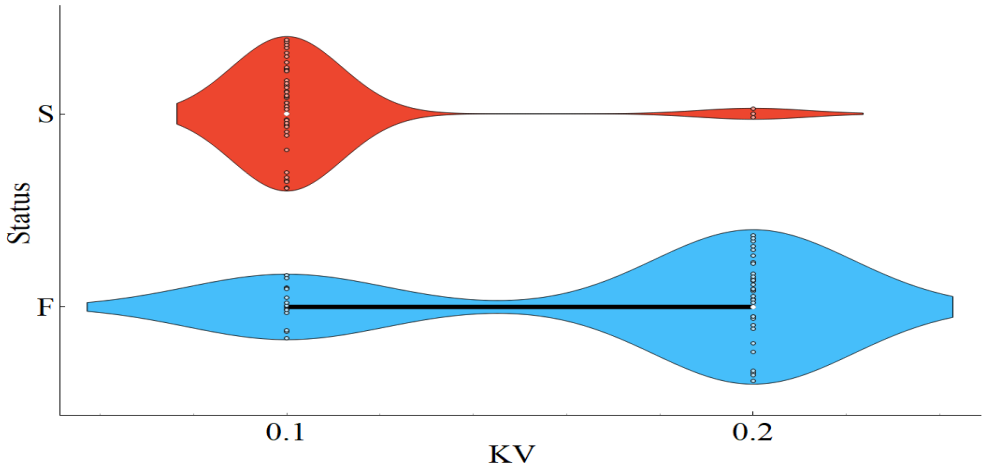

(g) K_v

Fig. 4.34 Standard kernel density Violin charts showcasing various input parameters

4.9 Statistical summary of the simulated dataset for dynamic modeling

To identify distributional tendencies that could be statistically summarised, a preliminary analysis of the simulation data was conducted prior to creating a prediction model. According to statistics, the values of these variables span wide ranges, indicating that the database includes a range of soil types and slope scenarios. For each characteristic, this section examines several statistics to see if the data or parameters have a "skewness" distribution. Because the seven sources have various SI units and meanings, they are all analysed independently. The means,

medians, modes, lowest and maximum values, standard deviations, and dispersion are given for the relevant data in Table 4.4 and Fig. 4.35 displays the mean and variability of normal distribution of different parameters.

Table 4.4 Statistical breakdowns of the five variables in the database under consideration

Indices	Mean	Median	Mode	Max.	Min.	Standard Deviation	Dispersion
Unit Weight	18.4467	18.875	18.875	22	13.1	1.724	0.093
Cohesion	33.6348	22.5	15	124.6	1	34.43	1.0181
Internal Friction angle	26.059	25	22	36	17	5.864	0.224
Angle of slope	39.391	37.25	20	80	10	22.369	0.565
Height of slope	18.093	18.093	18.093	65	10.7	10.298	0.566
Horizontal pseudostatic coefficient	0.2152	0.15	0.15	0.5	0	0.116	0.537
Vertical pseudostatic coefficient	0.13913	0.1	0.1	0.2	0.1	0.049	0.35078

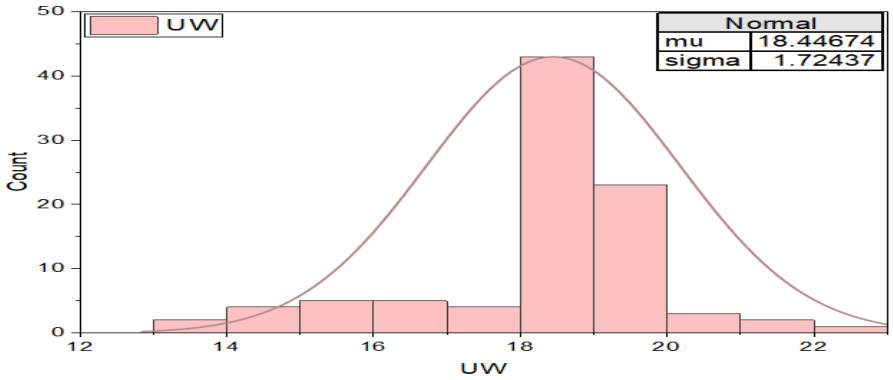

(a) UW

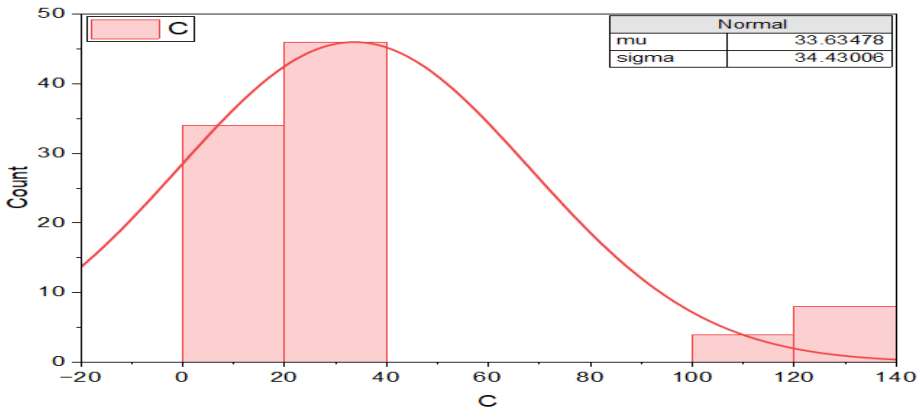
C
Normal
mu 33.63478
sigma 34.43006
Count
C

(b) C

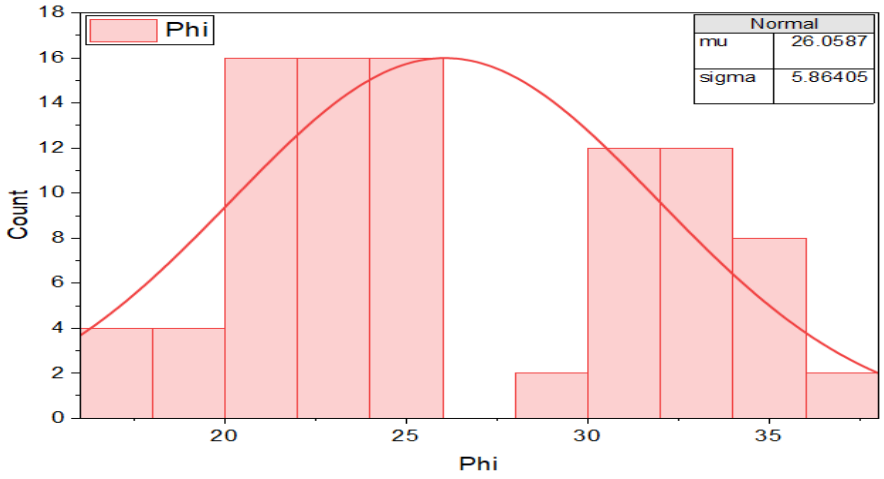
Phi
Normal
mu 26.0587
sigma 5.86405
Count
Phi

(c) Phi

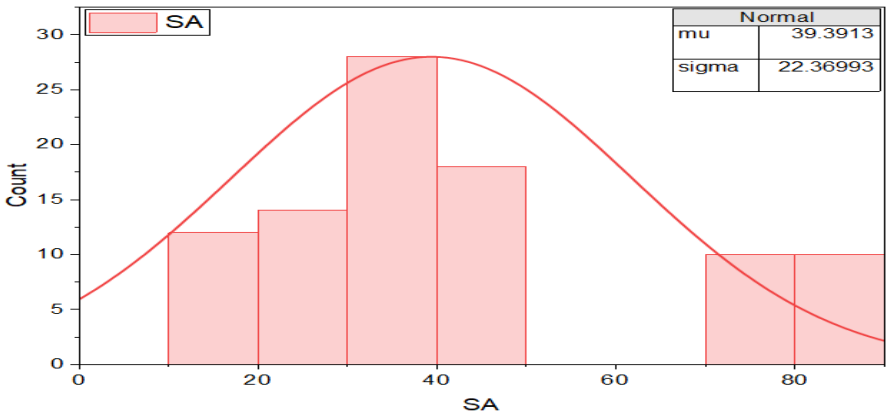
SA
Normal
mu 39.3913
sigma 22.36993
Count
SA

(d) SA

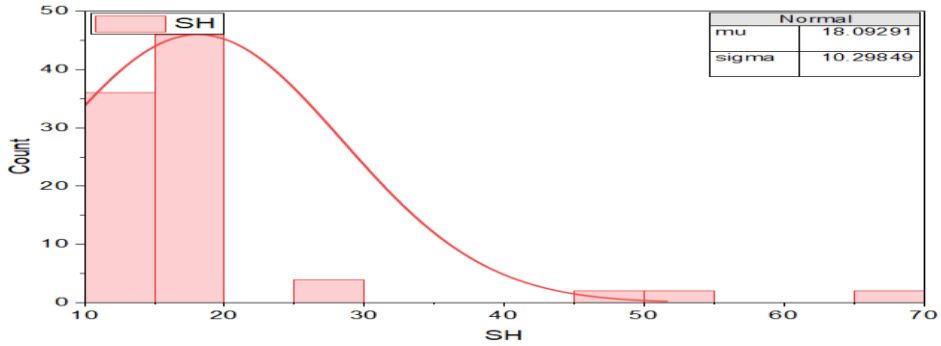

(e) SH

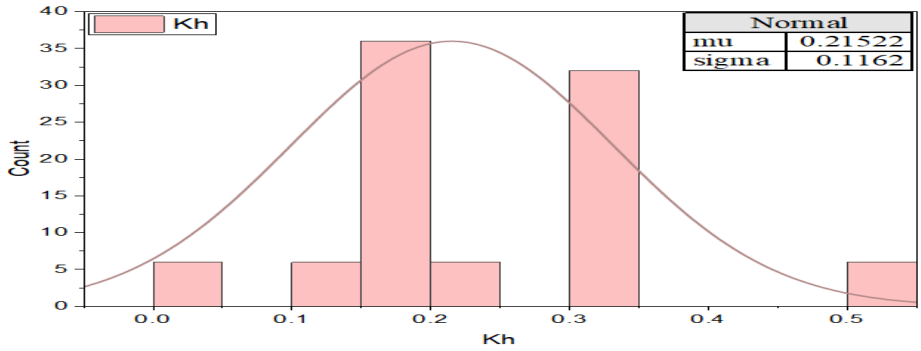

(f) K_h

Fig. 4.35 Distribution histogram of different indexes

4.10 Assessment of correlations among parameters for dynamic modeling

Evaluating slope stability was complex due to its variability. Limit Equilibrium Methods (LEMs) were used to calculate the factor of safety (FOS) for each slope individually. Prediction algorithms assessed slope conditions based on categorized data. Standardizing this data before training was crucial. Additionally, analyzing the relationships among the seven factors was essential, as incorrect assumptions could lead to false conclusions. The effectiveness of the prediction models relied on identifying meaningful correlations between these attributes. The "Pearson's correlation coefficient" equation, whose values range from -1 to 1, can be used to find the correlation between any two items (Cohen et al., 2009). A correlation value nearer one suggests a strong association between the components, whilst a number farther away suggests a weaker relationship. Using drawing software, a "correlation matrix" was created to help visualise the ranges and affiliations of the variables and improve comprehension of the connections in Fig. 4.36. This matrix demonstrated the independent significance of each feature in determining slope stability by examining the correlations between the index parameters that are used as inputs in ML prediction

models.

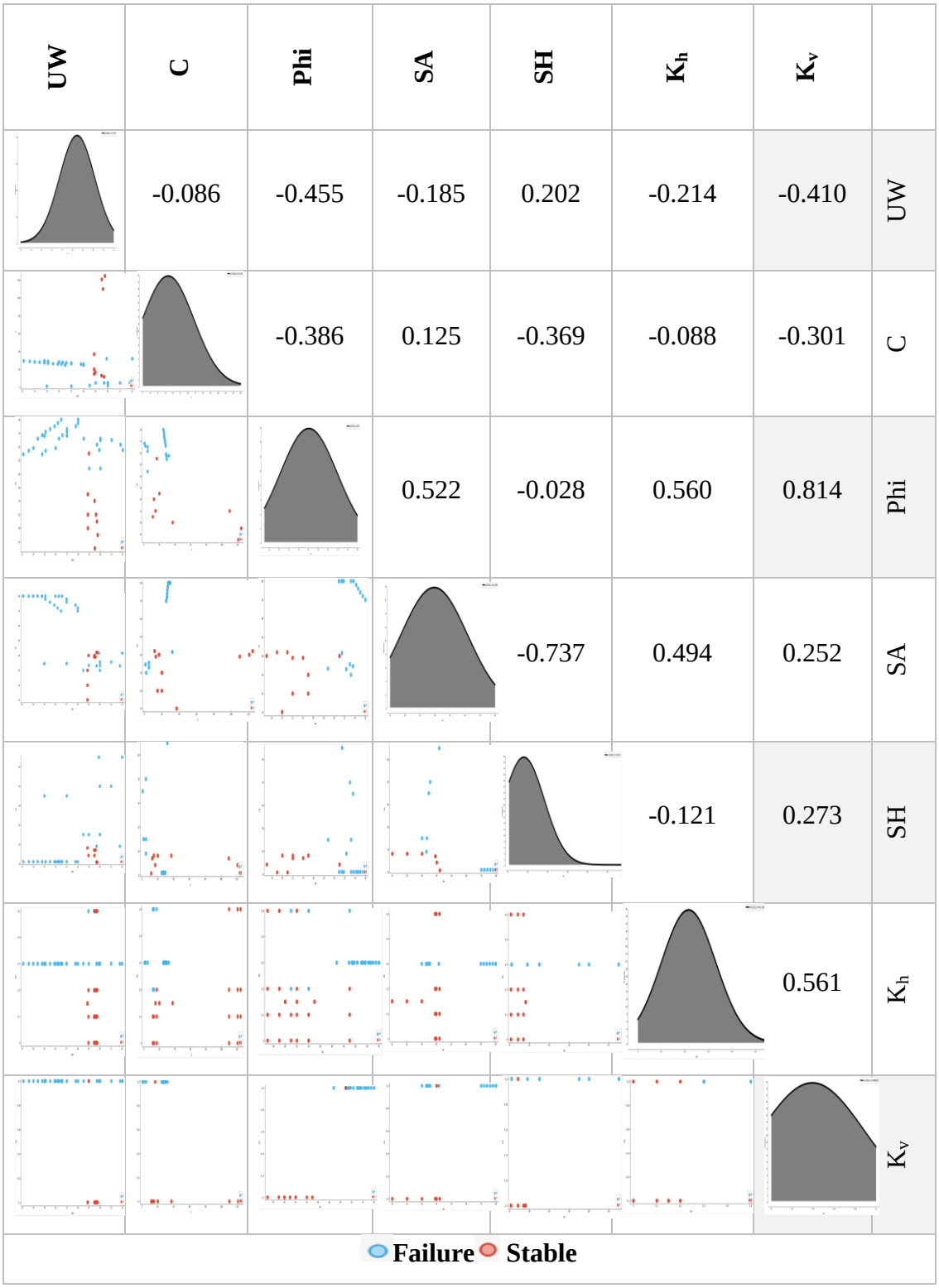

Fig. 4.36 Correlation matrix for parameters undergoing dynamic modeling

4.11 Model based predictions (dynamic)

4.11.1 Traditional Machine Learning Models (dynamic)

The seven supervised models utilised in this study are SVM, KNN, DT, RF, LR, Adaboost and GB. A highly effective supervised machine learning technique for classification and regression applications is the Support Vector Machine (SVM). Its primary objective is to determine the best hyperplane to split the data into several groups (Samui, 2008). Decision trees are flexible and easily understood machine learning models that are frequently employed in both regression and classification applications. They serve as a fundamental building block for more intricate algorithms like Random Forests and Gradient Boosting and offer practical insights and prediction capabilities across a range of fields (Hwang et al., 2009). K-Nearest Neighbours (KNN), a supervised machine learning technique, is simple and widely used. It can be applied to both regression and classification tasks. Since it is instance-based and non-parametric, it makes predictions based on the similarity of data points rather than making any assumptions about the distribution of the underlying data. One well-known and commonly applied statistical and machine learning technique for binary classification problems is logistic regression (Bhagat et al., 2022). Random Forest is a versatile and efficient ensemble learning technique that may be applied to regression and classification tasks. In order to produce more precise and reliable predictions, this decision tree extension trains many decision trees and then aggregates their predictions (Xie et al., 2022). Adaptive Boosting, or AdaBoost, is an ensemble learning method that builds a strong prediction model by combining weak learners (Lin et al., 2021). Gradient Boosting is widely used in several machine learning competitions and real-world applications due to its high accuracy and robustness (Feng et al., 2018).

4.11.2 Parameters and Techniques undertaken for dynamic modeling

Slope stability is examined in this study using both qualitative and quantitative criteria. Numerical constraints include UW, C, Phi, SA, SH, K_h, and K_v. On the other hand, the qualitative aspects take into account the prominence of the rocks and soil, failure patterns, and physical features. The primary goal is to

determine a slope's stability, or whether it is stable or prone to failure, and this is done by numerical computations. However, the lack of sufficient instances of field data makes it difficult to quantify qualitative qualities. In order to address this, the researchers developed prediction models based on these seven factors using machine learning techniques. Slopes are classified as "stable" or "unstable" in these models. Because interstitial water pressure has different rules for assigning values and is unpredictable in real-world situations, the modelling notably does not take this into account. The study confirms the accuracy of the five indicators selected to describe slope stability based on an examination of 92 slope data case sets. Using a multi-fold method and traditional cross-validation procedures, a slope stability forecasting model is built on the selected testing dataset. After this procedure is completed five times, the mean of those estimations is the end result. The "Python" programming language makes it easier to construct randomised cross-validation. Due to space constraints, the article can only show "scatter plots" and "linear fitting curves" in Fig. 4.37 to illustrate the correlations between various parameters and unit weight. Various visualizations aid in elucidating the potential impacts of various variables on slope stability.

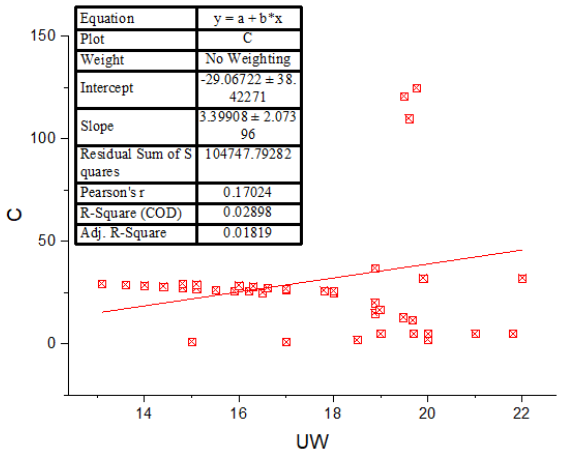

(a)

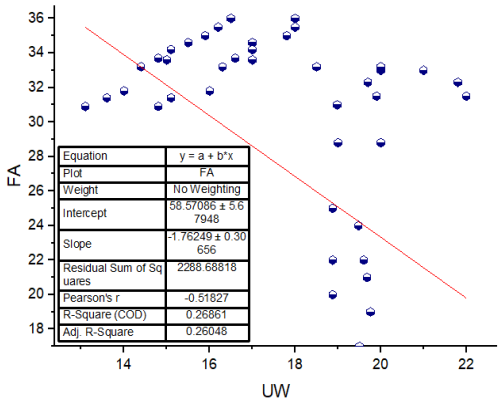

(b)

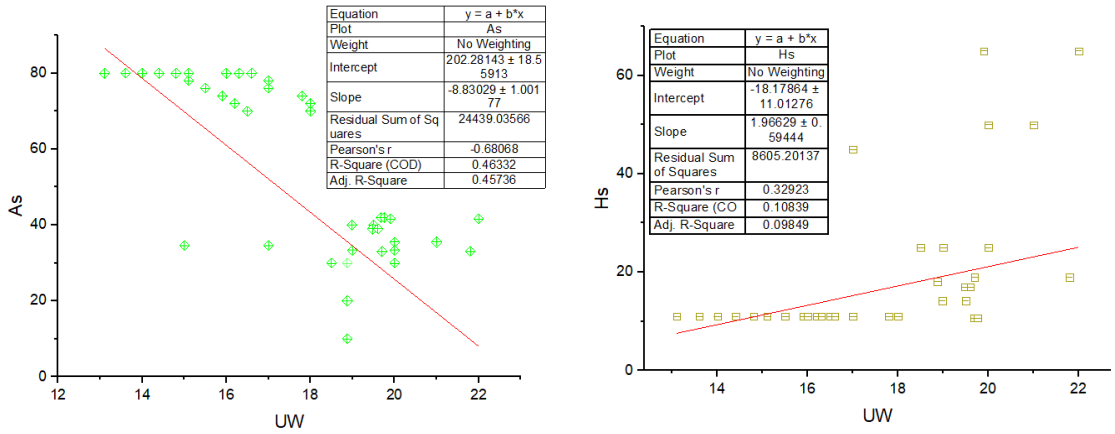

(c) (d)

Fig. 4.37 Line and scatter plots of various parameters fit with regression

4.11.3 Models Evaluation (dynamic)

Key evaluation metrics already discussed above are used to evaluate the performance of the machine learning models in binary classification scenarios (where there are two classes, sometimes labelled as positive and negative).

4.12 Examination of results from predictions (dynamic)

4.12.1 Evaluation of the model using the raw data

The outcomes of seven machine learning models used as well as one stacked SVM-Boost model are compared in this section. The model outputs were tested using a variety of performance indicators. This approach is frequently used in training and model building to assess a model and decide if it is appropriate. However, the results of the training phase indicated that the proposed AdaBoost model may be considered perfect. Along with one stacking strategy called SVM-Boost, which combines Support Vector Machine and AdaBoost to do the random cross evaluation, seven different machine learning algorithms are demonstrated.

AUC is a crucial machine learning statistic that offers a trustworthy and understandable assessment of a model's ability to classify binary data, especially when the datasets are unbalanced. Adaboost provides the best average AUC (0.956), with GB (0.952) and SVM-Boost (0.955) following closely after. With an average classification accuracy of 0.878, SVM-Boost demonstrates the strongest prediction

ability. Accuracy scores for SVM and AdaBoost were 0.865 and 0.834, respectively. AdaBoost is an ensemble learning strategy that adds extra weight for misclassified events to iteratively improve the performance of weak learners (like decision trees). SVM, on the other hand, is a powerful binary cataloguing method that finds the best hyperplane for each class inside a feature space. SVM's ability to recognise a solid decision boundary and AdaBoost's ability to focus on challenging cases during training can be combined to provide a successful outcome. This combination can sometimes lead to improved performance, especially when dealing with complex or challenging-to-separate information. The conjecture models SVM-Boost, AdaBoost, and SVM are shown in Table 4 with F1 values higher than 83%. Additionally, the AUC values of SVM-Boost, AdaBoost, and SVM with Gradient Boosting are higher than 95%. According to performance metrics, SVM-Boost and SVM are therefore regarded as the most accurate predictors, which also increases the novelty factor of the study report. Metrics including accuracy, precision, recall, F1-score, and AUC of ROC are used to compare the testing stage outcomes in Table 4.5.

Table 4.5 Metrics for assessment across multiple ML techniques

Evaluation Metrics	Folds	AdaBoost	Gradient Boosting	kNN	Logistic Regression	Random Forest	SVM	Tree	SVM-Boost
Area under the Curve	2	0.9602837	0.9567376	0.9156028	0.8921986	0.9177305	0.9413712	0.9451537	0.9607565
	3	0.9607565	0.9550827	0.9141844	0.9269504	0.9333333	0.9399527	0.9482270	0.9598109

Classification Accuracy								
20	10	5	3	2	Average	20	10	5
0.8260870	0.8260870	0.8260870	0.8478261	0.8478261	0.9569267	0.9612293	0.9510638	0.9513002
0.8043478	0.8369565	0.8478261	0.8369565	0.8369565	0.9523404	0.9508274	0.9463357	0.9527187
0.8152174	0.8152174	0.8043478	0.7717391	0.7608696	0.9193853	0.9340426	0.9186761	0.9144208
0.7826087	0.8152174	0.8260870	0.8043478	0.7826087	0.9214184	0.9328605	0.9276596	0.9274232
0.8152174	0.8260870	0.8043478	0.8478261	0.7934783	0.9245863	0.9390071	0.9245863	0.9082742
0.8695652	0.8695652	0.8586957	0.8695652	0.8586957	0.9406619	0.9513002	0.9416076	0.9290780
0.8043478	0.8260870	0.8478261	0.8260870	0.8260870	0.9418913	0.9349882	0.9423168	0.9387707
0.8913043	0.8913043	0.8586957	0.8586957	0.8913043	0.9556028	0.9527187	0.9543735	0.9503546

Precision		F1 Score						
3	2	Average	20	10	5	3	2	Average
0.8478261	0.8483420	0.8346880	0.8259225	0.8260870	0.8259225	0.8478261	0.8476820	0.8347826
0.8386240	0.8381677	0.8323579	0.8041628	0.8366673	0.8473938	0.8368987	0.8366667	0.8326087
0.7744565	0.7786896	0.7906681	0.8120319	0.8120319	0.8024765	0.7707897	0.7560106	0.7934783
0.8047399	0.7829389	0.8020672	0.7826087	0.8152392	0.8259225	0.8041625	0.7824028	0.8021739
0.8591847	0.7944410	0.8167105	0.8151519	0.8250965	0.8032335	0.8469594	0.7931112	0.8173913
0.8970252	0.8809955	0.8634271	0.8676938	0.8676938	0.8570269	0.8676938	0.8570269	0.8652174
0.8265409	0.8282494	0.8257327	0.8041628	0.8255929	0.8473938	0.8259223	0.8255917	0.8260870
0.8676212	0.9110672	0.877311	0.8902692	0.8902692	0.8576378	0.8581096	0.8902692	0.8782609

Recall									
Average	20	10	5	3	2	Average	20	10	5
0.8347826	0.8260870	0.8260870	0.8260870	0.8478261	0.8478261	0.8360083	0.8288933	0.8260870	0.8288933
0.8326087	0.8043478	0.8369565	0.8478261	0.8369565	0.8369565	0.8358859	0.8070304	0.8413561	0.8542511
0.7934783	0.8152174	0.8152174	0.8043478	0.7717391	0.7608696	0.8066705	0.8335281	0.8335281	0.8131503
0.8021739	0.7826087	0.8152174	0.8260870	0.8043478	0.7826087	0.8030749	0.7833488	0.8154537	0.8288933
0.8173913	0.8152174	0.8260870	0.8043478	0.8478261	0.7934783	0.8243668	0.8168231	0.8368566	0.8145285
0.8652174	0.8695652	0.8695652	0.8586957	0.8695652	0.8586957	0.8906133	0.8970252	0.8970252	0.8809955
0.8260870	0.8043478	0.8260870	0.8478261	0.8260870	0.8260870	0.8296544	0.8070304	0.8322001	0.8542511
0.8782609	0.8913043	0.8913043	0.8586957	0.8586957	0.8913043	0.8948595	0.9110672	0.9110672	0.8734744

4.12.2 ROC Curve for dynamic analysis

The ROC curve is a key tool for evaluating binary classification models, showing the trade-off between sensitivity and the false positive rate. As illustrated in Figures 4.38 and 4.39, Adaboost achieved the highest mean AUC (0.956), followed by SVM-Boost (0.955) and GB (0.952), while kNN had the lowest (0.91). SVM and SVM-Boost delivered the most accurate and reliable results, closely aligning with those from LEM. GB also showed strong performance and can serve as a reliable alternative. These machine learning models can effectively support future slope stability assessments and guide appropriate stabilization measures.

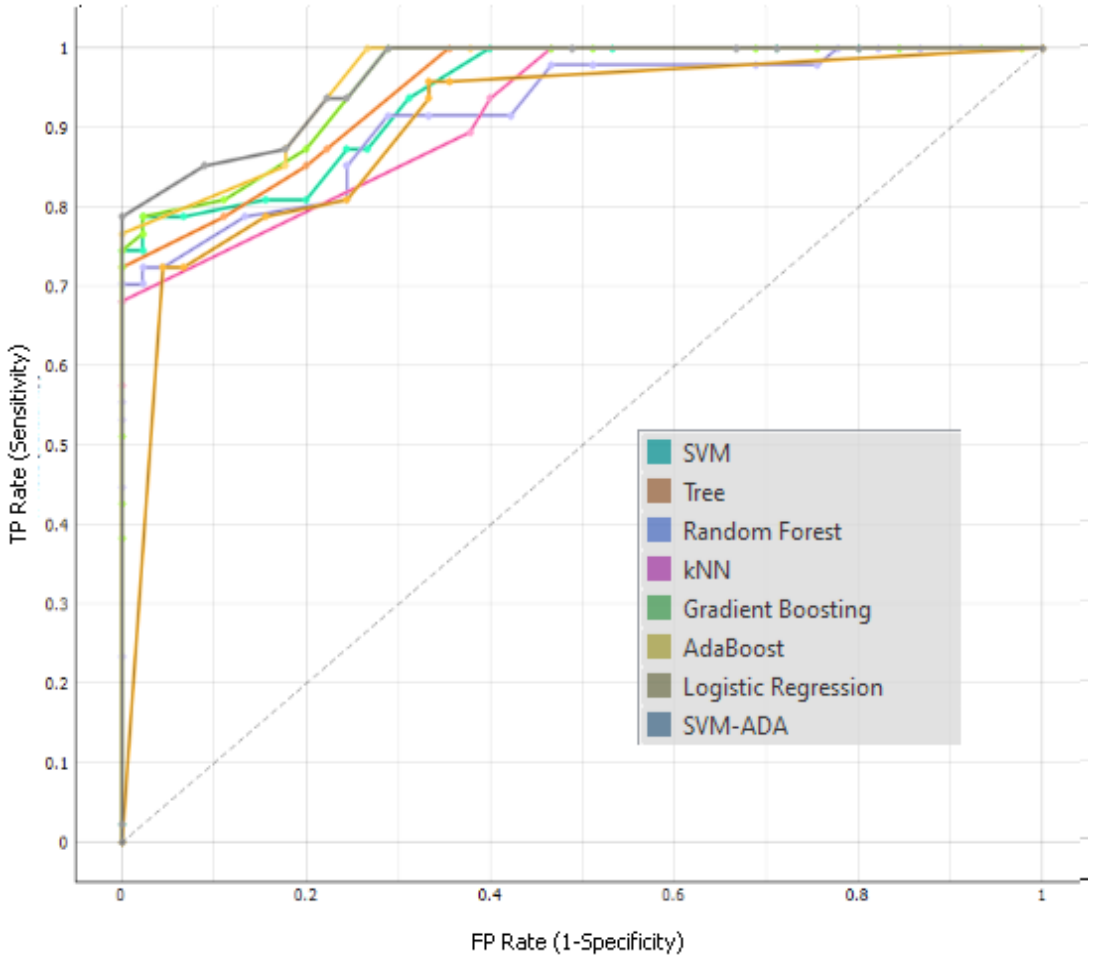

Fig. 4.38 ROC Curve (Failure)

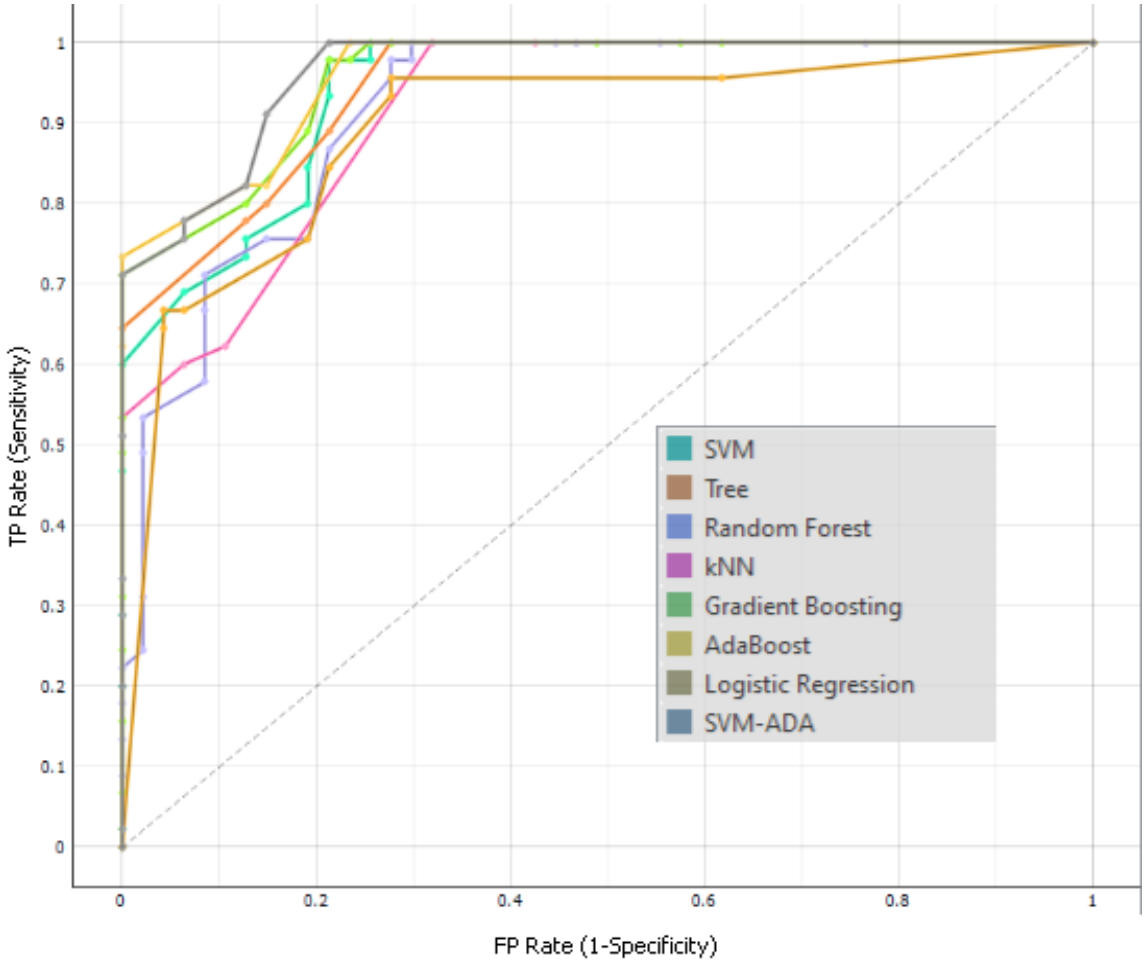

Fig. 4.39 ROC Curve (Failure)

4.12.3 Sensitivity Analysis for dynamic analysis

By comprehending how modifications to the input variables (criteria) impact the model's output or results, this aims to identify the quantitative and qualitative factors that most significantly affect slope stability. This is accomplished by using the CRITIC technique and a differentiation coefficient known as "Standard Deviation/Average" to separately establish the weightage for each parameter (Bhadra et al., 2022). Weighting is a crucial consideration based on the seven input factors displayed in Fig. 5.20. In percentage terms, this coefficient is 2.77, 30.35, 6.67, 16.84, 16.88, 16.01, and 10.46 for UW, C, Phi, As, Hs, Kh, and Kv, respectively. Out of all these attributes, cohesiveness has the biggest influence shown in Fig 4.40.

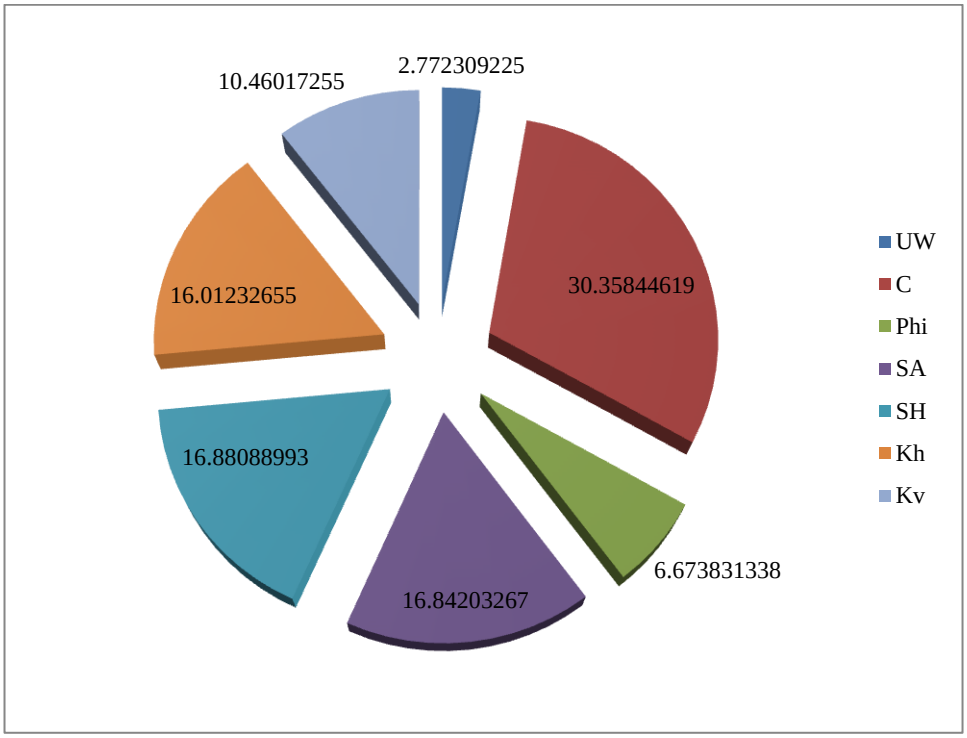

Fig. 4.40 Indicator representing each parameter's weight

4.12.4 Contrasting predicted outcomes with GeoStudio (dynamic)

Commercial software called GeoStudio was utilised to oversee the results of the prediction method that resulted in the F.S. evaluation. GeoStudio is a two-dimensional, fully integrated software suite that offers six finite element applications in many sub-models in addition to LEM-based stability analysis. In this investigation, the F.S. was calculated using the SLOPE/W and Morgenstern Price's approach. The information from this table was used by the SLOPE/W program and machine learning methods. Boundary conditions, stability solutions, behavioural and material characteristic assignment, and geometric modelling are all components of the multi-stage modelling approach that SLOPE/W employed. The estimated FOS and the outcomes of the ML prediction model were contrasted. Table 4.6 combines data from the FOS prediction model with the SLOPE/W program outcomes (F and S stand for Unstable and Stable, respectively). This table demonstrates how predictive models, particularly SVM-Boost, produce results that are near the FOS value when using their reasoning technique.

Table 4.6 Test outcomes regarding the stability condition criteria in Kalimpong (dynamic condition)

	C	UNIT WT.	FA	H_s	A_s	K_h	K_v	Prediction from SLOPE/W	SVM	AdaBoost	Stack- SVMBoost
L1 Dry	5	20	33	50	35.5	0.3	0.2	F	F	F	F
L1 Sat.	5	21	33	50	35.5	0.3	0.2	F	S	F	F
L2 Dry	2	18.5	33.2	25	30	0.3	0.2	F	F	F	F
L2 Sat.	2	20	33.2	25	30	0.3	0.2	F	F	F	F
L3 Dry	1	15	33.6	45	34.6	0.3	0.2	F	F	F	F
L3 Sat.	1	17	33.6	45	34.6	0.3	0.2	F	S	F	F
L4 Dry	5	19.7	32.3	19	33	0.3	0.2	F	F	S	F
L4 Sat.	5	21.8	32.3	19	33	0.3	0.2	F	F	F	F
L5 Dry	32	19.9	31.5	65	41.6	0.3	0.2	F	F	F	F
L5 Sat.	32	22	31.5	65	41.6	0.3	0.2	F	S	S	S
L6 Dry	5	19	28.8	25	33.3	0.3	0.2	F	F	F	F
L6 Sat.	5	20	28.8	25	33.3	0.3	0.2	F	F	F	F

4.13 Results after stabilization done by Soil nailing

Furthermore, soil nailing can be combined with other stabilization methods such as shotcrete or mesh facing to enhance surface stability and erosion control, providing a comprehensive solution for slope stabilization. Its adaptability, cost-effectiveness, and ability to provide robust reinforcement make soil nailing a preferable choice for addressing challenging slope stabilization projects. In this

project, soil nailing technique with Fe 415 Steel nails has been implemented. In Fig. 4.41-4.64, slope models have been represented for all locations with nails which stabilize these slopes under dry and saturated conditions for static and dynamic loading respectively. The presented table 4.7 illustrates FoS values for six slope locations (L1 to L6) under varying conditions—static and dynamic loading both in dry and saturated states before and after stabilization measures were implemented. The data clearly demonstrates the effectiveness of the soil nailing stabilization technique as all locations show a significant improvement in FoS across every condition post-intervention. After stabilization, all FoS values improved, with many exceeding 2.0 in static dry conditions reflecting a marked enhancement in slope stability. This improvement highlights the stabilizing method's capacity to substantially reduce slope failure risks, especially under adverse moisture and seismic influences.

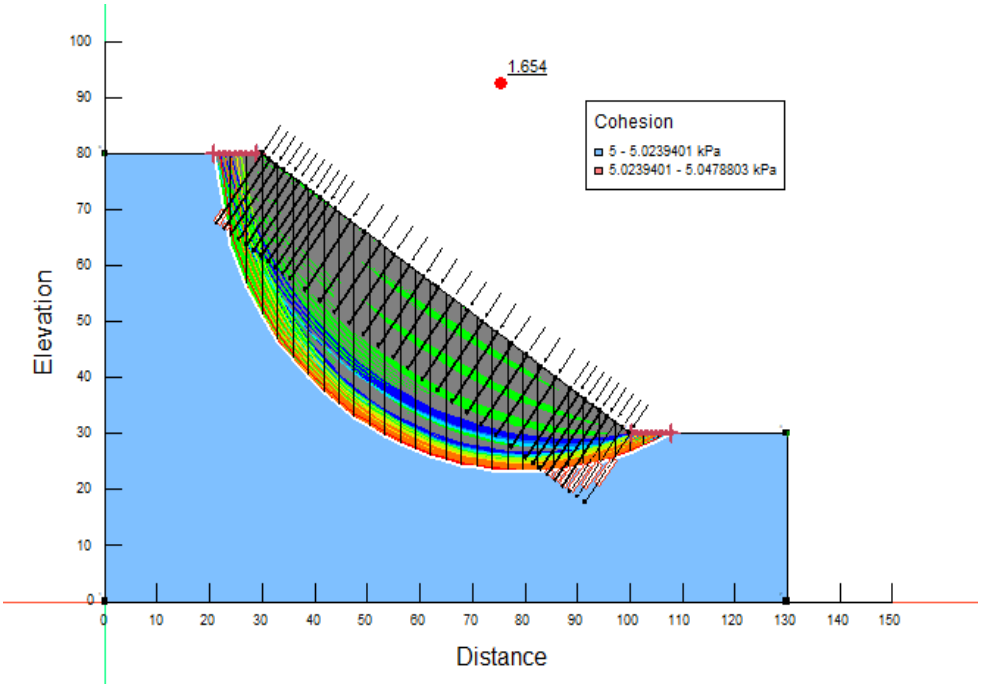

Fig. 4.41 Slope stabilization for L1 in Dynamic Dry condition (FOS=1.654)

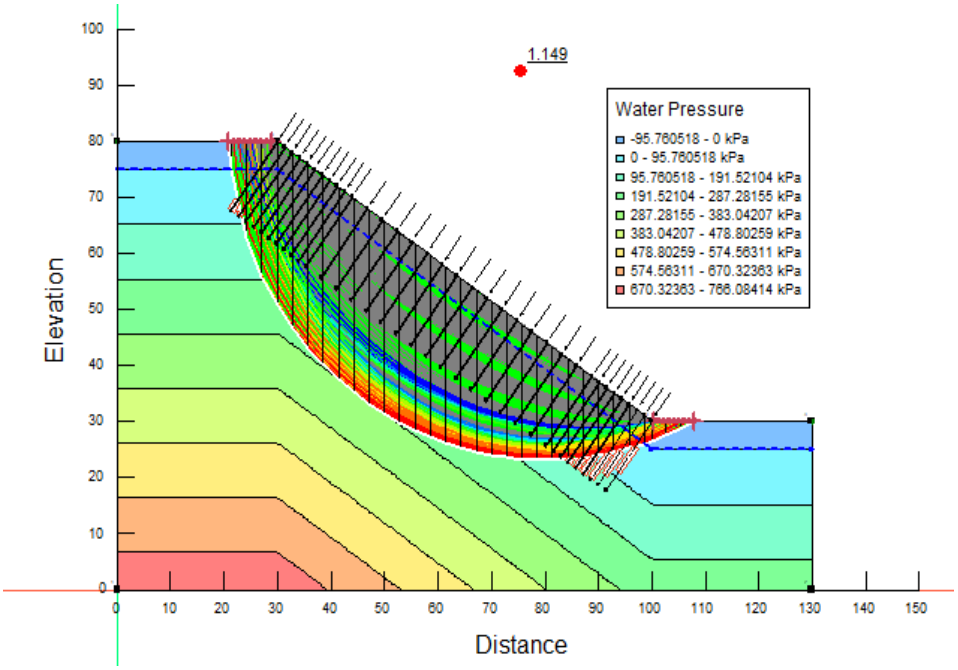

Fig. 4.42 Slope stabilization for L1 in Dynamic Saturated condition (FOS=1.149)

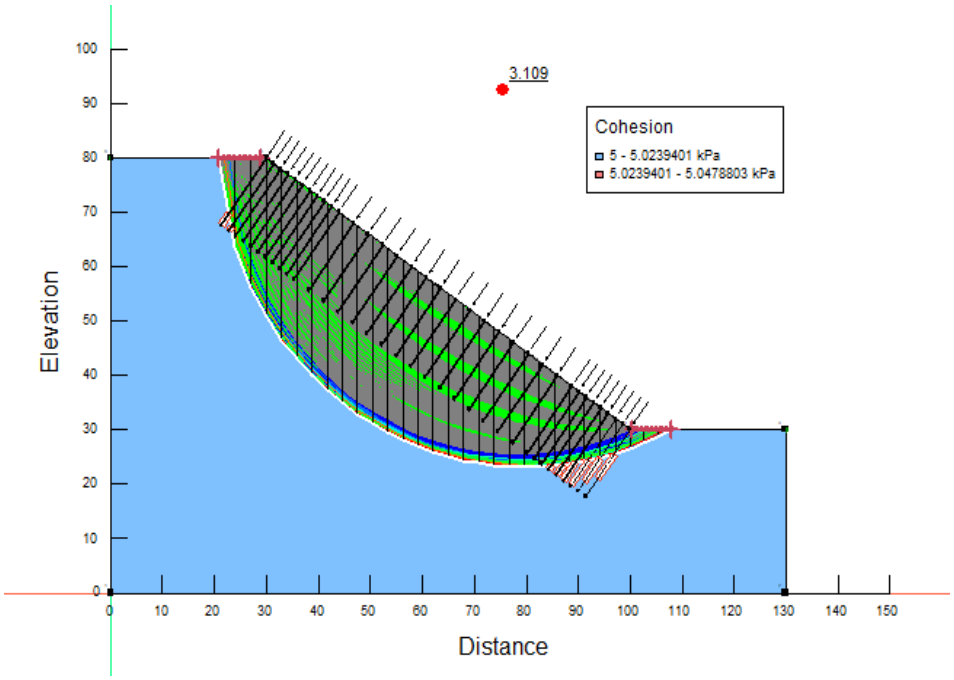

Fig. 4.43 Slope stabilization for L1 in Static Dry condition (FOS=3.109)

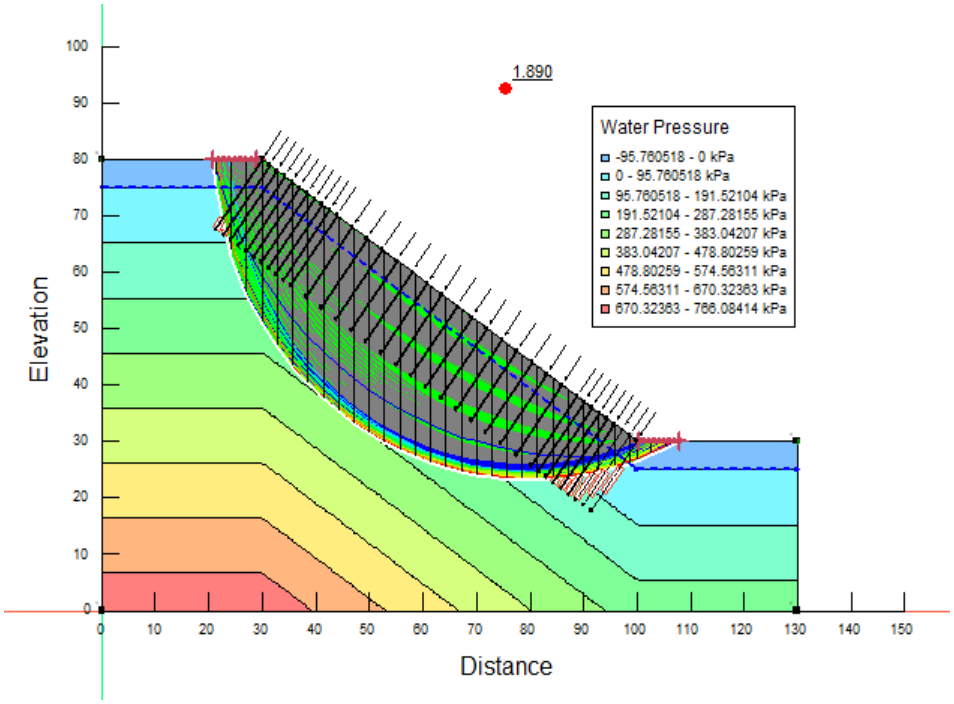

Fig. 4.44 Slope stabilization for L1 in Static Saturated condition (FOS=1.890)

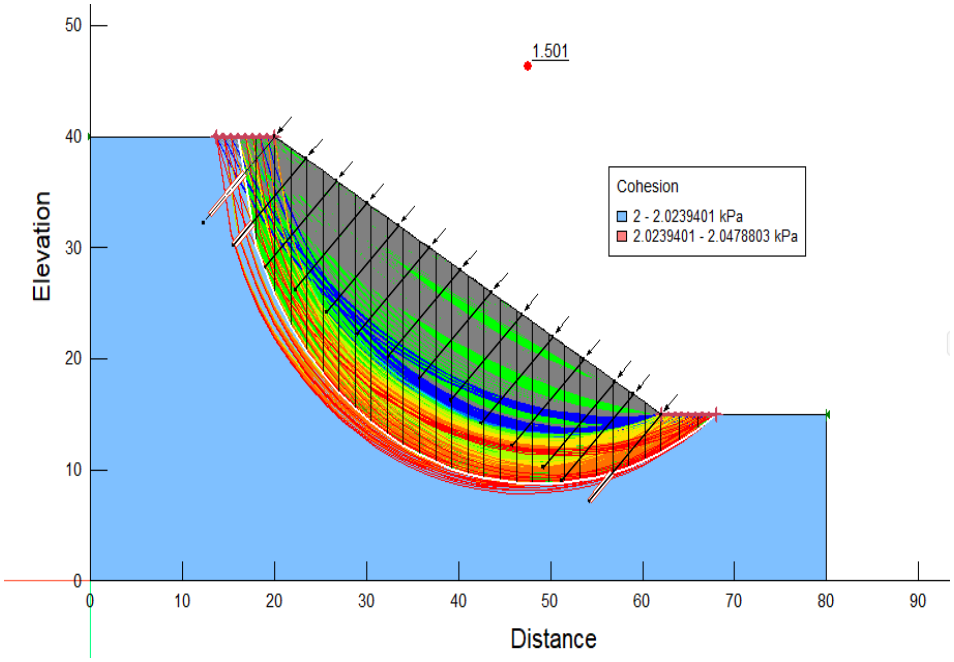

Fig. 4.45 Slope stabilization for L2 in Dynamic Dry condition (FOS=1.501)

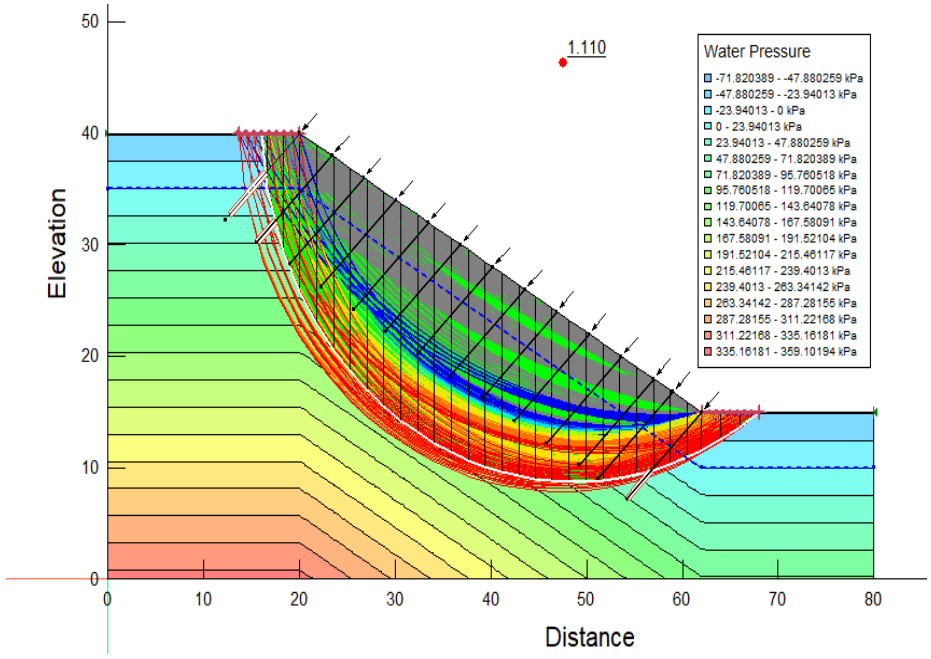

Fig. 4.46 Slope stabilization for L2 in Dynamic Saturated condition (FOS=1.110)

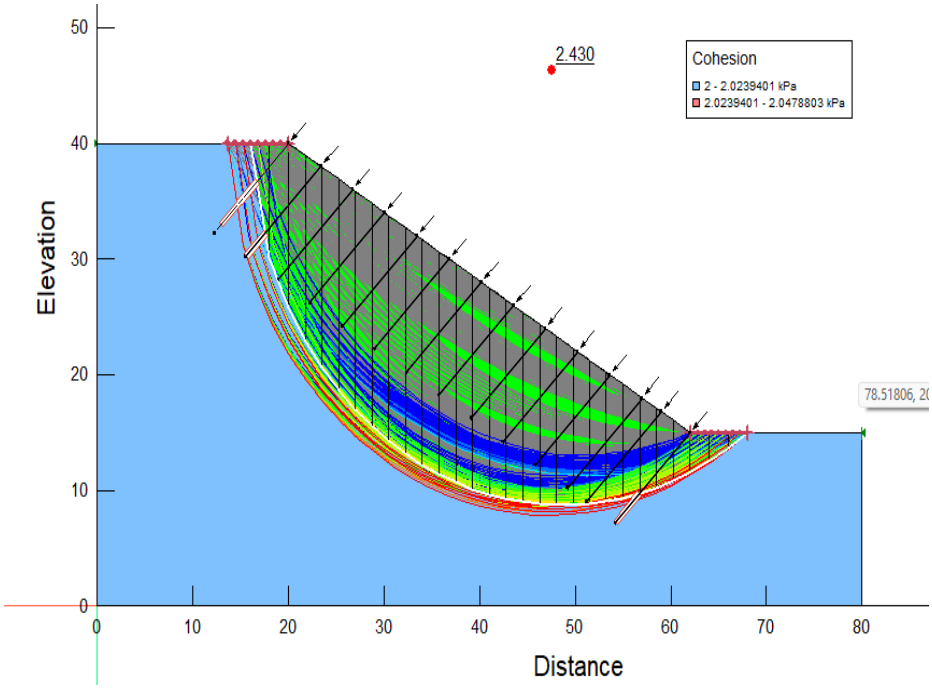

Fig. 4.47 Slope stabilization for L2 in Static Dry condition (FOS=2.430)

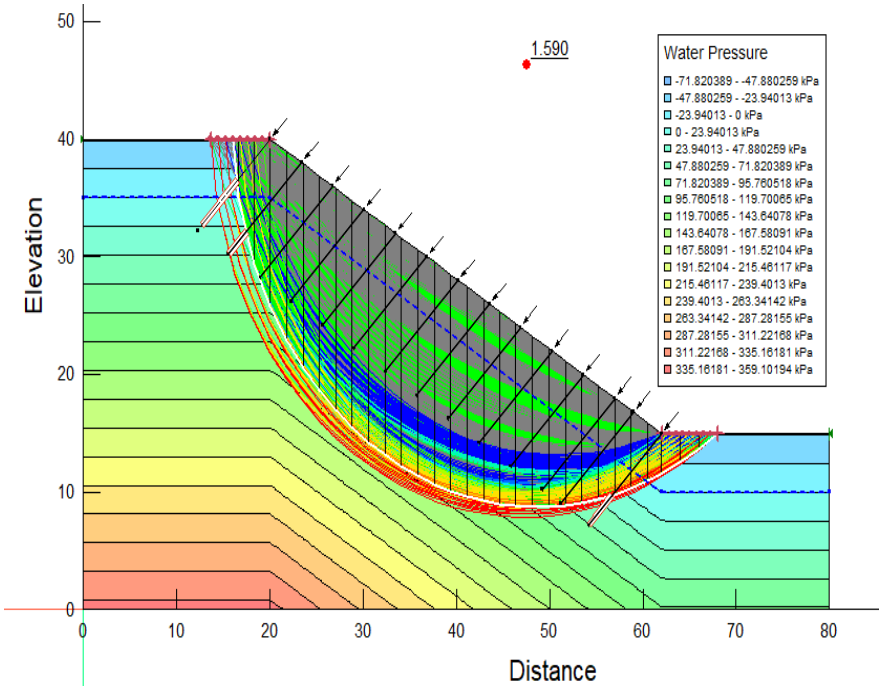

Fig. 4.48 Slope stabilization for L2 in Static Saturated condition (FOS=1.590)

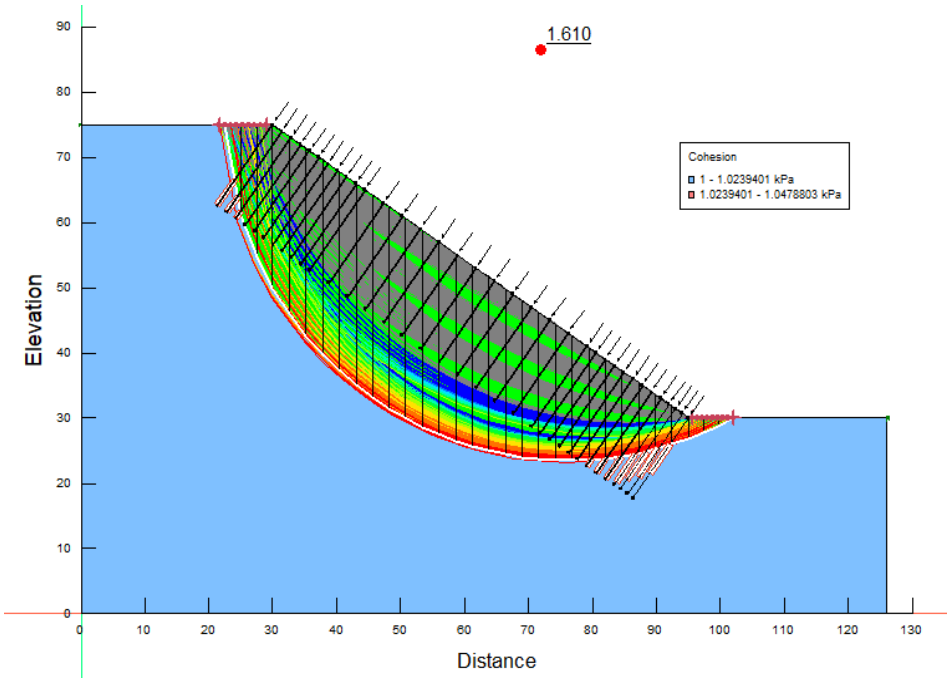

Fig. 4.49 Slope stabilization for L3 in Dynamic Dry condition (FOS=1.610)

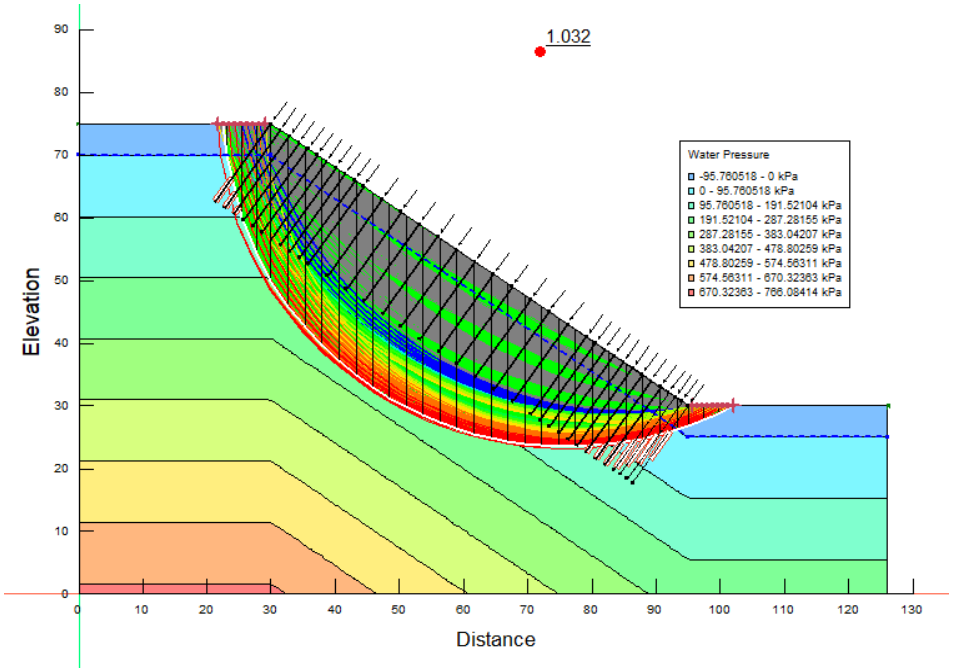

Fig. 4.50 Slope stabilization for L3 in Dynamic Saturated condition (FOS=1.032)

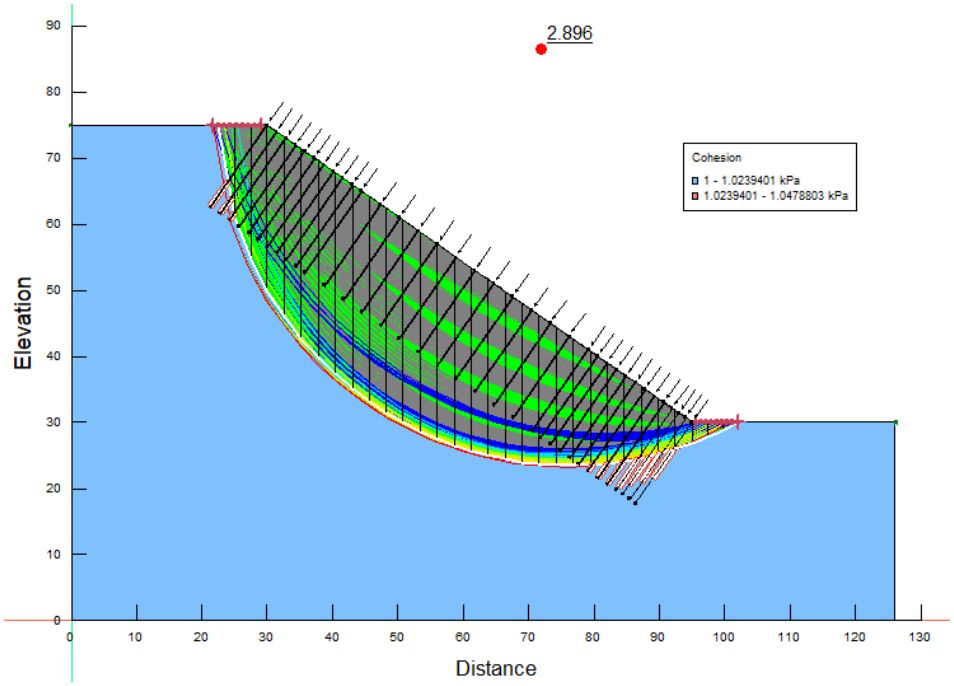

Fig. 4.51 Slope stabilization for L3 in Static Dry condition (FOS=2.896)

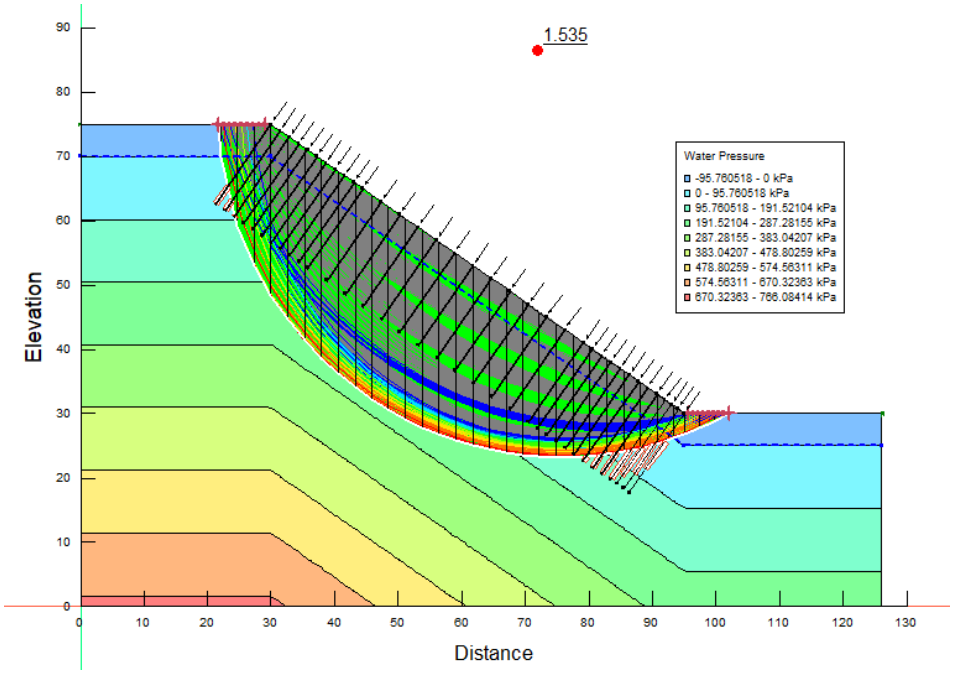

Fig. 4.52 Slope stabilization for L3 in Static Saturated condition (FOS=1.535)

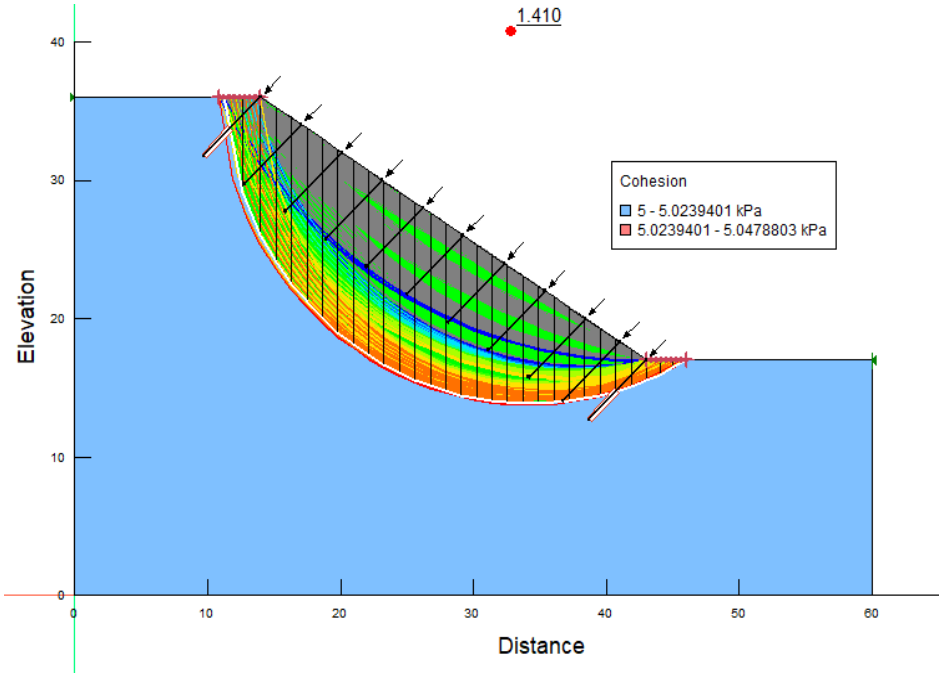

Fig. 4.53 Slope stabilization for L4 in Dynamic Dry condition (FOS=1.410)

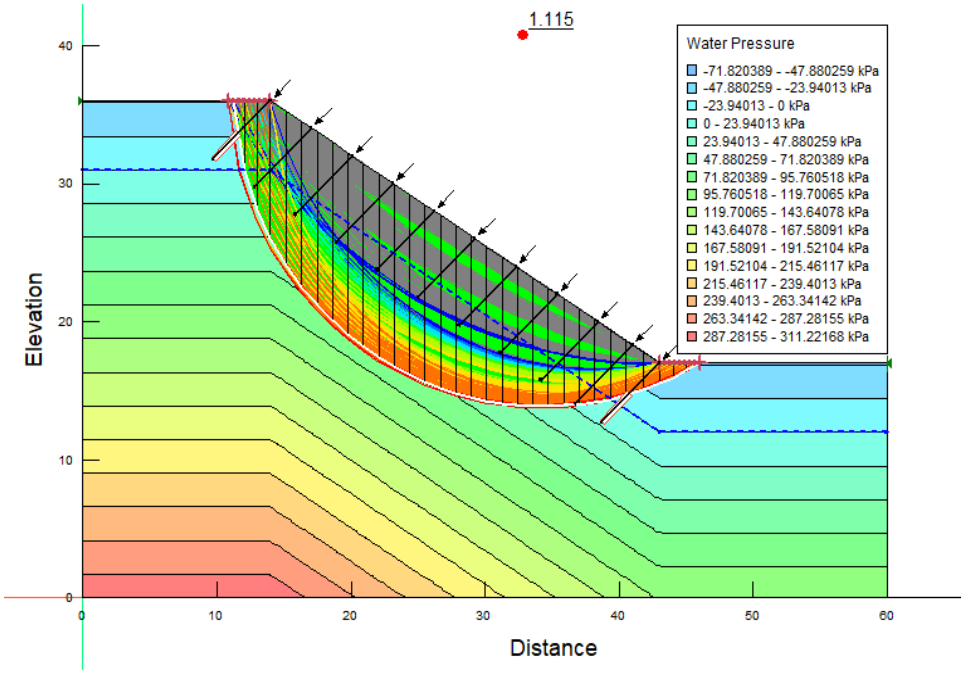

Fig. 4.54 Slope stabilization for L4 in Dynamic Saturated condition (FOS=1.115)

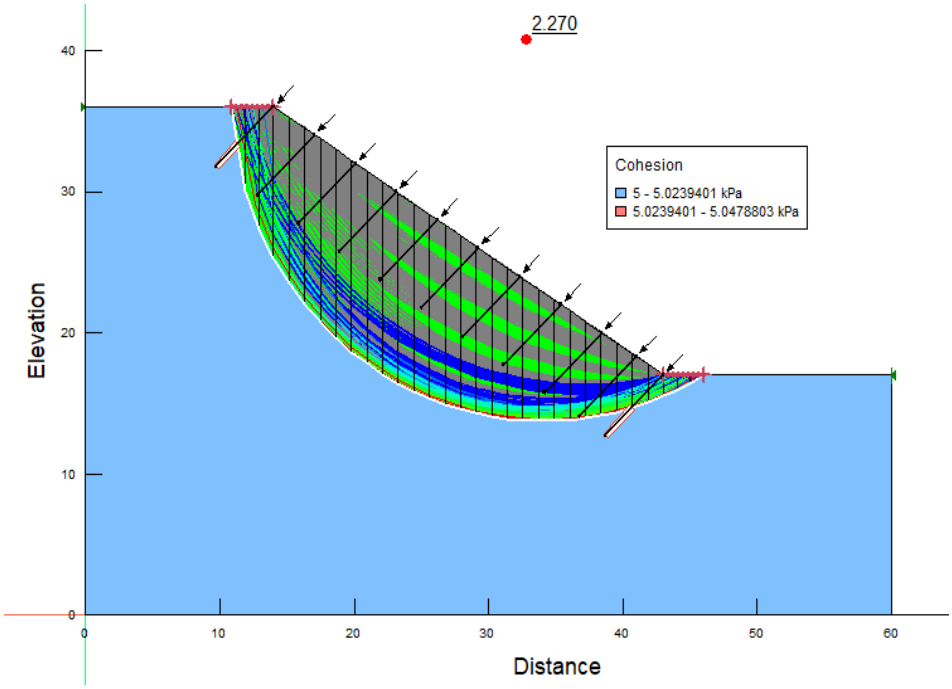

Fig. 4.55 Slope stabilization for L4 in Static Dry condition (FOS=2.270)

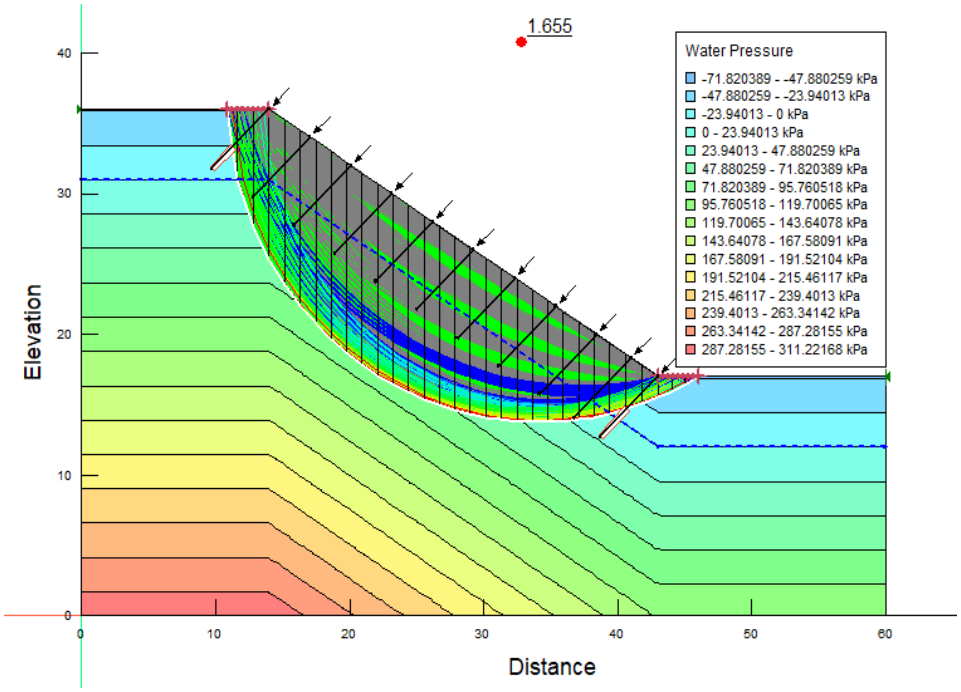

Fig. 4.56 Slope stabilization for L4 in Static Saturated condition (FOS=1.655)

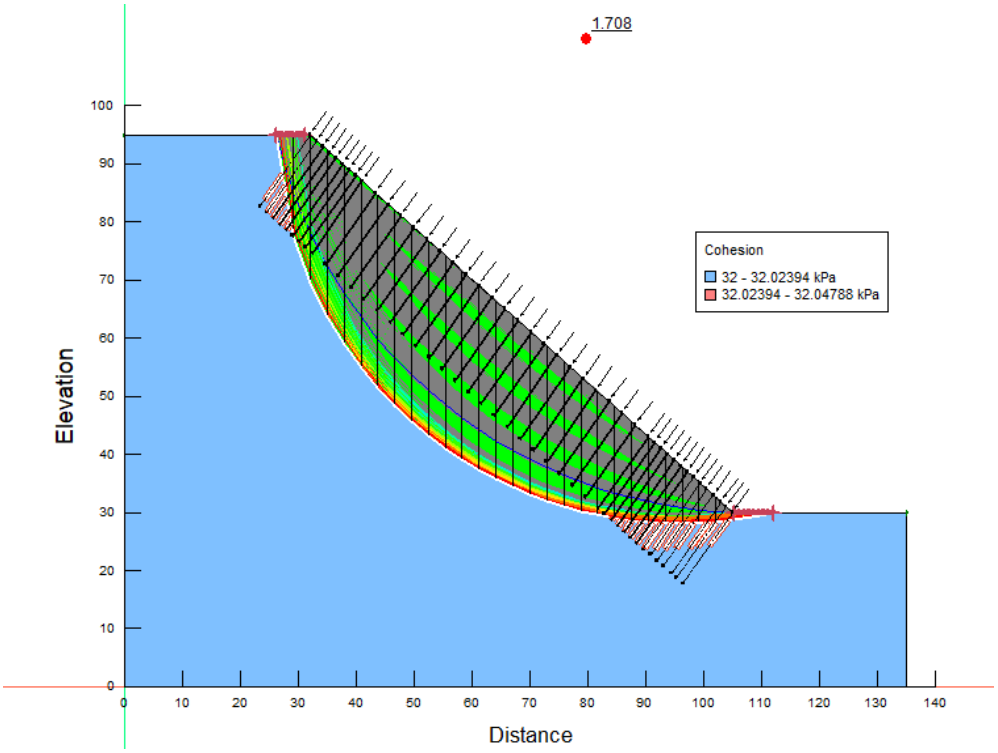

Fig. 4.57 Slope stabilization for L5 in Dynamic Dry condition (FOS=1.708)

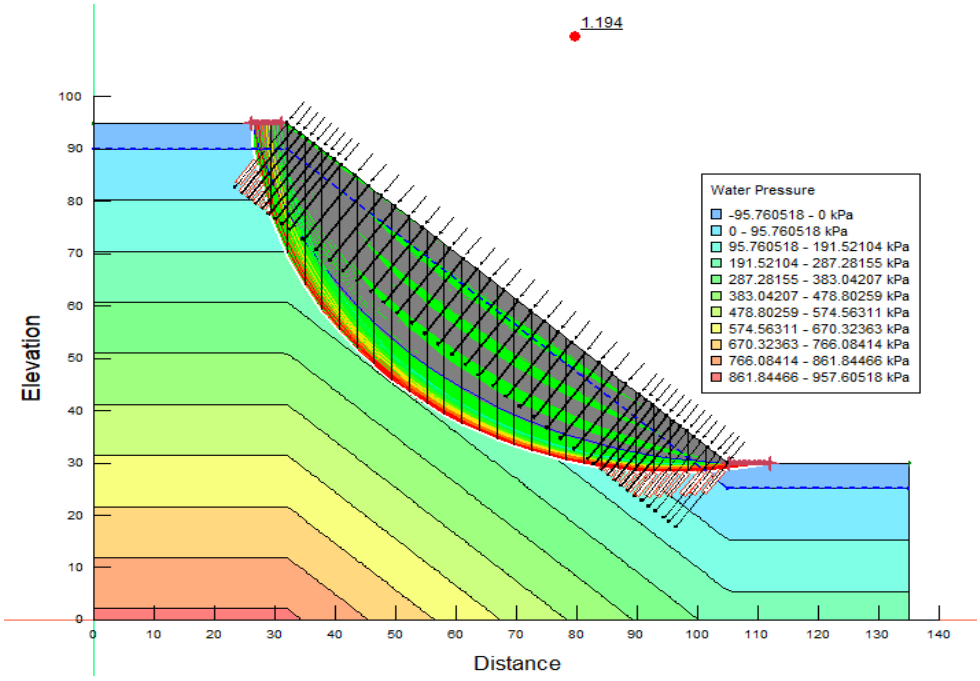

Fig. 4.58 Slope stabilization for L5 in Dynamic Saturated condition (FOS=1.194)

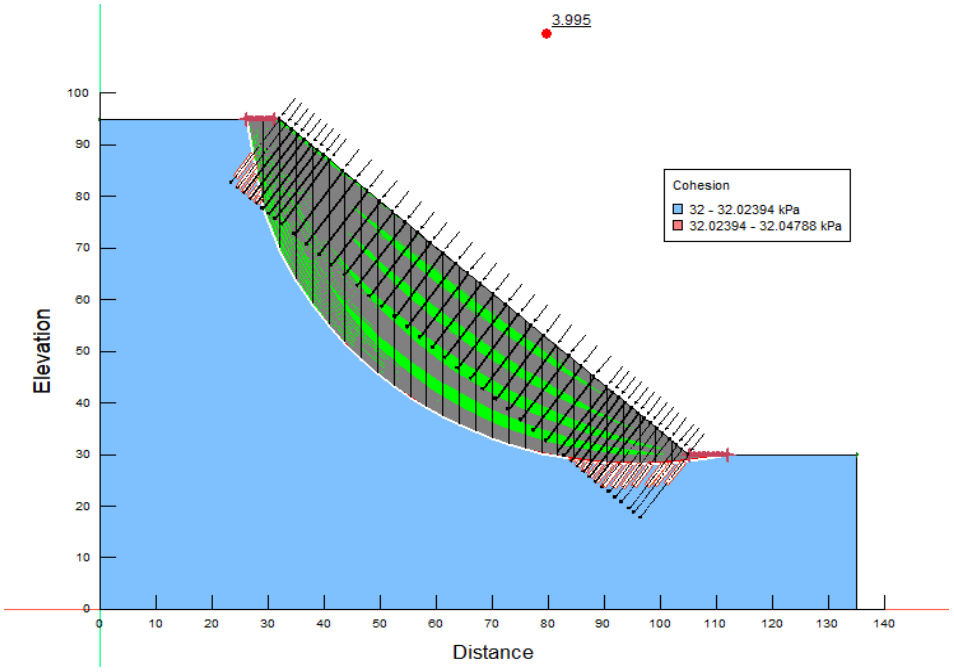

Fig. 4.59 Slope stabilization for L5 in Static Dry condition (FOS=3.995)

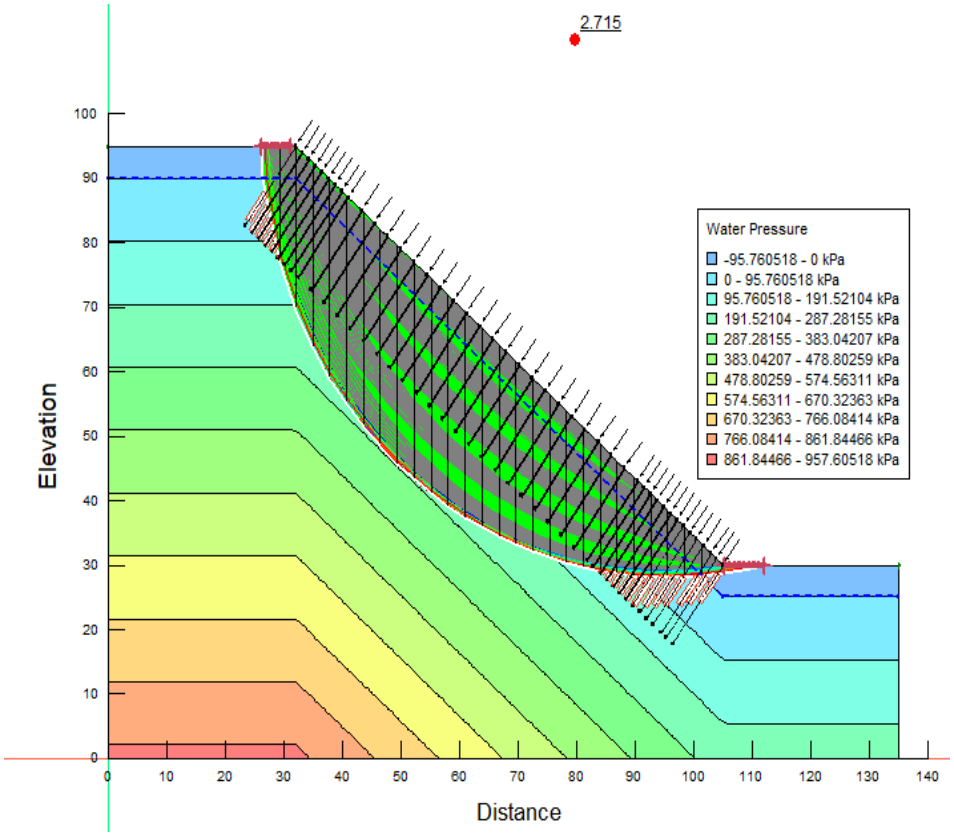

Fig. 4.60 Slope stabilization for L5 in Static Saturated condition (FOS=2.715)

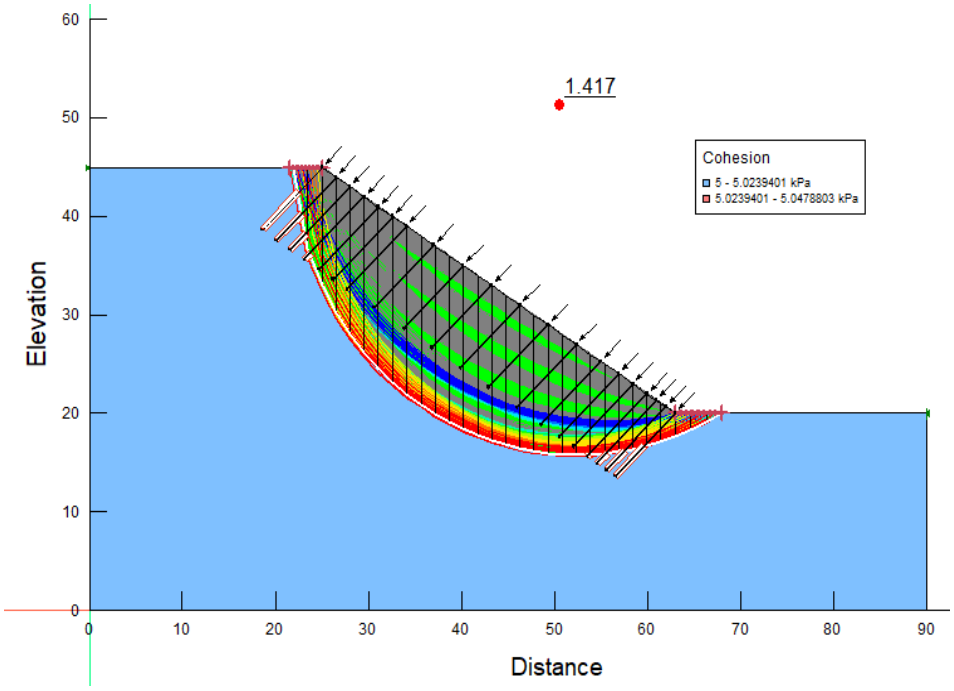

Fig. 4.61 Slope stabilization for L6 in Dynamic Dry condition (FOS=1.417)

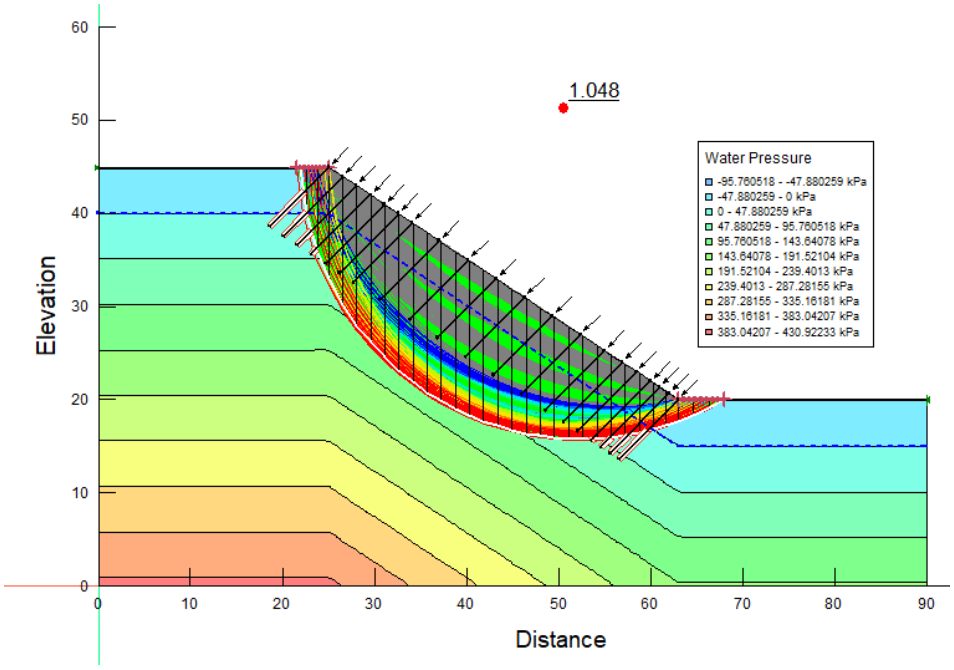

Fig. 4.62 Slope stabilization for L6 in Dynamic Saturated condition (FOS=1.048)

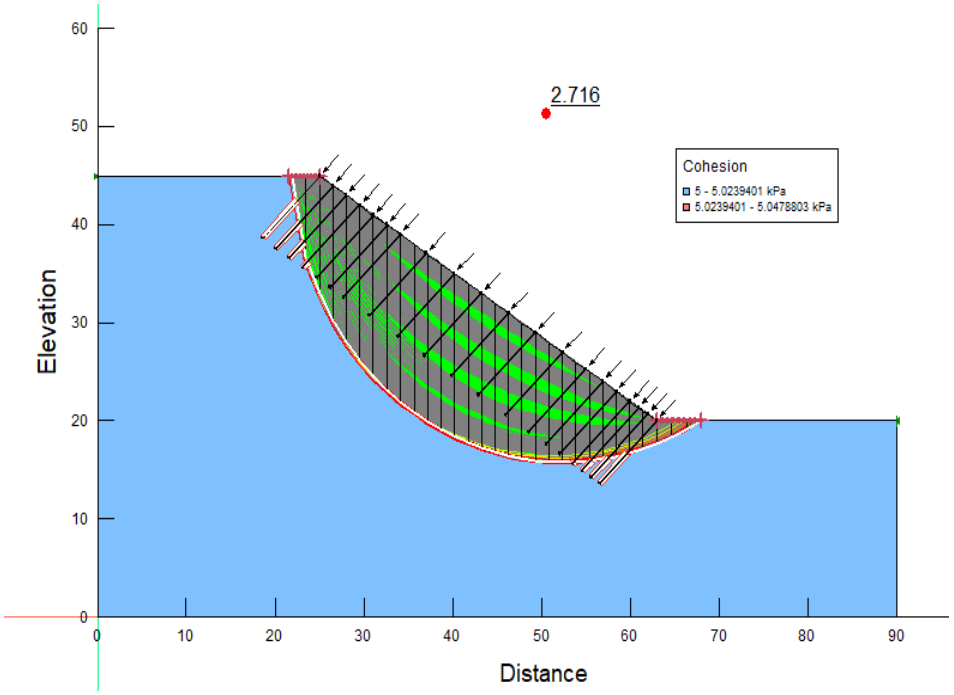

Fig. 4.63 Slope stabilization for L6 in Static Dry condition (FOS=2.716)

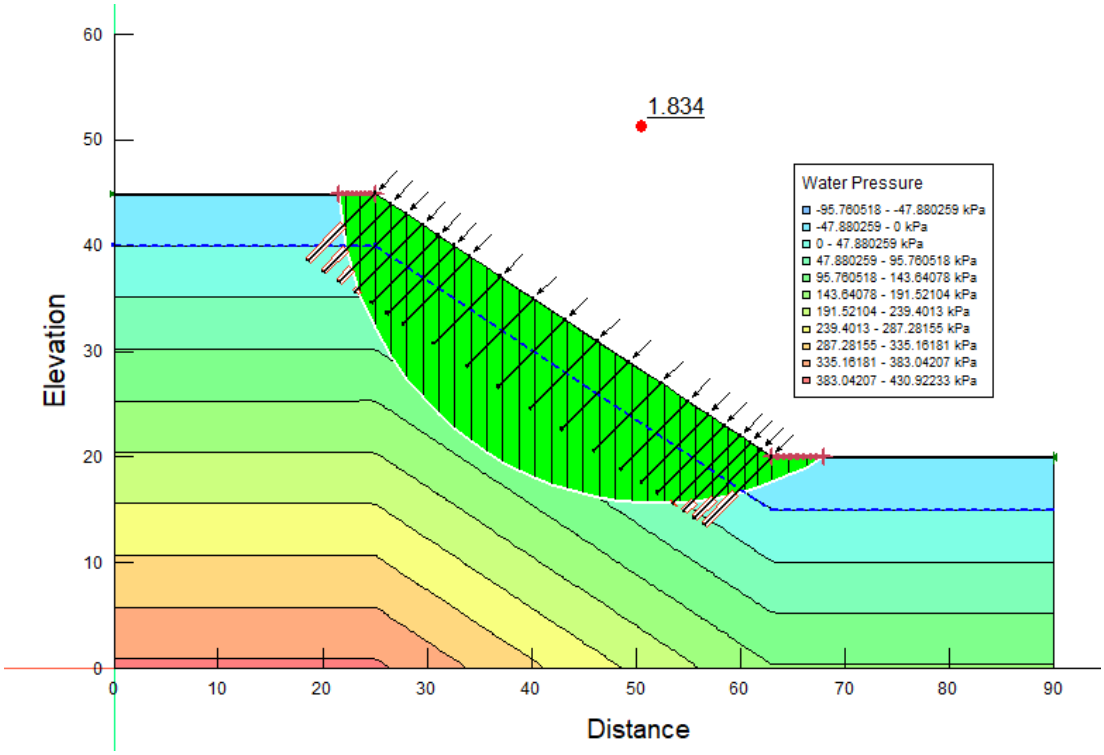

Fig. 4.64 Slope stabilization for L6 in Static Saturated condition (FOS=1.834)

Table 4.7 Comparison of factor of safety before and after stabilization

Site/State		L1	L2	L3	L4	L5	L6
Static Dry	Before stabilization	1.293	1.243	1.123	1.253	1.137	1.215
	After stabilization	3.109	2.430	2.896	2.270	3.995	2.716
Static Saturated	Before stabilization	0.808	1.098	0.716	1.173	0.684	0.905
	After stabilization	1.890	1.590	1.535	1.655	2.715	1.834
Dynamic Dry	Before	0.659	0.759	0.728	0.773	0.707	0.660

	stabilization						
	After stabilization	1.654	1.501	1.610	1.410	1.708	1.417
Dynamic Saturated	Before stabilization	0.533	0.711	0.476	0.760	0.477	0.597
	After stabilization	1.149	1.110	1.032	1.115	1.194	1.048

CHAPTER 5
CONCLUSION, FUTURE SCOPE AND SOCIAL IMPACT

5.1 Overview of Objectives and Methodologies

The primary objective of the study was to perform a detailed slope stability analysis in the Kalimpong region, accounting for both static and dynamic loading conditions. This included the identification of critical sites prone to landslides, field and laboratory investigations for determining geotechnical parameters, slope modeling under varying hydrological conditions (dry and saturated), and evaluating stabilization techniques. The research employed both deterministic LEM and probabilistic (frequency ratio-based GIS mapping) approaches to assess slope safety comprehensively.

The methodology comprised multiple stages: first, critical slope sites in Kalimpong were identified through field surveys and existing landslide records. Then, soil samples were extracted and tested to determine key parameters such as cohesion, internal friction angle, and unit weight. The models of these slopes were then simulated in geotechnical software using LEMs, particularly Bishop's Simplified Method and M-P Method, to compute the FOS under different conditions. Furthermore, GIS-based landslide susceptibility mapping was carried out using FR models, incorporating various conditioning parameters such as slope angle, elevation, aspect, lithology, distance to roads and faults, and rainfall data.

5.2 Integrated Slope Stability Assessment and Stabilization Strategy in Kalimpong Region

This research presents a comprehensive evaluation of slope stability in the Kalimpong region by integrating numerical modeling, geospatial susceptibility mapping, and site-specific stabilization measures. The analysis was conducted using the LEM through GeoStudio's SLOPE/W software, simulating both static and dynamic conditions under dry and saturated states to mirror real-world environmental scenarios. Under static dry conditions, slopes generally demonstrated

marginal to moderate stability, with FOS values between 1.3 and 1.6. However, these values dropped significantly by 15–25% under saturated conditions, indicating the destabilizing effects of elevated pore water pressures during monsoons. Dynamic analysis, incorporating pseudo-static seismic forces based on Zone IV classification under IS 1893, revealed a further decline in FOS, especially under saturated conditions, where values fell below 1.0 in several cases. This clearly pointed to an elevated landslide risk due to the combined impact of rainfall infiltration, reduction in effective stress, and seismic activity. Slopes composed of weak weathered phyllite and schist formations, particularly those with steep gradients exceeding 35° and aligned with tectonic discontinuities, were found to be highly prone to translational and flow-type failures, especially during prolonged rainfall.

To supplement the geotechnical analysis, a GIS-based FR model was employed for landslide susceptibility mapping across the Kalimpong region. The model utilized SRTM-based DEM and remote sensing data to generate thematic layers based on six key causative factors: slope angle, aspect, elevation, distance to roads, proximity to lineaments/faults, and rainfall. The FR model quantified the spatial correlation between historical landslides and these conditioning parameters, producing a LSI. The resulting LSZ map categorized the terrain into four zones: very low, low, moderate, and high susceptibility. Notably, around 38% of the study area was classified under moderate to high susceptibility zones, with the most vulnerable areas located along steep road cuts, fractured lithologies, and poorly drained, deforested slopes. Slope gradients over 35°, road proximity within 100 meters, and annual rainfall exceeding 2200 mm were identified as high-risk factors with FR values greater than 1.5. These findings provide a critical framework for local authorities to plan infrastructure reinforcement, control land use, and deploy early warning systems, thereby bridging the gap between scientific risk assessment and real-world hazard mitigation.

In response to the identified slope instability, the study proposed soil nailing as an effective, adaptable stabilization measure tailored to the terrain of Kalimpong. Steel bars were inserted into the slopes at engineered angles and spacing,

enhancing internal shear resistance and reducing deformation without large-scale excavation. GeoStudio SLOPE/W was used to reanalyze slopes with soil nailing and drainage elements incorporated under critical saturated-dynamic conditions. The models showed a substantial increase in FOS, often improving from values below 1.0 to a safer range between 1.25 and 1.45. This validated soil nailing's effectiveness, especially for steep slopes and space-constrained areas such as road cuts and populated hillsides. Its ease of installation, low environmental impact, and cost-efficiency make it highly suitable for widespread application in Himalayan hill towns. The success of soil nailing, reinforced by quantitative modeling and real-world applicability, affirms its value as a central component of slope management strategies. Together, the integrated approach of this thesis—combining LEM-based analysis, GIS-driven risk mapping, and validated stabilization—offers a holistic and replicable model for sustainable slope safety and landslide risk reduction in mountainous regions.

5.3 Limitations of the Study

While the study provides a robust framework for slope stability assessment and mitigation, it acknowledges several limitations:

- Temporal Data Gaps: The frequency ratio method relies on historical landslide inventories. Incomplete or outdated records can affect the accuracy of susceptibility models.
- Simplified Modeling Assumptions: The limit equilibrium method, though widely used, assumes predefined failure surfaces and neglects strain-softening behavior or progressive failure mechanisms. Advanced FEM simulations could further refine the analysis.
- Limited Field Implementation: Although the effectiveness of stabilization techniques was validated through simulation, large-scale field implementation was outside the scope of this study. Thus, long-term performance under varying climatic cycles remains to be monitored.

- Data Resolution: The use of 30m SRTM DEM may under-represent micro-topographic variations critical in slope failure mechanisms, particularly in narrow valleys and small hillslopes.

5.4 Scope for Future Research

This research lays a solid foundation for future investigations and innovations in slope stability assessment in mountainous terrains. Potential areas for further exploration include:

1. Integration of Real-Time Monitoring: Installing instrumentation such as inclinometers, piezometers, and ground-based LiDAR can provide continuous data for early warning and adaptive management of slopes.
2. Application of Machine Learning Models: Advanced algorithms like Random Forests, Support Vector Machines, or Deep Learning Neural Networks can be employed to further improve susceptibility prediction and identify hidden patterns in the data.
3. 3D Numerical Modeling: Future work can explore 3D slope modeling using FEM or hybrid approaches to simulate complex geometries and loading conditions, especially in the context of large-scale landslides or infrastructure expansion.
4. Climate Change Projections: Given the increasing intensity and unpredictability of rainfall patterns due to climate change, future models should integrate precipitation forecasting and runoff modeling to assess future slope behavior.
5. Community-Based Slope Management: Integrating local knowledge, training, and community monitoring can ensure effective and sustainable implementation of stabilization techniques, especially in remote or rural settings.

5.5 Social Impact

The findings of this thesis have far-reaching social implications for the communities residing in the Kalimpong region and similar landslide-prone

Himalayan terrains. By identifying critical slopes and proposing effective, site-specific stabilization techniques, the research contributes directly to safeguarding lives, homes, roads, and vital infrastructure. The GIS-based landslide susceptibility maps developed through this work serve as vital tools for local governments and disaster management authorities to implement early warning systems, formulate evacuation plans, and guide safe land-use policies. Moreover, the use of cost-effective and sustainable stabilization strategies such as soil nailing, vegetative cover, and improved drainage offers practical solutions that can be adopted even in resource-constrained settings. The outcomes promote greater resilience in hill communities by reducing vulnerability to landslides, enabling uninterrupted access to healthcare, education, and livelihood, and fostering a culture of preparedness. Ultimately, this research not only advances engineering knowledge but also enhances public safety, economic stability, and long-term environmental stewardship in high-risk regions. The findings of this thesis have important implications for regional planning, disaster risk reduction, and infrastructure development in Kalimpong and similar hilly regions. The GIS-based susceptibility maps provide a decision-making framework for municipal bodies, disaster management authorities, and infrastructure planners. By overlaying critical infrastructure—such as roads, bridges, and schools—with the high-risk zones delineated in the susceptibility maps, authorities can prioritize retrofitting and reinforcement efforts.

Additionally, the study advocates the incorporation of slope stability assessment into the early phases of infrastructure development, especially in terrains influenced by the Main Central Thrust and other active geological structures. This proactive approach can prevent costly retrofitting and minimize risks to life and property. Urban expansion and road widening projects, which have historically accelerated slope failures in the region, should undergo rigorous geotechnical screening as recommended in the study. Development permissions in high-susceptibility zones must be linked to slope treatment commitments, including mandatory drainage systems and mechanical reinforcement.

The research undertaken in this thesis successfully addresses the critical

issue of slope instability in the Kalimpong region through a combination of empirical, analytical, and geospatial techniques. It bridges the gap between theoretical geotechnical modeling and practical, field-applicable solutions, offering a comprehensive roadmap for future slope management in hilly, tectonically active regions. The proposed stabilization measures, validated models, and GIS-based susceptibility zones provide a ready-to-use toolkit for planners, engineers, and policymakers alike, ensuring that Kalimpong and similar Himalayan towns are better equipped to handle landslide hazards in a sustainable, resilient manner.

REFERENCES

[1] Abdalla, J. A., Attom, M. F. & Hawileh, R. 2015. Prediction of minimum factor of safety against slope failure in clayey soils using artificial neural network. Environmental Earth Sciences, 73, 5463-5477.

[2] Abella, E. C. & Van Westen, C. 2007. Generation of a landslide risk index map for Cuba using spatial multi-criteria evaluation. Landslides, 4, 311-325.

[3] Agam, M., Hashim, M., Murad, M. & Zabidi, H. 2016. Slope sensitivity analysis using spencer's method in comparison with general limit equilibrium method. Procedia Chemistry, 19, 651-658.

[4] Ahangari Nanehkaran, Y., Pusatli, T., Chengyong, J., Chen, J., Cemiloglu, A., Azarafza, M. & Derakhshani, R. 2022. Application of Machine Learning Techniques for the Estimation of the Safety Factor in Slope Stability Analysis. Water, 14, 3743.

[5] Ai-Jun, Y. & Yong-Hua, S. 2003. A method for stability of slope engineering with complicated rock-mass. China Civil Engineering Journal, 36, 34-37.

[6] Alejano, L., Ferrero, A. M., Ramírez-Oyanguren, P. & Fernández, M. Á. 2011. Comparison of limit-equilibrium, numerical and physical models of wall slope stability. International Journal of Rock Mechanics Mining Sciences 48, 16-26.

[7] Aleotti, P. & Chowdhury, R. 1999. Landslide hazard assessment: summary review and new perspectives. J Bulletin of Engineering Geology the environment, 58, 21-44.

[8] Ali, A., Huang, J., Lyamin, A., Sloan, S., Griffiths, D., Cassidy, M. & Li, J. 2014. Simplified quantitative risk assessment of rainfall-induced landslides modelled by infinite slopes. J Engineering Geology, 179, 102-116.

[9] Alimohammadlou, Y., Najafi, A. & Yalcin, A. 2013. Landslide process and impacts: A proposed classification method. J Catena, 104, 219-232.

[10] Ansari, T. A., Singh, K., Singh, T. & Tripathi, J. N. 2020. Stability analysis of road cut slope near Devprayag in Lesser Himalaya, India. J Journal of

Earth System Science, 129, 1-13.

[11] Arbanas, S. M. & Arbanas, Ž. 2015. Landslides: A guide to researching landslide phenomena and processes. Transportation Systems and Engineering: Concepts, Methodologies, Tools, and Applications. IGI Global.

[12] Armaghani, D. J., Mamou, A., Maraveas, C., Roussis, P. C., Siorikis, V. G., Skentou, A. D. & Asteris, P. G. 2021. Predicting the unconfined compressive strength of granite using only two non-destructive test indexes. Geomech. Eng 25, 317-330.

[13] Asteris, P. G., Rizal, F. I. M., Koopialipoor, M., Roussis, P. C., Ferentinou, M., Armaghani, D. J. & Gordan, B. 2022. Slope stability classification under seismic conditions using several tree-based intelligent techniques. Applied Sciences, 12, 1753.

[14] Auty, K. M., Zaman, R. U. & Kamal, N. N. 2024. Innovative Approaches to Stability of Embankment-A Role of Chemical Stabilization in Erosion Mitigation. Department of Civil and Environmental Engineering (CEE), Islamic University

[15] Azarafza, M., Hajialilue Bonab, M. & Derakhshani, R. 2022. A novel empirical classification method for weak rock slope stability analysis. Scientific Reports 12, 14744.

[16] Azarafza, M., Nikoobakht, S., Asghari-Kaljahi, E. & MOSHREFY-FAR, M. Stability analysis of jointed rock slopes using block theory (case study: gas flare site in phase 7 of South Pars Gas Complex). Proceedings of the 32th National & 1st International Geosciences Congress of Iran, 2014.

[17] Baker, R., Shukha, R., Operstein, V. & Frydman, S. 2006. Stability charts for pseudo-static slope stability analysis. Soil Dynamics and Earthquake Engineering, 26, 813-823.

[18] Bar, N., Kostadinovski, M., Tucker, M., Byng, G., Rachmatullah, R., Maldonado, A., Pötsch, M., Gaich, A., Mcquillan, A. & Yacoub, T. 2020. Rapid and robust slope failure appraisal using aerial photogrammetry and 3D slope stability models. J International Journal of Mining Science Technology, 30, 651-658.

[19] Bathurst, R. & Jones, C. 2001. Earth retaining structures and reinforced

slopes. Geotechnical and geoenvironmental engineering handbook. Springer.

[20] Baynes F.J. (2008) Anticipating problem soils on linear projects. In: Conference proceedings on problem soils in South Africa, 3–4 November 2008, pp 9–21.

[21] Begum, N., Maiti, A., Chakravarty, D. & Das, B. S. 2021. Diffuse reflectance spectroscopy based rapid coal rank estimation: A machine learning enabled framework. Spectrochimica Acta Part A: Molecular Biomolecular Spectroscopy, 263, 120150.

[22] Bhadra, D., Dhar, N. & Salam, M. A. 2022. Sensitivity analysis of the integrated AHP-TOPSIS and CRITIC-TOPSIS method for selection of the natural fiber. Materials today: proceedings, 56, 2618-2629.

[23] Bhagat, N. K., Mishra, A. K., Singh, R. K., Sawmliana, C. & Singh, P. 2022. Application of logistic regression, CART and random forest techniques in prediction of blast-induced slope failure during reconstruction of railway rock-cut slopes. Engineering Failure Analysis, 137, 106230.

[24] Bhambri, R., Mehta, M., Singh, S., Jayangondaperumal, R., Gupta, A. K. & Srivastava, P. 2017. Landslide inventory and damage assessment in the Bhagirathi Valley, Uttarakhand, during June 2013 flood. J Himalayan Geology, 38, 193-205.

[25] Biondi, G., Cascone, E. & Maugeri, M. J. S. D. 2002. Flow and deformation failure of sandy slopes. Soil Dynamics and Earthquake Engineering, 22, 1103-1114.

[26] Bird, J. F. & Bommer, J. J. 2004. Earthquake losses due to ground failure. Engineering geology, 75, 147-179.

[27] Bjerrum, L. J. G. 1967. Engineering geology of Norwegian normally-consolidated marine clays as related to settlements of buildings. 17, 83-118.

[28] Bouajaj, A., Bahi, L., Ouadif, L. & Awa, M. 2016. Slope stability analysis using GIS. J The International Archives of the Photogrammetry, Remote Sensing Spatial Information Sciences, 42, 151-153.

[29] Bui, X.-N., Nguyen, H., Choi, Y., Nguyen-Thoi, T., Zhou, J. & Dou, J. 2020. Prediction of slope failure in open-pit mines using a novel hybrid artificial intelligence model based on decision tree and evolution algorithm.

Scientific reports, 10, 1-17.

[30] Carrara, A., Cardinali, M., Detti, R., Guzzetti, F., Pasqui, V. & Reichenbach, P. 1991. GIS techniques and statistical models in evaluating landslide hazard. J Earth surface processes landforms, 16, 427-445.

[31] Cevik, A. 2011. Modeling strength enhancement of FRP confined concrete cylinders using soft computing. Expert Systems with Applications, 38, 5662-5673.

[32] Chang, S.-K., Lee, D.-H., Wu, J.-H. & Juang, C. H. 2011. Rainfall-based criteria for assessing slump rate of mountainous highway slopes: A case study of slopes along Highway 18 in Alishan, Taiwan. J Engineering geology, 118, 63-74.

[33] Chawla, A., Chawla, S., Pasupuleti, S., Rao, A., Sarkar, K. & Dwivedi, R. 2018. Landslide Susceptibility Mapping in Darjeeling Himalayas, India. Advances in Civil Engineering 2018, 1-17.

[34] Chen, J., Huang, H., Cohn, A. G., Zhang, D. & Zhou, M. 2022. Machine learning-based classification of rock discontinuity trace: SMOTE oversampling integrated with GBT ensemble learning. International Journal of Mining Science Technology, 32, 309-322.

[35] Cheng, M.-Y. & Hoang, N.-D. 2016. Slope collapse prediction using Bayesian framework with k-nearest neighbor density estimation: case study in Taiwan. Journal of Computing in Civil Engineering, 30, 04014116.

[36] Cheng, Y. M., Lansivaara, T. & Wei, W. 2007. Two-dimensional slope stability analysis by limit equilibrium and strength reduction methods. Computers and Geotechnics, 34, 137-150.

[37] Chuhan, Z., Pekau, O., Feng, J. & Guanglun, W. 1997. Application of distinct element method in dynamic analysis of high rock slopes and blocky structures. Soil Dynamics and Earthquake Engineering, 16, 385-394.

[38] Chung, C.-J. F. & Fabbri, A. G. 1999. Probabilistic prediction models for landslide hazard mapping. J Photogrammetric engineering remote sensing, 65, 1389-1399.

[39] Cohen, I., Huang, Y., Chen, J., Benesty, J., Benesty, J., Chen, J., Huang, Y. & Cohen, I. 2009. Pearson correlation coefficient. Noise reduction in speech

processing, 1-4.

[40] Collins, B. D. & Znidarcic, D. 2004. Stability analyses of rainfall induced landslides. Journal of geotechnical and geoenvironmental engineering 130, 362-372.

[41] Cred, U. 2020. The human cost of disasters 2000-2019. J United Nations Office of the Disarmament Affairs.

[42] Crozier, M. 2010. Landslide geomorphology: An argument for recognition, with examples from New Zealand. J Geomorphology, 120, 3-15.

[43] Cruden, D. 1991. A simple definition of a landslide: Bulletin of the International Association of Engineering Geology, no. 43.

[44] Cruden, D. M. 1996. Cruden, dm, varnes, dj, 1996, landslide types and processes, transportation research board, us national academy of sciences, special report, 247: 36-75. J Transp Res Board, 247, 36-57.

[45] Cui, W., Wang, X.-H., Zhang, G.-K. & LI, H.-B. 2021. Identification of unstable bedrock promontory on steep slope based on UAV photogrammetry. Bulletin of Engineering Geology and the Environment, 80, 7193-7211.

[46] Dai Fc, Lee CF (2003) A spatiotemporal probabilistic modelling of storm-induced shallow landslides using aerial photographs and logistic regression. Earth Surf Process Landforms 28(5):527–545

[47] Daraei, A., Herki, B. M., Sherwani, A. F. H. & Zare, S. 2018. Slope stability in swelling soils using cement grout: a case study. J International Journal of Geosynthetics Ground Engineering, 4, 1-10.

[48] Das, S. K. 2013. Artificial neural networks in geotechnical engineering: modeling and application issues. Metaheuristics in Water Geotech Transp Eng, 45, 231-267.

[49] Das, S., Pandit, K., Sarkar, S. & Kanungo, D. P. 2024. Stability and hazard assessment of the progressive zero landslide in the Kalimpong region of Darjeeling Himalaya, India. J Geotechnical Geological Engineering, 42, 1693-1709.

[50] Das, S., Sarkar, S. & Kanungo, D. P. 2022. GIS-based landslide susceptibility zonation mapping using the analytic hierarchy process (AHP)

method in parts of Kalimpong Region of Darjeeling Himalaya. J Environmental Monitoring Assessment, 194, 234.

[51] DAS, S., SARKAR, S. & KANUNGO, D. P. 2022. GIS-based landslide susceptibility zonation mapping using the analytic hierarchy process (AHP) method in parts of Kalimpong Region of Darjeeling Himalaya. J Environmental Monitoring Assessment, 194, 234.

[52] Demir, G., Aytekin, M. & Akgun, A. 2015. Landslide susceptibility mapping by frequency ratio and logistic regression methods: an example from Niksar–Resadiye (Tokat, Turkey). J Arabian Journal of Geosciences, 8, 1801-1812.

[53] Donald, I. B. & Chen, Z. 1997. Slope stability analysis by the upper bound approach: fundamentals and methods. J Canadian Geotechnical Journal, 34, 853-862.

[54] Duncan, J. M. 1996. State of the art: limit equilibrium and finite-element analysis of slopes. J Journal of Geotechnical engineering, 122, 577-596.

[55] Eberhardt, E., Stead, D. & Coggan, J. 2004. Numerical analysis of initiation and progressive failure in natural rock slopes—the 1991 Randa rockslide. J International Journal of Rock Mechanics Mining Sciences, 41, 69-87.

[56] Erzin, Y. & Cetin, T. 2012. The use of neural networks for the prediction of the critical factor of safety of an artificial slope subjected to earthquake forces. Scientia Iranica, 19, 188-194.

[57] Erzin, Y. & Cetin, T. 2013. The prediction of the critical factor of safety of homogeneous finite slopes using neural networks and multiple regressions. Computers and Geosciences, 51, 305-313.

[58] Erzin, Y., Nikooy, M., Nikooz, M. & Cetin, T. 2016. The use of self-organizing feature map networks for the prediction of the critical factor of safety of an artificial slope. Neural Network World, 26, 461.

[59] Fan, X., Dufresne, A., Subramanian, S. S., Strom, A., Hermanns, R., Stefanelli, C. T., Hewitt, K., Yunus, A. P., Dunning, S. & Capra, L. 2020. The formation and impact of landslide dams–State of the art. J Earth-Science Reviews, 203, 103116.

[60] Fattahi, H. 2017. Prediction of slope stability using adaptive neuro-fuzzy

inference system based on clustering methods. Journal of Mining and Environment, 8, 163-177.

[61] Fauziah A., Yahaya A.S., Farooqi M.A. (2006) Characterization and geotechnical properties of Penang residual soils with emphasis on landslides. Am J Environ Sci 2(4):121–128.

[62] Fay, L., Akin, M. & Shi, X. 2012. Cost-effective and sustainable road slope stabilization and erosion control, Transportation research board.

[63] Feng, X., Li, S., Yuan, C., Zeng, P. & Sun, Y. 2018. Prediction of slope stability using naive Bayes classifier. KSCE Journal of Civil Engineering, 22, 941-950.

[64] Ferentinou, M. & Sakellariou, M. 2007. Computational intelligence tools for the prediction of slope performance. Computers Geotechnics, 34, 362-384.

[65] Firincioglu, B. S. & Ercanoglu, M. 2021. Insights and perspectives into the limit equilibrium method from 2D and 3D analyses. J Engineering Geology, 281, 105968.

[66] Fredlund, D. Analytical methods for slope stability analysis. 1984. Proceedings of the 4th International Symposium on Landslides.

[67] Gerrard, J. 1994. The landslide hazard in the Himalayas: geological control and human action. Geomorphology and natural hazards. Elsevier.

[68] Gokceoglu, C., Sonmez, H. & Ercanoglu, M. 2000. Discontinuity controlled probabilistic slope failure risk maps of the Altindag (settlement) region in Turkey. J Engineering Geology, 55, 277-296.

[69] Gordan, B., Armaghani, D. J., Adnan, A. & Rashid, A. 2016. A new model for determining slope stability based on seismic motion performance. Soil Mechanics and Foundation Engineering, 53, 344-351.

[70] Goswami, R. 2012. Subaerial and submarine geomorphology and links between onshore and offshore erosion in the Ionian Sea, Italy, The University of Manchester (United Kingdom).

[71] Gray, D. H. & Sotir, R. B. 1992. Biotechnical stabilization of highway cut slope. J Journal of Geotechnical Engineering, 118, 1395-1409.

[72] Greenwood, J. R., Norris, J. & Wint, J. 2004. Assessing the contribution of vegetation to slope stability. J Proceedings of the Institution of Civil

Engineers-Geotechnical Engineering, 157, 199-207.

[73] Guo, J., Cui, Y., Xu, W., Yin, Y., Li, Y. & Jin, W. 2022. Numerical investigation of the landslide-debris flow transformation process considering topographic and entrainment effects: a case study. J Landslides, 1-16.

[74] Gupta, V., Bhasin, R. K., Kaynia, A. M., Kumar, V., Saini, A., Tandon, R. & Pabst, T. 2016. Finite element analysis of failed slope by shear strength reduction technique: a case study for Surabhi Resort Landslide, Mussoorie township, Garhwal Himalaya. J Geomatics, Natural Hazards Risk, 7, 1677-1690.

[75] Hassan, Z., Haidir, A., Saad, F. N. M., Ayob, A., Rahim, M. A. & Ghazaly, Z. M. Spatial interpolation of historical seasonal rainfall indices over Peninsular Malaysia. E3S Web of Conferences, 2018. EDP Sciences, 02048.

[76] Highland, L. M. & Bobrowsky, P. 2008. The landslide handbook-A guide to understanding landslides, US Geological Survey.

[77] Hoang, N.-D. & Bui, D. T. 2017. Slope stability evaluation using radial basis function neural network, least squares support vector machines, and extreme learning machine. Handbook of neural computation. Elsevier.

[78] Hong, Y., Shao, Z., Wu, K., Shi, G., Wu, S. & Jiang, S. 2023. An extended 3D limit analysis of slope stability considering prestressed anchor cables reinforcement. J Archives of Civil Mechanical Engineering, 23, 59.

[79] Howland, J. 1980. Probabilistic seismic stability analysis of earth slopes.

[80] Hryciw, R. D. 1991. Anchor design for slope stabilization by surface loading. J Journal of Geotechnical Engineering, 117, 1260-1274.

[81] Huang, C.-C. & Chen, Y.-H. 2004. Seismic stability of soil retaining walls situated on slope. J geotechnical geoenvironmental engineering, 130, 45-57.

[82] Huang, C. Z., Cao, Y. H. & Sun, W. H. Generalized limit equilibrium method for slope stability analysis. Applied Mechanics and Materials, 2012. Trans Tech Publ, 557-568.

[83] Hungr, O. 1987. An extension of Bishop's simplified method of slope stability analysis to three dimensions. J Geotechnique, 37, 113-117.

[84] Hungr, O., Leroueil, S. & Picarelli, L. 2014. The Varnes classification of

landslide types, an update. J Landslides, 11, 167-194.

[85] Hutchinson, J. 1988. General report: Morphological and geotechnical parameters of landslides in relation to geology and hydrogeology.

[86] Hwang, S., Guevarra, I. F. & Yu, B. 2009. Slope failure prediction using a decision tree: A case of engineered slopes in South Korea. Engineering Geology, 104, 126-134.

[87] Hynes-Griffin, M. E. & Franklin, A. G. 1984. Rationalizing the seismic coefficient method. Army Engineer Waterways Experiment Station Vicksburg Ms Geotechnical Lab.

[88] Jeldes, I. A., Drumm, E. C. & Schwartz, J. S. 2013. The low compaction grading technique on steep reclaimed slopes: Soil characterization and static slope stability. J Geotechnical Geological Engineering, 31, 1261-1274.

[89] Jiang, S.-H., Huang, J., Qi, X.-H. & Zhou, C.-B. 2020. Efficient probabilistic back analysis of spatially varying soil parameters for slope reliability assessment. J Engineering Geology, 271, 105597.

[90] Jing-Shan, B., Guo-Dong, X. & Li-Ping, J. 2001. Seismic response and dynamic stability analysis of soil slopes. Earthquake Engineering and Engineering Vibration, 21, 116-120.

[91] Johari, A., Mousavi, S. & Hooshmand Nejad, A. 2015. A seismic slope stability probabilistic model based on Bishop's method using analytical approach. Scientia Iranica, 22, 728-741.

[92] Kabir, M. U., Islam, M. S., Nazrul, F. B. & Shahin, H. M. 2023. Comparative Stability and Behaviour Assessment of a Hill Slope on Clayey Sand Hill Tracts. International Journal of Engineering Trends and Technology, 11–24.

[93] Kalatehjari, R., A Rashid, A. S., Ali, N. & Hajihassani, M. 2014. The contribution of particle swarm optimization to three-dimensional slope stability analysis. The Scientific World Journal, 2014.

[94] Kanungo, D., Pain, A. & Sharma, S. 2013. Finite element modeling approach to assess the stability of debris and rock slopes: a case study from the Indian Himalayas. J Natural hazards, 69, 1-24.

[95] Kardani, N., Bardhan, A., Samui, P., Nazem, M., Zhou, A. & Armaghani, D.

J. 2021. A novel technique based on the improved firefly algorithm coupled with extreme learning machine (ELM-IFF) for predicting the thermal conductivity of soil. Engineering with Computers, 1-20.

[96] Karray, M., Hussien, M. N., Delisle, M.-C. & Ledoux, C. 2018. Framework to assess pseudo-static approach for seismic stability of clayey slopes. J Canadian Geotechnical Journal, 55, 1860-1876.

[97] Kayabasi, A., Yesiloglu-Gultekin, N. & Gokceoglu, C. 2015. Use of non-linear prediction tools to assess rock mass permeability using various discontinuity parameters. Engineering Geology, 185, 1-9.

[98] Kechik, F. A., Ibrahim, A., Hassan, Z. A., Matlan, S. J., Taib, A. M. & Abd Rahman, N. 2023. Analysis of influence of air-entry values to unsaturated soil properties. J Physics Chemistry of the Earth, Parts A/B/C, 129, 103340.

[99] Kezdi Á. (1980) Handbook of soil mechanics, Vol. 2, Soil Testing, Amsterdam.

[100] Khanna, K., Martha, T. R., Roy, P. & Kumar, K. V. 2021. Effect of time and space partitioning strategies of samples on regional landslide susceptibility modelling. Landslides, 18, 2281-2294.

[101] Krishnamoorthy, A. 2007. Factor of safety of a slope subjected to seismic load. Electronic Journal of Geotechnical Engineering, 12.

[102] Krishnan, A. R., Kasim, M. M., Hamid, R. & Ghazali, M. F. 2021. A modified CRITIC method to estimate the objective weights of decision criteria. Symmetry, 13, 973.

[103] Kristo, C., Rahardjo, H. & Satyanaga, A. 2019. Effect of hysteresis on the stability of residual soil slope. J International soil water conservation research, 7, 226-238.

[104] Kokutse, N. K., Temgoua, A. G. T. & Kavazović, Z. 2016. Slope stability and vegetation: Conceptual and numerical investigation of mechanical effects. J Ecological Engineering, 86, 146-153.

[105] Koner R., Chakravarty D. (2016) Characterisation of overburden dump materials: a case study from the Wardha valley coal field. Bull Eng Geol Environ, 75:1311–1323.

[106] Koukis G, Tsiambaos G, Sabatakakis N (1994) Slope movements in the

Greek territory: a statistical approach. In: International congress of the international association of engineering. Geology, 4621–4628

[107] Kumar, A., Sharma, R. K. & Mehta, B. S. 2020. Slope stability analysis and mitigation measures for selected landslide sites along NH-205 in Himachal Pradesh, India. J Journal of Earth System Science, 129, 135.

[108] Kumarasinghe, U. 2021. A review on new technologies in soil erosion management. J Journal of research technology engineering, 2, 120-127.

[109] Kumar, M., Rana, S., Pant, P. D. & Patel, R. C. 2017. Slope stability analysis of balia nala landslide, kumaun lesser himalaya, nainital, uttarakhand, India. J Journal of Rock Mechanics Geotechnical Engineering, 9, 150-158.

[110] Kumar, V., Gupta, V. & Jamir, I. 2018. Hazard evaluation of progressive Pawari landslide zone, Satluj valley, Himachal Pradesh, India. J Natural Hazards, 93, 1029-1047.

[111] Kumar, V., Gupta, V. & Sundriyal, Y. 2019. Spatial interrelationship of landslides, litho-tectonics, and climate regime, Satluj valley, Northwest Himalaya. J Geological Journal, 54, 537-551.

[112] Kumsar, H., Aydan, Ö. & Ulusay, R. 2000. Dynamic and static stability assessment of rock slopes against wedge failures. J Rock Mechanics Rock Engineering, 33, 31-51.

[113] Lacasse, S., Nadim, F., Lacasse, S. & Nadim, F. 2009. Landslide risk assessment and mitigation strategy. J Landslides–disaster risk reduction, 31-61.

[114] Lee, D.-H., Lai, M.-H., Wu, J.-H., Chi, Y.-Y., Ko, W.-T. & Lee, B.-L. 2013. Slope management criteria for Alishan Highway based on database of heavy rainfall-induced slope failures. J Engineering geology, 162, 97-107.

[115] Lee, S. & Pradhan, B. 2007. Landslide hazard mapping at Selangor, Malaysia using frequency ratio and logistic regression models. J Landslides, 4, 33-41.

[116] Lee, S. & Talib, J. A. 2005. Probabilistic landslide susceptibility and factor effect analysis. J Environmental geology, 47, 982-990.

[117] Leshchinsky, D. & San, K.-C. 1994. Pseudostatic seismic stability of slopes:

Design charts. Journal of Geotechnical Engineering, 120, 1514-1532.

[118] Lin, S., Zheng, H., Han, C., Han, B. & Li, W. 2021. Evaluation and prediction of slope stability using machine learning approaches. Frontiers of Structural Civil Engineering, 15, 821-833.

[119] Liu, C., Qi, S., Tong, L. & Zhao, F.-S. 2004. Stability analysis of slope under earthquake with FLAC3D. Chinese Journal of Rock Mechanics and Engineering, 23, 2730-2733.

[120] Liu, S., Shao, L. & Li, H. 2015. Slope stability analysis using the limit equilibrium method and two finite element methods. Computers and Geotechnics, 63, 291-298.

[121] Liu, X. & Wang, Y. 2023. Analytical solutions for annual probability of slope failure induced by rainfall at a specific slope using bivariate distribution of rainfall intensity and duration. J Engineering Geology, 313, 106969.

[122] Liu, Y. & Geo, F. 2015. Dynamic stability analysis on a slope supported by anchor bolts and piles. J Electronic Journal of Geotechnical Engineering, 20, 1887-1900.

[123] Liu, Z., Shao, J., Xu, W., Chen, H. & Zhang, Y. 2014. An extreme learning machine approach for slope stability evaluation and prediction. Natural hazards, 73, 787-804.

[124] Li J, Wang F (2010) Study on the forecasting models of slope stability under data mining. In Earth and Space: Engineering, Science, Construction, and Operations in Challenging Environments (pp. 765-776)

[125] Li, Y. & Yang, X. 2019. Soil-slope stability considering effect of soil-strength nonlinearity. International Journal of Geomechanics, 19, 04018201.

[126] Löbmann, M. T., Geitner, C., Wellstein, C. & Zerbe, S. 2020. The influence of herbaceous vegetation on slope stability–a review. J Earth-Science Reviews, 209, 103328.

[127] Loukidis, D., Bandini, P. & Salgado, R. 2003. Stability of seismically loaded slopes using limit analysis. Geotechnique, 53, 463-479.

[128] Lucas, D. & De Graaf, P. Iterative geotechnical pit slope design in a structurally complex setting: a case study from Tom Price, Western

Australia. Slope Stability 2013: Proceedings of the 2013 International Symposium on Slope Stability in Open Pit Mining and Civil Engineering, 2013. Australian Centre for Geomechanics, 513-526.

[129] Lugo Hubp, J. 1999. Landslide recognition: identification, movement and causes. J Investigaciones geográficas, 163-163.

[130] Lu, P. & Rosenbaum, M. 2003. Artificial neural networks and grey systems for the prediction of slope stability. Natural Hazards, 30, 383-398.

[131] Mafi, R., Javankhoshdel, S., Cami, B., Jamshidi Chenari, R. & Gandomi, A. H. 2021. Surface altering optimisation in slope stability analysis with non-circular failure for random limit equilibrium method. Georisk: Assessment Management of Risk for Engineered Systems Geohazards 15, 260-286.

[132] Malviya, D. K., Samanta, M., Dash, R. K. & Kanungo, D. P. 2024. Anthropogenically induced instability in road cut slopes along NH-39, Manipur, North-East Indian Himalaya: assessment and mitigation measures. J Environment, Development Sustainability, 26, 6239-6268.

[133] Mangnejo, D. A., Oad, S., Kalhoro, S. A., Ahmed, S., Laghari, F. & Siyal, Z. 2019. Numerical analysis of soil slope stabilization by soil nailing technique. J Engineering, Technology Applied Science Research, 9, 4469-4473.

[134] Manouchehrian, A., Gholamnejad, J. & Sharifzadeh, M. 2014. Development of a model for analysis of slope stability for circular mode failure using genetic algorithm. Environmental Earth Sciences, 71, 1267-1277.

[135] Markiewicz, A., Koda, E., Kiraga, M., Wrzesiński, G., Kozanka, K., Naliwajko, M. & Vaverková, M. D. 2024. Polymeric Products in Erosion Control Applications: A Review. J Polymers, 16, 2490.

[136] Mathe, L. & Ferentinou, M. Rock slope stability analysis adopting Eurocode 7, a limit state design approach for an open pit. IOP Conference Series: Earth and Environmental Science, 2021. IOP Publishing, 012201.

[137] Matthews, C., Farook, Z. & Helm, P. 2014. Slope stability analysis–limit equilibrium or the finite element method. Ground Engineering, 48, 22-28.

[138] Mehdipour, B., Hashemolhosseini, H., Nadi, B. & Mirmohamadsadeghi, M. 2020. Investigating the effect of geocell changes on slope stability in unsaturated soil. J Tehnički glasnik, 14, 66-75.

[139] Melo, C. & Sharma, S. Seismic coefficients for pseudostatic slope analysis. 13th World conference on earthquake engineering, 2004. 15.

[140] Michalowski, R. 1995. Slope stability analysis: a kinematical approach. J Geotechnique, 45, 283-293.

[141] Mizal-Azzmi, N., Mohd-Noor, N. & Jamaludin, N. 2011. Geotechnical approaches for slope stabilization in residential area. J Procedia Engineering, 20, 474-482.

[142] Mohamed, T. & Kasa, A. Application of fuzzy set theory to evaluate the stability of slopes. Applied Mechanics and Materials, 2014. Trans Tech Publ, 566-571.

[143] Mora C, S. & Vahrson, W.-G. 1994. Macrozonation methodology for landslide hazard determination. J Bulletin of the Association of Engineering Geologists, 31, 49-58.

[144] Morgenstern, N. U. & Price, V. E. 1965. The analysis of the stability of general slip surfaces. Geotechnique, 15, 79-93.

[145] Msilimba G., and Holmes P. (2005) A Landslide Hazard Assessment and Vulnerability Appraisal Procedure: Vunguvungu/Banga Catchment, Northern Malawi, Natural Hazards: Journal of the International Society for the Prevention and Mitigation of Natural Hazards, 34(2): 199-216.

[146] Mugagga F., Kakembo V., Buyinza M. (2011) A characterization of the physical properties of soil and the implications for landslide occurrence on the slopes of Mount Elgon, Eastern Uganda. Nat Hazards, 60:1113–1131.

[147] Nath, S. K., Sengupta, A. & Srivastava, A. 2021. Remote sensing GIS-based landslide susceptibility & risk modeling in Darjeeling–Sikkim Himalaya together with FEM-based slope stability analysis of the terrain. J Natural Hazards, 108, 3271-3304.

[148] Nanehkaran, Y. A., Licai, Z., Chengyong, J., Chen, J., Anwar, S., Azarafza, M. & Derakhshani, R. 2023. Comparative analysis for slope stability by using machine learning methods. J Applied Sciences, 13, 1555.

[149] Newmark, N. M. 1965. Effects of earthquakes on dams and embankments. Geotechnique, 15, 139-160.

[150] Niroumand, H., Kassim, K. A., Ghafooripour, A. & Nazir, R. 2012. The role

of geosynthetics in slope stability. J Electronic Journal of Geotechnical Engineering, 17, 2739-2746.

[151] Nithya, S. E. & Prasanna, P. R. 2010. An integrated approach with GIS and remote sensing technique for landslide hazard zonation. J International Journal of Geomatics Geosciences, 1, 66-75.

[152] Nohani E, Moharrami M, Sharafi S, Khosravi K, Pradhan B, Pham BT, Lee S, Melesse AM (2019) Landslide susceptibility mapping using different GIS-based bivariate models. Water 11(7):1402

[153] Nouri, H., Fakher, A. & Jones, C. 2008. Evaluating the effects of the magnitude and amplification of pseudo-static acceleration on reinforced soil slopes and walls using the limit equilibrium horizontal slices method. Geotextiles and Geomembranes, 26, 263-278.

[154] Pardeshi, S. D., Autade, S. E. & Pardeshi, S. S. 2013. Landslide hazard assessment: recent trends and techniques. J SpringerPlus, 2, 1-11.

[155] Petley, D. 2012. Global patterns of loss of life from landslides. J Geology, 40, 927- 930.

[156] Phong, T. V., Phan, T. T., Prakash, I., Singh, S. K., Shirzadi, A., Chapi, K., Ly, H.-B., Ho, L. S., Quoc, N. K. & Pham, B. T. 2021. Landslide susceptibility modeling using different artificial intelligence methods: A case study at Muong Lay district, Vietnam. Geocarto International, 36, 1685-1708.

[157] Pourghasemi, H. R., Pradhan, B. & Gokceoglu, C. 2012. Application of fuzzy logic and analytical hierarchy process (AHP) to landslide susceptibility mapping at Haraz watershed, Iran. Natural hazards 63, 965-996.

[158] Powers, P. S., Chiarle, M. & Savage, W. Z. 1996. A digital photogrammetric method for measuring horizontal surficial movements on the Slumgullion earthflow, Hinsdale County, Colorado. J Computers Geosciences, 22, 651-663.

[159] Puniya, M. K., Kaushik, A. K., Mukherjee, S., Kar, N. R., Biswas, M. & Choudhary, R. 2023. Structural geology and stability issue of the Giral lignite mine, Rajasthan, India. Structural Geology and Tectonics Field

Guidebook—Volume 2. Springer.

[160] Qi, C. & Tang, X. 2018. Slope stability prediction using integrated metaheuristic and machine learning approaches: A comparative study. Computers Industrial Engineering, 118, 112-122.

[161] Qi, C., Wu, J., Liu, J. & Kanungo, D. P. 2016. Assessment of complex rock slope stability at Xiari, southwestern China. J Bulletin of Engineering Geology the Environment, 75, 537-550.

[162] Rahardjo, H., Hritzuk, K., Leong, E. & Rezaur, R. 2003. Effectiveness of horizontal drains for slope stability. J Engineering Geology, 69, 295-308.

[163] Rahardjo H, Lim TT, Chang MF, Fredlund DG (1995) Shear-strength characteristics of a residual soil. Can Geotechn J 32(1):60–77

[164] Ramakrishnan, S., Kumar, V., Sadiq, M., Arulraj, M. & Venugopal, K. 2003. An Integrated Approach For Landslide Disaster Management Planning Using Photogrammetry And 3D GIS Techniques. J International Archives Of Photogrammetry Remote Sensing Spatial Information Sciences, 34, 1237-1241.

[165] Raschka, S., Patterson, J. & Nolet, C. 2020. Machine learning in python: Main developments and technology trends in data science, machine learning, and artificial intelligence. Information, 11, 193.

[166] Rawat, S. & Gupta, A. 2016. An experimental and analytical study of slope stability by soil nailing. J Electron J Geotech Eng, 21, 5577-5597.

[167] Ray, P. C., Parvaiz, I., Jayangondaperumal, R., Thakur, V., Dadhwal, V. & Bhat, F. 2009. Analysis of seismicity-induced landslides due to the 8 October 2005 earthquake in Kashmir Himalaya. J Current science, 1742-1751.

[168] Remondo, J., González, A., De Terán, J. R. D., Cendrero, A., Fabbri, A. & Chung, C.-J. F. 2003. Validation of landslide susceptibility maps; examples and applications from a case study in Northern Spain. J Natural Hazards, 30, 437-449.

[169] Roy, P., Ghosal, K. & Paul, P. K. 2022. Landslide susceptibility mapping of Kalimpong in Eastern Himalayan Region using a Rprop ANN approach. Journal of Earth System Science 131, 130.

[170] Sah, M. & Mazari, R. 1998. Anthropogenically accelerated mass movement, Kulu Valley, Himachal Pradesh, India. J Geomorphology, 26, 123-138.

[171] Sah NK, Sheorey PR, Upadhyaya LN (1994) Maximum likelihood estimation of slope stability. In International journal of rock mechanics and mining sciences & geomechanics abstracts (Vol. 31, No. 1, pp. 47-53). Pergamon.

[172] Sakellariou, M. & Ferentinou, M. 2005a. A study of slope stability prediction using neural networks. Geotechnical and Geological Engineering, 23, 419-445.

[173] Sakellariou, M. & Ferentinou, M. 2005b. A study of slope stability prediction using neural networks. Geotechnical Geological Engineering, 23, 419-445.

[174] Samson, A., Bowa, V. M., Chileshe, P. R., Chinyanta, S. & Manda, E. 2024. Analytical and numerical modelling of the effects of buttressing on slide-head toppling failure. J Mining, Metallurgy Exploration, 41, 1873-1889.

[175] Samui, P. 2008. Slope stability analysis: a support vector machine approach. Environmental Geology, 56, 255-267.

[176] Samui, P. 2013. Support vector classifier analysis of slope. Geomatics, Natural Hazards Risk 4, 1-12.

[177] Santi, P., Hewitt, K., Vandine, D. & Barillas Cruz, E. 2011. Debris-flow impact, vulnerability, and response. J Natural hazards, 56, 371-402.

[178] Santoso, A. M., Phoon, K.-K. & Quek, S.-T. 2011. Effects of soil spatial variability on rainfall-induced landslides. J Computers Structures, 89, 893-900.

[179] Sarkar, S., Pandit, K., Sharma, M. & Pippal, A. 2018. Risk assessment and stability analysis of a recent landslide at Vishnuprayag on the Rishikesh–Badrinath highway, Uttarakhand, India. J Current Science, 1527-1533.

[180] Schmidhuber, J. 2015. Deep learning in neural networks: An overview. Neural networks 61, 85-117.

[181] Schor, H. J. & Gray, D. H. 1995. Landform grading and slope evolution. J Journal of Geotechnical Engineering 121, 729-734.

[182] Schuster, R. L. & Wieczorek, G. F. 2018. Landslide triggers and types.

Landslides. Routledge.

[183] Seed, H. B. 1979. Considerations in the earthquake-resistant design of earth and rockfill dams. Geotechnique, 29, 215-263.

[184] Selby M.G. (1993) Hillslope materials and processes. Oxford University Press, New York.

[185] Sharma, M., Samanta, M. & Sarkar, S. 2019. Soil nailing: an effective slope stabilization technique. J Landslides: Theory, practice modelling, 173-199.

[186] Shrestha, S. & Kang, T.-S. 2019. Assessment of seismically-induced landslide susceptibility after the 2015 Gorkha earthquake, Nepal. Bulletin of Engineering Geology and the Environment, 78, 1829-1842.

[187] Shroder Jr, J. F. & Bishop, M. P. 1998. Mass movement in the Himalaya: new insights and research directions. J Geomorphology, 26, 13-35.

[188] Siad, L. 2003. Seismic stability analysis of fractured rock slopes by yield design theory. Soil dynamics and earthquake engineering, 23, 21-30.

[189] Siyahi, B. G. & Bilge, G. 1998. A pseudo-static stability analysis in normally consolidated soil slopes subjected to earthquake. Teknik Dergi/Technical Journal of Turkish Chamber of Civil Engineers, 9, 457-461.

[190] Steck, A. 2003. Geology of the NW Indian Himalaya. J Eclogae Geologicae Helvetiae, 96, 147-196.

[191] Sousa, R., Karam, K. S., Costa, A. L., Einstein, H. H. & Geohazards 2017. Exploration and decision-making in geotechnical engineering–a case study. J Georisk: Assessment Management of Risk for Engineered Systems Geohazards, 11, 129-145.

[192] Suhatril, M., Osman, N., Azura Sari, P., Shariati, M. & Marto, A. 2019. Significance of surface eco-protection techniques for cohesive soils slope in Selangor, Malaysia. J Geotechnical Geological Engineering, 37, 2007-2014.

[193] Suman, S., Khan, S., Das, S. & Chand, S. 2016. Slope stability analysis using artificial intelligence techniques. Natural Hazards, 84, 727-748.

[194] Tang, C., Zhu, J., Qi, X. & Ding, J. 2011. Landslides induced by the Wenchuan earthquake and the subsequent strong rainfall event: A case study in the Beichuan area of China. Engineering Geology, 122, 22-33.

[195] Tao, Y., Xue, Y., Zhang, Q., Yang, W., Li, B., Zhang, L., Qu, C. & Zhang,

K. 2021. Risk Assessment of Unstable Rock Masses on High-Steep Slopes: An Attribute Recognition Model. Soil Mechanics Foundation Engineering, 58, 175-182.

[196] Thakur, V., Jayangondaperumal, R. & Malik, M. 2010. Redefining Medlicott–Wadia's main boundary fault from Jhelum to Yamuna: An active fault strand of the main boundary thrust in northwest Himalaya. J Tectonophysics, 489, 29-42.

[197] Thiede, R. C., Ehlers, T. A., Bookhagen, B. & Strecker, M. R. 2009. Erosional variability along the northwest Himalaya. J Journal of Geophysical Research: Earth Surface, 114.

[198] Tiwari, B. & Douglas, R. 2012. Application of GIS tools for three-dimensional slope stability analysis of pre-existing landslides. GeoCongress 2012: State of the Art and Practice in Geotechnical Engineering.

[199] Urciuoli, G. & Pirone, M. 2013. Subsurface drainage for slope stabilization. J Landslide Science Practice: Volume 6: Risk Assessment, Management Mitigation, 577-585.

[200] Van Westen, C. J., Jaiswal, P., Ghosh, S., Martha, T. R. & Kuriakose, S. L. 2012. Landslide inventory, hazard and risk assessment in India. J Terrigenous mass movements: detection, modelling, early warning mitigation using geoinformation technology, 239-282.

[201] Varnes, D. 1978. Slope movement types and processes. J Landslides: analysis control.

[202] Verma, A., Singh, T., Chauhan, N. K. & Sarkar, K. 2016. A hybrid FEM–ANN approach for slope instability prediction. Journal of The Institution of Engineers : Series A, 97, 171-180.

[203] Wang, Y., Cao, Z. & Au, S.-K. 2011. Practical reliability analysis of slope stability by advanced Monte Carlo simulations in a spreadsheet. Canadian Geotechnical Journal, 48, 162-172.

[204] Wang, Y., Wen, H., Sun, D. & Li, Y. 2021. Quantitative assessment of landslide risk based on susceptibility mapping using random forest and geodetector. J Remote Sensing, 13, 2625.

[205] Wang, Z. & Lin, M. 2021. Finite element analysis method of slope stability

based on fuzzy statistics. Earth Sciences Research Journal, 25, 123-130.

[206] Wasowski, J., Keefer, D. K. & Lee, C.-T. 2011. Toward the next generation of research on earthquake-induced landslides: current issues and future challenges. Engineering Geology, 122, 1-8.

[207] Wei, W., Li, X., Liu, J., Zhou, Y., Li, L. & Zhou, J. 2021a. Performance evaluation of hybrid WOA-SVR and HHO-SVR models with various kernels to predict factor of safety for circular failure slope. Applied Sciences, 11, 1922.

[208] Wei, X., Zhang, L., Yang, H.-Q., Zhang, L. & Yao, Y.-P. 2021b. Machine learning for pore-water pressure time-series prediction: Application of recurrent neural networks. Geoscience Frontiers, 12, 453-467.

[209] Wieczorek, G. F. 1996. Landslides: investigation and mitigation. Chapter 4-Landslide triggering mechanisms. J Transportation Research Board Special Report.

[210] Wines, D. 2016. A comparison of slope stability analyses in two and three dimensions. J Journal of the Southern African Institute of Mining Metallurgy, 116, 399-406.

[211] Winterkorn, H. F. & Pamukcu, S. 1991. Soil stabilization and grouting. Foundation engineering handbook. Springer.

[212] Wulf, H., Bookhagen, B. & Scherler, D. 2012. Climatic and geologic controls on suspended sediment flux in the Sutlej River Valley, western Himalaya. J Hydrology Earth System Sciences, 16, 2193-2217.

[213] Xie, H., Dong, J., Deng, Y. & Dai, Y. 2022. Prediction model of the slope angle of rocky slope stability based on random forest algorithm. Mathematical Problems in Engineering, 2022, 1-10.

[214] Xie, M., Esaki, T., Zhou, G. & Mitani, Y. 2003. Geographic information systems-based three-dimensional critical slope stability analysis and landslide hazard assessment. J Journal of Geotechnical Geoenvironmental engineering, 129, 1109-1118.

[215] Xie, M., Wang, Z., Liu, X. & Xu, B. 2011. Three-dimensional critical slip surface locating and slope stability assessment for lava lobe of Unzen volcano. J Journal of Rock Mechanics Geotechnical Engineering, 3, 82-89.

[216] Yang, H., Wang, Z. & Song, K. 2020. A new hybrid grey wolf optimizer-feature weighted-multiple kernel-support vector regression technique to predict TBM performance. Engineering with Computers, 1-17.

[217] Yin, Y., Wang, F. & Sun, P. 2009. Landslide hazards triggered by the 2008 Wenchuan earthquake, Sichuan, China. J Landslides, 6, 139-152.

[218] Yue, Z. & Kang, X. Different contributions of two shear strength parameters to soil slope stability with limit equilibrium method based slice techniques. IOP Conference Series: Earth and Environmental Science, 2021. IOP Publishing, 062009.

[219] Zhang, H., Nguyen, H., Bui, X.-N., Pradhan, B., Asteris, P. G., Costache, R. & Aryal, J. 2021. A generalized artificial intelligence model for estimating the friction angle of clays in evaluating slope stability using a deep neural network and Harris Hawks optimization algorithm. Engineering with Computers 1-14.

[220] Zhao, J., Nguyen, H., Nguyen-Thoi, T., Asteris, P. G. & Zhou, J. 2021. Improved Levenberg–Marquardt backpropagation neural network by particle swarm and whale optimization algorithms to predict the deflection of RC beams. Engineering with Computers 1-23.

[221] Zhao, L., Huang, Y., Chen, Z., Ye, B. & Liu, F. 2020a. Dynamic failure processes and failure mechanism of soil slope under random earthquake ground motions. J Soil Dynamics Earthquake Engineering and Engineering Vibration, 133, 106147.

[222] Zhou, J., Li, E., Yang, S., Wang, M., Shi, X., Yao, S. & Mitri, H. S. 2019. Slope stability prediction for circular mode failure using gradient boosting machine approach based on an updated database of case histories. Safety Science, 118, 505-518.

[223] Zhou KP, Chen ZQ (2009) Stability prediction of tailing dam slope based on neural network pattern recognition. In 2009 Second International Conference on Environmental and Computer Science (pp. 380-383). IEEE.

[224] Zhu, D. 2008. Investigations on the accuracy of the simplified Bishop method. Landslides and Engineered Slopes. From the Past to the Future, Two Volumes+ CD-ROM. CRC Press.

[225] Zhu, D., Lee, C. & Jiang, H. 2003. Generalised framework of limit equilibrium methods for slope stability analysis. Geotechnique 53, 377-395.

[226] Zhu, D., Lee, C., Qian, Q. & Chen, G. 2005. A concise algorithm for computing the factor of safety using the Morgenstern Price method. Canadian geotechnical journal, 42, 272-278.

[227] Zolkepli, M., Ishak, M. & Zaini, M. Slope stability analysis using modified Fellenius's and Bishop's method. IOP Conference Series: Materials Science and Engineering, 2019. IOP Publishing, 012004.

Proof of Papers Published SCI/SCIE Indexed Journals

Iranian Journal of Science and Technology, Transactions of Civil Engineering
https://doi.org/10.1007/s40996-023-01156-0

RESEARCH PAPER

Prophetical Modeling Using Limit Equilibrium Method and Novel Machine Learning Ensemble for Slope Stability Gauging in Kalimpong

Vaishnavi Bansal[1] · Raju Sarkar[1]

Received: 25 April 2023 / Accepted: 20 May 2023

Abstract
Slope stability assessment is necessary to evaluate the safety of natural or man-made slopes. This analysis is crucial for determining the potential risk that could result in landslides or other hazardous situations. This research investigates the landslide predictability of crucial locations in Kalimpong, Darjeeling Himalayas, which are characterized by complicated geology in tough terrains. The study concentrated on the factor of safety determination process for dry and saturated conditions utilizing the GeoStudio commercial software "SLOPE/W" based on limit equilibrium method and provide an analytical comparison using computational intelligence and machine learning approaches. Support vector machine, decision tree, random forest, logistic regression, naïve Bayes, k-nearest neighbors algorithm, and AdaBoost are used as machine learning classifiers having a strong capability of predicting slope failures and perils. Five parameters, namely cohesion, internal friction angle, unit weight, slope angle, and slope height, are chosen as random variables and stability condition as output. Inter-criteria correlation (CRITIC)-based method is utilized to perform sensitivity analysis denoting the greatest impacting parameter, i.e., slope height. Novel ensemble approach R-Boost is identified to give maximum accuracy in comparison to all seven machine learning methods. By multifold cross-validation, R-Boost has the greatest forecasting skill, with an average classification accuracy of 0.725 and in terms of area under the curve, random forest (RF) represents an average value of 0.81, followed by R-Boost at 0.798. Among all predictive models, particularly R-Boost followed by RF provides quite similar results as obtained by SLOPE/W. This technique will be particularly beneficial in preventing, anticipating, and reducing the impact of these sorts of catastrophic disasters, which function as substantial barriers to the nation's socioeconomic progress

Keywords Limit equilibrium method · Slope stability · Kalimpong · Machine learning · Factor of safety

1 Introduction

Slope failures are the easiest natural hazard to prevent, reduce, or resolve (Collins and Znidarcic 2004). Landslides occur on a large portion of land surfaces except snow-covered areas in India (Chawla et al. 2018). This translates to a total area of 0.42 million km^2, out of which 43% area is found in the North-Eastern Himalayan Region (NEHR) according to GSI 2014. According to the National Crime Records Bureau's (NCRB) statistics on inadvertent fatalities (2010–2019), landslides kill around 304 people in India each year. Surprisingly, recent changes in global climatic conditions have resulted in catastrophic weather events that increase the likelihood of landslides (Zou et al. 2021) and their frequency is being aggravated by uncontrolled urbanization and unorganized land-use changes in steep terrains (Khanna et al. 2021; Phong et al. 2021; Pourghasemi et al. 2012). The Kalimpong district is located in the NEHR and is susceptible to small- and large-scale landslides, particularly during the monsoon season, which lasts from July to September. The Kalimpong area has a steeply slanting mountainous topography that is constantly drained by heavy rains, making it very prone to landslides. The major town is located on a ridge near the Teesta River, but other rivers like Relli, Neora, Geesh, Leesh, Jaldhaka, and Murti, as well as several tiny streams, drain Kalimpong. These water bodies create active denudation among slopes on the valley side by erosion, which makes them steeper. The interCuvial (Area occurring between two phases or streams) area has been

✉ Vaishnavi Bansal
vaishnavi_2k19phdce08@dtu.ac.in

Raju Sarkar
rajusarkar@dce.ac.in

[1] Department of Civil Engineering, Delhi Technological University, Delhi 110042, India

Published online: 23 June 2023

Iranian Journal of Science and Technology, Transactions of Civil Engineering (2024) 48:2785–2807
https://doi.org/10.1007/s40996-024-01344-6

RESEARCH PAPER

Comparative Analysis of Slope Stability for Kalimpong Region under Dynamic Loading Using Limit Equilibrium Method and Machine Benchmark Learning Classifiers

Vaishnavi Bansal[1] · Raju Sarkar[1]

Received: 19 September 2023 / Accepted: 30 December 2023 / Published online: 8 February 2024

Abstract
Significant slope destabilisation may become more likely due to the speed at which urbanisation is occurring, as well as the growing necessity for geoengineering initiatives or the growth of the road network. Slope stability analysis is done to lower the risk of landslides and slope failures. The study area, Kalimpong, is well-known for its lush greenery and stunning views and is situated in the Eastern Himalayas. However, it also constantly confronts the risk of landslides because of its rugged topography, potential seismic zone, and heavy monsoon rains. In this study, the results of the factor of safety computed by limit equilibrium (conventional) method have been compared analytically using computational intelligence and machine learning methodologies for both dry and saturated conditions under dynamic loading. Conventional machine learning techniques are combined with seven prediction models. The following algorithms have been chosen for slope stability analysis: support vector machine, *k*-nearest neighbours, decision tree, random forest, logistic regression, AdaBoost, and gradient boosting. Random cross-validation is used to assess each model's dependability. The stability condition is the result of the random selection of seven parameters: cohesiveness, unit weight, slope height, angle of the slope, internal friction angle, horizontal and vertical pseudo-static coefficient. Moreover, the coefficient of variation method is employed to assess the importance of every indicator in forecasting slope stability. As per the sensitivity analysis, slope stability is primarily affected by cohesiveness. With an average classification accuracy of 0.878, ensembling approach SVM-Boost demonstrates the best prediction abilities among the models tested using multifold cross-validation. The accuracy ratings of SVM and AdaBoost were 0.865 and 0.834, respectively. When combined with SLOPE/W advances, novel SVM-Boost exhibits the highest exactitude, hegemony, and best outcomes in slope stability prediction. Future earthquakes, strong rainfall, and human activity could cause the slope to collapse. The outcome demonstrates machine learning's enormous potential for enhancing slope stability assessments and provides a means of raising the effectiveness and safety of slope management.

Keywords Slope stabilisation · Numerical modelling · Machine learning · Slope/W · Kalimpong

1 Introduction

Rapid urbanisation and the increasing needs of geoengineering projects like dams, tunnels, bridges, and road widening could exacerbate large-scale slope destabilisation (Pradhan and Siddique 2020). Landslides are induced by gravity and entail the descending and lateral movement of slope-forming materials through a variety of motions such as falling, sliding, flowing, and any combination of the aforementioned. Regular slope failure on both naturally occurring and artificially constructed slopes is significant because it endangers lives, hinders socioeconomic development, and degrades habitat (Leroueil 2001). Except for snow-covered areas in India, a substantial percentage of terrestrial surfaces experience landslides (Chawla et al. 2018). As per the GSI 2014 report, the cumulative expanse covers approximately 0.42 million square kilometres, with the "North-eastern Himalayan Region" (NEHR) accounting for 43% of this area. Based on the "National Crime Records Bureau" (NCRB) data on unintentional fatalities during the period 2010–2019, it is

✉ Raju Sarkar
rajusarkar@dce.ac.in

Vaishnavi Bansal
vaishnavi_2k19phdce08@dtu.ac.in

[1] Department of Civil Engineering, Delhi Technological University, Delhi 110042, India

Proof of Papers Presented in Proceedings of the Conferences

Maulana Azad National Institute of Technology, Bhopal

ICET 2023

Springer

Certificate of Appreciation

This is to certify that the paper titled **Geo-environmental study of rainfall induced slope fail-ure in Kalimpong by numerical modelling- A case study**

Authored by **Vaishnavi Bansal, Prof. Raju Sarkar**

was presented in Second International Conference on **Innovations in Clean Energy Technologies (ICET-2023)** at **Energy Centre, Maulana Azad National Institute of Technology, Bhopal, Madhya Pradesh, India** from **8th-10th April 2023.**

Dr. Gaurav Dwivedi
Organizing Secretary

Dr. Archana Soni
Organizing Secretary

Dr. Prashant Baredar
Organizing Chairman

International Conference on

SUSTAINABLE INFRASTRUCTURE: INNOVATIONS, OPPORTUNITIES AND CHALLENGES (SIIOC 2023)

G20 भारत 2023 INDIA

CERTIFICATE

OF PARTICIPATION

Presented to

Ms Vaishnavi Bansal

SIIOC 2023

For successfully participating and presenting a paper entitled, "NUMERICAL ANALYSIS AND IMPLICATIONS OF FLUCTUATING WATER LEVELS ON SLOPE STABILITY ", authored by Vaishnavi Bansal, Prof. Raju Sarkar at the International Conference on Sustainable Infrastructure: Innovations, Opportunities, and Challenges (SIIOC 2023) held during 20 - 21 April 2023 at NITK, Surathkal.

Dr. Raviraj H. M Dr. Pavan G. S
Organizing Secretaries

Prof. B. R. Jayalekshmi
HOD, Civil Engg. Dept.

DELHI TECHNOLOGICAL UNIVERSITY
(Formerly Delhi College of Engineering)
Shahbad Daulatpur, Main Bawana Road,
Delhi-42

PLAGIARISM VERIFICATION

Title of the Thesis **"Slope Stability Assessment in Kalimpong region of Darjeeling Himalayas"**

Total Pages: 140 Name of Scholar: **Vaishnavi Bansal**

Supervisor (s): **Prof. Raju Sarkar**

Department: **Civil Engineering**

This is to report that the above thesis was scanned for similarity detection. Process and outcome is given below:

Software used: **Turnitin** Similarity Index: 9 **% after excluding self-citations**

Total Word Count: 28016

Date: **30/10/2025**

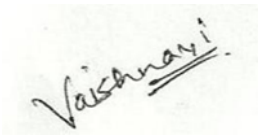

Candidate's Signature **Signature of Supervisor(s)**

PLAGIARISM REPORT

vaishnavi bansal thesis 1.pdf

Delhi Technological University

Document Details

Submission ID
trn:oid:::27535:119094532

Submission Date
Oct 30, 2025, 2:19 PM GMT+5:30

Download Date
Oct 30, 2025, 2:24 PM GMT+5:30

File Name
vaishnavi bansal thesis 1.pdf

File Size
5.0 MB

140 Pages

28,016 Words

156,478 Characters

9% Overall Similarity

The combined total of all matches, including overlapping sources, for each database.

Filtered from the Report

- Bibliography
- Quoted Text
- Small Matches (less than 10 words)

Exclusions

- 2 Excluded Sources

Match Groups

- 128 Not Cited or Quoted 7%
  Matches with neither in-text citation nor quotation marks
- 43 Missing Quotations 2%
  Matches that are still very similar to source material
- 0 Missing Citation 0%
  Matches that have quotation marks, but no in-text citation
- 0 Cited and Quoted 0%
  Matches with in-text citation present, but no quotation marks

Top Sources

- 5% Internet sources
- 3% Publications
- 4% Submitted works (Student Papers)

BRIEF PROFILE

I, Vaishnavi Bansal, completed B. Tech in Civil Engineering from Uttar Pradesh Technical University, Lucknow, India, and M.Tech from National Institute of Technology, Kurukshetra (Haryana, India). Currently I am working as an Assistant Professor in the Department of Civil Engineering at JSS Academy of Technical Education, Noida since 11-Aug- 2015. I have enrolled Ph.D. in Department of Civil Engineering at Delhi Technological University, Delhi-42, (India) under the supervision of Prof. Raju Sarkar. I have published 2 SCI/SCIE in reputed journals and 13 Scopus/conference papers till date. My specialization lies in geotechnical engineering with a focus on slope stability and landslide hazard assessment. I am also focused on integrating interdisciplinary approaches for sustainable slope stabilization in hilly terrains, field investigations, GIS-based mapping, and numerical modeling techniques for geohazard analysis.